



HAL
open science

Photobiological properties of photoactive nanoparticles for the treatment of cancer

Vadzim Reshetov

► **To cite this version:**

Vadzim Reshetov. Photobiological properties of photoactive nanoparticles for the treatment of cancer. Human health and pathology. Université de Lorraine, 2012. English. NNT: 2012LORR0114 . tel-01749318v1

HAL Id: tel-01749318

<https://hal.univ-lorraine.fr/tel-01749318v1>

Submitted on 29 Mar 2018 (v1), last revised 5 Dec 2012 (v2)

HAL is a multi-disciplinary open access archive for the deposit and dissemination of scientific research documents, whether they are published or not. The documents may come from teaching and research institutions in France or abroad, or from public or private research centers.

L'archive ouverte pluridisciplinaire **HAL**, est destinée au dépôt et à la diffusion de documents scientifiques de niveau recherche, publiés ou non, émanant des établissements d'enseignement et de recherche français ou étrangers, des laboratoires publics ou privés.



AVERTISSEMENT

Ce document est le fruit d'un long travail approuvé par le jury de soutenance et mis à disposition de l'ensemble de la communauté universitaire élargie.

Il est soumis à la propriété intellectuelle de l'auteur. Ceci implique une obligation de citation et de référencement lors de l'utilisation de ce document.

D'autre part, toute contrefaçon, plagiat, reproduction illicite encourt une poursuite pénale.

Contact : ddoc-theses-contact@univ-lorraine.fr

LIENS

Code de la Propriété Intellectuelle. articles L 122. 4

Code de la Propriété Intellectuelle. articles L 335.2- L 335.10

http://www.cfcopies.com/V2/leg/leg_droi.php

<http://www.culture.gouv.fr/culture/infos-pratiques/droits/protection.htm>

Ecole Doctorale BioSE (Biologie-Santé-Environnement)

Thèse

Présentée et soutenue publiquement pour l'obtention du titre de

DOCTEUR DE L'UNIVERSITE DE LORRAINE

Mention : « Sciences de la Vie et de la Santé »

par **Vadzim RESHETOV**

**Propriétés photobiologiques de nanoparticules photoactivables utilisées pour
le traitement de cancers**

**Photobiological properties of photoactive nanoparticles for the treatment of
cancer**

Le 29 Octobre 2012

Membres du jury :

Rapporteurs : Madame Beate RÖDER	Professeur, Humboldt-Universität, Berlin
Madame Athena KASSELOURI	Docteur, Université Paris Sud, Paris
Examineurs : Monsieur François GUILLEMIN	Professeur, CRAN Université de Lorraine CNRS CAV, Vandœuvre-lès-Nancy
Monsieur Boris DZHAGAROV	Professeur, Institut de Physique de l'Académie de Sciences de Biélorussie, Minsk
Madame Lina BOLOTINE	Docteur, CRAN Université de Lorraine CNRS CAV, Co-Directeur de thèse
Monsieur Vladimir ZORIN	Docteur, Université d'Etat Biélorusse, Minsk Co-Directeur de thèse

Centre de Recherche en Automatique de Nancy (CRAN), Université de Lorraine, CNRS UMR 7039,
Centre Alexis Vautrin, 6, Avenue de Bourgogne 54511 Vandœuvre-lès-Nancy, France;

Research Laboratory of Biophysics and Biotechnology, Physics Faculty, Belarusian State University, 4,
pr. Nezavisimosti, 220030 Minsk, Belarus

ACKNOWLEDGEMENTS

I dedicate this thesis to my fiancée, Darya, and to my parents. Without your love, devotion, encouragement, advice, support and patience throughout these years I would have never accomplished this goal. Through all the periods of despair, all the hardships and the pitfalls of life you have carried me. You believed in me when all the hope was lost, and it is you who have made me what I am now. Yours is the single most important contribution to this work, which would be meaningless without you, as would be the life itself. I am forever indebted to you. I thank you, with all my heart and all my love.

I would like to thank my Co-Director of PhD Studies, **Dr Vladimir Zorin**, for intellectual encouragement, scientific advice and discussions and guidance, and for steering me in the right direction. We have worked together for 7 long years, - 3 years at the university, my Master's degree, and PhD years, which in totality were the making years for me as a researcher.

I am grateful to my Co-Director of PhD Studies, **Dr Lina Bolotina**, for giving me the opportunity to work in her research group, for her time and for long discussions of the research problems as well as of the research articles in the process of writing, and for directing me to the exciting world of the European science.

I sincerely thank **Professor François Guillemin** for allowing me the possibility to work under his direction of Centre Alexis Vautrin, for precious and precise discussion of my thesis and for presiding over the thesis jury. It was a privilege, Sir, to have known you and worked with you – this experience I will carry with me for life, with an image of a Scientist and a Man.

I am indebted to **Professor Beate Röder** for accepting to review my thesis manuscript, and whose vast experience in bio- and photophysics, formidable commentaries and questions have greatly contributed to the finalization of this work. I thank you for your keen interest in this thesis, and for giving me a wonderful opportunity to discuss it with you.

I am very grateful to **Dr Athena Kasselouri** for reviewing my thesis manuscript. It was an honor for me to have my work evaluated by this distinguished scientist, and I have profited greatly from her insightful and profound questions on the work.

I wholeheartedly thank **Professor Boris Dzhagarov** for his kind and gracious acceptance to take part in the thesis defense as a member of the jury, for the fundamental discussion that we have had during the defense. I thank you, Sir, for the opportunity to have worked in your distinguished laboratory with **Mr Alexander Stasheuski** on the experiments on singlet oxygen fluorescence, the experience that has indeed advanced my studies.

During my PhD years, I had the pleasure of collaborating with several outstanding researchers, to whom I would like to express my gratitude.

I thank **Dr Julie Garrier** of Centre Alexis Vautrin research laboratory, with whom I have had a long and fruitful collaboration on the chick embryos, and discussions that were very valuable for me, and who has taught me the art of working with the eggs in the laboratory.

I am eternally grateful to **Dr Behnoush Maherani** of LIBio laboratory, who has introduced me to the physico-chemical side of the liposome technology, and has helped with many a research problem that have arisen during the PhD years. I thank **Professor Michel Linder** for the opportunity to have worked in his laboratory with Dr Maherani.

I have enjoyed collaboration with **Ms Aurélie François** of Centre Alexis Vautrin research laboratory on my last, the most demanding and the most exciting *in vivo* project on mice. I am grateful for her willing help and for teaching me how to work with the animals.

I had the opportunity to work in the laboratory of **Professor Wim Jiskoot** of the Leiden/Amsterdam Centre for Drug Research, who has graciously invited me, and provided an important help with a part of my PhD project. I thank **Dr Vasco Filipe** for teaching me the fundamentals of the Nanoparticle Tracking Analysis. I sincerely appreciate his help with these measurements.

I would like to thank **Dr Dominique Dumas** of Plate forme d'Imagerie et de Biophysique cellulaire of Nancy for teaching me the art of working with confocal microscopy, and for long collaboration of 3 years.

My research benefited significantly from the help of **Dr Henri-Pierre Lassalle**, with whom we have discussed spectroscopic and microscopic aspects of many ongoing projects.

I appreciate the hard work of **Ms Agnieszka Siupa** of Nanosight Ltd, UK, on the analysis of nanoparticles.

I thank **Ms Tatiana Shmigol** and **Professor Alexander Potapenko** of the Russian National Research Medical University for the help with the resonance light scattering experiments.

I am very grateful to the members of the research group of Dr Zorin – **Dr Tatiana Zorina**, **Mrs Irina Kravchenko** and **Mr Ivan Khludeev**. They were instrumental in teaching

me the fundamentals of laboratory research work, spectroscopy and chromatography experiments. I will always remember the warm atmosphere of the laboratory created by these devoted scientists.

I express my gratitude to **Dr Susanna Gräfe** of Biolitec AG, Germany, for the help with HPLC measurements.

I thank **Dr Marie-Ange D'Hallewin** for the discussions of our research articles, for her critical view, and ever-present search for the ideal scientific representation of the work.

I thank **Dr Denise Bechet** and **Ms Estelle Bastien** for their help during the PhD years. Finally, I would like to thank all the other members of the Centre Alexis Vautrin research laboratory, my colleagues, for the years that we have worked under one roof, often helping each other with advice, a willing hand, or a laugh.

I acknowledge the fellowship of the Ministry of Foreign and European Affairs of France for the PhD studies.

TABLE OF CONTENTS

ABBREVIATIONS	4
LIST OF FIGURES	5
LIST OF TABLES.....	6
GENERAL INTRODUCTION	7
CHAPTER I. INTRODUCTION	8
1. Photodynamic therapy of cancer	8
1.1. Historical aspects	8
1.2. Principles of photodynamic therapy	8
1.2.1. Applications, advantages and limitations of photodynamic therapy	9
1.2.2. Photophysical and photochemical processes in photodynamic therapy	10
1.3. Mechanisms of tumor photoeradication: direct, vascular, immune effects	13
1.4. Photosensitizers	16
1.4.1. An ideal photosensitizer	16
1.4.2. Distribution of the photosensitizer in the body	18
1.4.3. Photosensitizers approved clinically/in trials	19
1.4.4. Photosensitizer generations	19
1.4.5. meta-Tetra(hydroxyphenyl)chlorin	20
2. Drug delivery systems: an overview of systemic nanocarriers	24
2.1. A rational design of drug delivery systems and drug suitability	24
2.2. Advantages of drug delivery systems	25
2.3. Types of drug delivery systems	26
3. Liposomes for anticancer therapy.....	30
3.1. Liposome classification, structure and basic properties	30
3.2. Properties and behavior of liposomes as a drug delivery system	32
3.2.1. Effects of liposomal formulation on drug pharmacokinetics	32
3.2.2. Liposomal clearance	34
3.2.3. Liposome destruction in circulation	35
3.2.4. Drug release from liposomal formulation	36
3.2.5. Liposome-cell interaction	38
3.2.6. Long-circulating liposomes	39
3.2.7. Tumor targeting of liposomes.....	42
3.2.7.1. Passive targeting	43

3.2.7.2. Active targeting	44
4. Liposomes for photodynamic therapy of cancer	46
4.1. Photophysical properties and localization of photosensitizers in liposomes.....	46
4.1.1. Localization of photosensitizers in liposomes.....	47
4.1.2. Singlet oxygen generation by liposomal photosensitizers.....	47
4.2. Liposomal photosensitizers in biological systems.....	48
4.2.1. Phototoxicity of liposomal photosensitizers <i>in vitro</i>	48
4.2.2. Photodynamic therapy with liposomal photosensitizers <i>in vivo</i>	49
4.3. Release of photosensitizers from liposomes.....	50
4.3.1. Mechanisms of drug release from liposomes	51
4.3.2. Methods of drug release measurement	51
4.4. Liposomal formulations of meta-tetra(hydroxyphenyl)chlorin.....	53
4.4.1. Photophysical properties of mTHPC in liposomes	53
4.4.2. mTHPC release from liposomes.....	55
4.4.2. <i>In vitro</i> studies	56
4.4.3. <i>In vivo</i> studies	57
OBJECTIVES.....	60
CHAPTER II. RESULTS	62
1. mTHPC photophysical properties and localization in liposomes. Release from liposomes to blood serum proteins	62
2. Comparison of fluorescence methods suitable for mTHPC release studies.....	72
3. Binding of liposomal mTHPC to serum proteins and the destruction of liposomes	80
GENERAL DISCUSSION	90
CONCLUSIONS AND OUTLOOK	95
REFERENCES	97
SCIENTIFIC OUTPUT	115
SUMMARY IN FRENCH	118

ABBREVIATIONS

BPD-MA – benzoporphyrin derivative mono-acid ring A

CAM – chorioallantoic membrane

DDS – drug delivery system

DLI – drug-light interval

DPPC – dipalmitoylphosphatidylcholine

DPPG – dipalmitoylphosphatidylglycerol

EPR – enhanced permeability and retention

ER – endoplasmic reticulum

Hp – hematoporphyrin

HpD – hematoporphyrin derivative

IV – intravenous

MPS – mononuclear phagocyte system

mTHPC – meta-tetra(hydroxyphenyl)chlorin

PEG – poly(ethylene glycol)

PDT – photodynamic therapy

PK – pharmacokinetics

PS – photosensitizer

RES – reticuloendothelial system

LIST OF FIGURES

Figure 1. Jablonski energy diagram for PS. VR – vibrational relaxation, IC – internal conversion, ISC – intersystem crossing.	11
Figure 2. Principle of PDT and tumor photoeradication (from [6]).	13
Figure 3. mTHPC chemical structure.	20
Figure 4. Schematic structures of DDS (from [117]).	27
Figure 5. Steric and fundamental organization of a liposome with one lipid bilayer and the general structure of lipid (from [167]).	30
Figure 6. Opsonin-mediated liposome uptake by Kupffer cells and hepatocytes (from [200]). ...	34
Figure 7. Principal nanocarrier internalization pathways in cells (from [227]).	39
Figure 8. Schematic diagram of PEG configuration regimens (mushroom, brush and pancake) for the polymer grafted to the surface of the lipid bilayer (from [240]).	40
Figure 9. Mechanism of steric protection by PEG. PEG chains (1) prevent opsonins (2) from being absorbed on the liposome surface (from [180]).	41
Figure 10. Schematic representation of passive and active mechanisms of liposomal drug accumulation in tumor (from [117]).	42

LIST OF TABLES

Table 1. Photosensitizers approved for clinics or undergoing clinical trials (from [1]).....	19
Table 2. Photophysical properties of mTHPC (in methanol)	20
Table 3. Examples of DDS and their clinical applications in cancer therapy	26
Table 4. Properties of rapid release and sustained release lipidic DDS (from [2])	37

General introduction

GENERAL INTRODUCTION

Photodynamic therapy (PDT) is a photochemical-based approach that uses a combination of a light-activatable drug (photosensitizer, PS) and the light of a specific wavelength to damage the target tumor tissue by generating reactive molecular species. Clinically, the photosensitizer is generally administered intravenously, and the tumor is irradiated with a suitable light source after a certain time delay termed the drug-light interval depending on the specific PS and the target disease. Currently, the development of liposomal nanocarriers to deliver photosensitizers to tumor targets has become a major direction in PDT research with the aim of adapting treatment protocols, reducing side effects, and improving PDT efficacy.

meta-tetra(hydroxyphenyl)chlorin (mTHPC) is a highly efficient 2nd generation photosensitizer, clinically approved for palliative treatment of head and neck cancer. Clinical application of mTHPC encounters several difficulties due to high hydrophobicity of this photosensitizer. In aqueous media like blood plasma, mTHPC strongly aggregates and as such is ineffective in producing singlet oxygen, thus resulting in a drop of its photosensitizing efficiency. The hydrophobic nature of mTHPC also complicates the administration of the drug. Thus, in order to improve its bioavailability and efficacy, mTHPC is formulated in liposomes which possess several attractive properties for anticancer drug delivery. Two liposomal formulations of mTHPC are available: conventional Foslip® and sterically stabilized Fospeg®.

Inclusion of a photosensitizer into lipid vesicles can significantly change its pharmacokinetic and photophysical properties. Thorough characterization of a liposomal drug system is essential for an adequate understanding of the system-target interactions generating the *in vivo* results. It is not clear from the studies of anticancer drugs what is the critical parameter to consider when optimizing liposomal PDT. Drug release is considered to be a crucial property of the liposomal drug formulation, along with the blood circulation and the spatio-temporal uptake in the tumor.

The objectives of this work were to characterize the properties of mTHPC in two liposomal formulations *in vitro* and estimate its release from the carriers. A technique of analyzing mTHPC release from liposomes *in vitro* and *in vivo* was developed, based on the effect of photoinduced fluorescence quenching.

Introduction

CHAPTER I. INTRODUCTION

1. PHOTODYNAMIC THERAPY OF CANCER

1.1. Historical aspects

Although photodynamic therapy (PDT) has been known in its ancient form for several thousand years, its modern era started in the 1960s with the discovery of hematoporphyrin derivative (HpD) [3]. It was used for fluorescence detection of tumors [4], and administered at much smaller doses than hematoporphyrin (Hp), thus serving as a promising diagnostic tool. The clinical application of PDT started in the 1970s, largely due to the efforts by Thomas Dougherty and his colleagues at Roswell Park Cancer Institute (University of Buffalo, USA). Their studies have shown long-term HpD-PDT efficacy in animal models and humans [5]. Chromatographic isolation of HpD led to the development of the photosensitizer Photofrin®, first approved for the treatment of bladder cancer in Canada in 1993, and currently approved in the US, Europe and Japan for the treatment of advanced and early stage lung cancer, superficial gastric cancer, oesophageal adenocarcinoma, cervical cancer and bladder cancer [6]. An increasing number of PDT-related studies led to a better understanding of the factors controlling PDT. The application of PDT has spread from the treatment of cancer and pre-cancerous lesions to antimicrobial PDT, wound healing, treatment of ocular macular degeneration and bone marrow purging [7]. Current research is focused on improving the photosensitizers, developing new drugs, light sources, and optimizing treatment protocols. The latter aims to improve the major PDT components, namely the drug (photophysical properties, the mode of administration, the delivery system and distribution in the body), the light (administration, characteristics, the light-drug interval), and utilize specific tumor characteristics. Understanding the interrelation between these factors is essential for the development of treatment strategies for PDT.

1.2. Principles of photodynamic therapy

Photodynamic therapy is a photochemical-based approach that uses a combination of a light-activatable drug (photosensitizer) and the light of a specific wavelength to damage the target tissue by generating reactive molecular species [1]. A third component is an adequate concentration of oxygen at the target site. The lack of any of the three components results in the absence of a PDT effect. Clinically, the photosensitizer (PS) is generally administered intravenously (IV) or topically, and the tumor is irradiated with a suitable light source after a

certain time delay termed the drug-light interval (DLI), depending on the specific PS and the target disease.

1.2.1. Applications, advantages and limitations of photodynamic therapy

There are several major clinical applications of PDT which have evolved in time with the development of new drugs, light sources and the understanding of the fundamental processes involved in PDT [8].

Cancer treatment

Historically the destruction of solid tumors was the initial indication for the palliative use of modern PDT. Today, as a considerable number of clinical trials testing various treatment modalities of cancer have shown only small differences in treatment outcomes [9, 10], PDT may offer a different therapeutic approach to advance the treatment of a superficial and early disease. The first tumor approved for treatment was refractory superficial bladder cancer [11]. Other approvals include the treatment of obstructive and early-stage bronchial cancers [12], esophageal dysplasia and carcinoma *in situ* [13], and unresectable cholangiocarcinoma. Excellent cosmetic outcomes make PDT suitable for patients with skin cancers [13, 14]. PDT has been shown to have high efficacy for basal cell carcinoma, including extensive or recurrent lesions. In malignant brain tumors, there have been several clinical trials of PDT as an adjunctive therapy for both primary and recurrent tumors, where the whole surgical cavity is illuminated immediately following radical resection in order to reduce the residual tumor burden and to increase the probability of long-term disease control. Prostate cancer PDT trials are ongoing, with the treatment of the whole prostate in patients who have recurred locally following radiation therapy [15] or as a primary therapy for focal tumors [16]. The development of second-generation PSs led to efficient clinical treatment of head and neck tumors: widespread and unresectable or recurrent tumors [17], early stage oral cancers [18] and nasopharyngeal tumors [19]. However, the effectiveness of the treatment of many cancer types with PDT remains yet to be proven due to the lack of well-designed clinical trials [1].

PDT has several potential advantages over surgery and radiotherapy [20, 1]: (1) it is minimally invasive; (2) it can be targeted accurately using the ability of PSs to localize in neoplastic lesions and with the precise delivery of light to the treatment sites with flexible fiberoptic devices; (3) repeated doses can be administered without inducing significant resistance or total-dose limitations associated with radiotherapy; and (4) the healing process results in little or no scarring; (5) none of the clinically approved PSs accumulate in cell nuclei, limiting DNA damage that could be carcinogenic or lead to the development of resistant clones; (6) the adverse effects of chemotherapy or radiation are absent, and the systemic toxicity is low; (7) PDT can be

used either before or after chemotherapy, radiotherapy or surgery without compromising these therapeutic modalities, (8) PDT can be performed in outpatient settings which reduces costs, and is convenient for the patient. PDT acts through the multitude of biological effects, however, due to the multiple interplaying factors, the treatment is complex and difficult to optimize.

Localized infections

The increase in antibiotic resistance among many species of pathogens may bring about the end of the antibiotic era that has lasted for the past 60 years [21]. The growth of multi-drug-resistant bacteria has led to a tremendous increase in research dedicated to finding alternative therapies [7]. PDT is considered as an alternative in the treatment of localized bacterial infection. It was shown to be effective against even multi-drug-resistant strains [22, 23]. Advantages of PDT include equal killing effectiveness regardless of antibiotic resistance, and the absence of induction of PDT resistance. Disadvantages are the cessation of the antimicrobial effect when the light is turned off, and a rather poor selectivity for microbial cells over the host tissue [7].

Macular degeneration

One of the major achievements of PDT was the clinical ophthalmological success in the treatment of age-related macular degeneration and eye diseases related to neovascularization [24]. Before PDT, the only treatment was the use of thermal laser coagulation, but this was marginally effective [8]. FDA approval of Visudyne® in 2000 as a first-line treatment led to more than 2 million treatments conducted to date [25].

Dermatology

PDT with aminolevulinic acid is an approved approach to the treatment of actinic keratosis or sun-damaged skin [26, 27] which is associated with development of skin cancer. PDT with this prodrug is widely used in cosmetic dermatology, e.g. in the treatment of acne, in hair removal (the treatment damages the hair follicles) and in skin re-modeling.

The adverse effects of PDT relate to pain during treatment protocols and a persistent skin photosensitization that has been somewhat circumvented by the latest PSs. However, compared to other techniques this is a small price to pay for a potential cancer cure. PDT is a localized treatment and will be ineffective against metastatic lesions, which are the most frequent cause of death in cancer patients [1], and is not applicable to systemic diseases. The major limitation of PDT in the present state of the art is the absence of precise dosimetry [8].

1.2.2. Photophysical and photochemical processes in photodynamic therapy

The absorption of light by a PS is the initial step in all photoreactions. The energy of the absorbed quantum promotes PS molecules from their ground electronic state to excited states. At room temperature, almost all the molecules are in their ground state, which is the electronic state

associated with the lowest energy and a configuration where all electrons are orbitally paired. During an electronic transition one of the electrons is excited from an initially occupied orbital of low energy to a previously unoccupied orbital of higher energy. The excited state S_1 has a different electronic distribution than the ground state S_0 , and is energetically less stable than S_0 . De-excitation must take place to permit the release of the surplus of energy. Several physical pathways leading to energy dissipation can follow, each with an associated probability of occurrence. These are represented in the Jablonski diagram (Fig. 1).

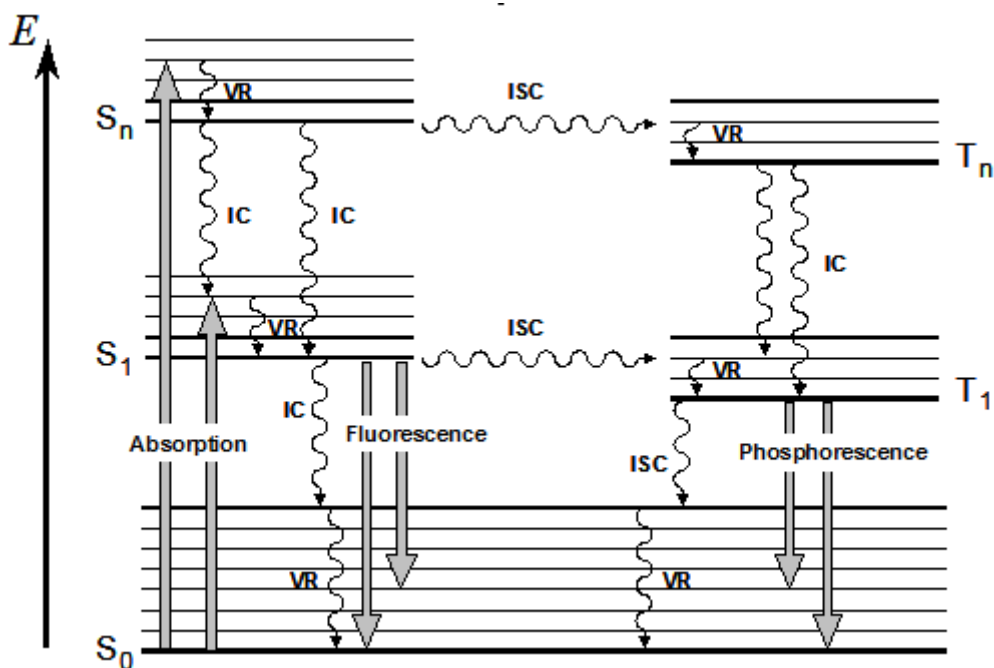


Figure 1. Jablonski energy diagram for PS. VR – vibrational relaxation, IC – internal conversion, ISC – intersystem crossing.

A molecule with a high vibrational level of the excited state S_n (n depending on the PS and excitation wavelength used) will quickly fall to the lowest vibrational level of this state in a process called vibrational relaxation. Also, a molecule in a higher excited state S_n will finally fall to the first excited singlet state S_1 by internal conversion. Then, the singlet state S_1 can rapidly return to the ground state level S_0 by two mechanisms, a radiative process (fluorescence), or a non-radiative process (internal conversion). During this internal conversion, the excess of energy of the singlet state is released as heat, which dissipates usually into the tissue or the solvent. As for the radiative process, a photon is emitted with the energy equal to the energy gap between the S_0 and the S_1 levels, implying that the fluorescence does not depend on the excitation wavelength. PS fluorescence emission forms a basis for fluorescence detection used in certain photodiagnostic applications.

In addition to radiationless and radiative processes, the excited singlet state may initiate photochemistry or undergo a change to a triplet state T_1 via intersystem crossing. The lifetime of the triplet state is much longer ($\tau > 10^{-7}$ s) than the lifetime of the singlet state ($\tau \sim 10^{-9}$ s), which

greatly increases the probability of a reaction with a neighboring molecule, and the biologically relevant photochemistry is often mediated by this state. There are several pathways for the triplet state T_1 to return to S_0 . De-activation can occur with the emission of a photon (phosphorescence), or by undergoing intersystem crossing followed by vibrational relaxation.

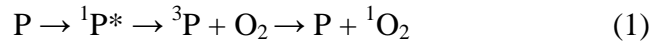
For most of the organic molecules, only the S_1 and T_1 can be considered as likely candidates for the initiation of photochemical and photophysical reactions. This is due to the fact that higher order electronic states ($n \geq 2$) undergo very rapid internal conversion from S_n to S_1 and from T_n to T_1 . However, under the special circumstance of multiphoton absorption (short pulse, high intensities of irradiation), the upper excited states may be populated and complex photophysical and photochemical processes can occur [28, 29].

T_1 can initiate photochemical reactions directly upon interaction with a substrate, giving rise to reactive free radicals (type I reaction), or transfer its energy to the ground-state oxygen molecules to produce highly reactive singlet oxygen molecules (type II reaction) [30]. The relatively longer lifetimes for the triplet excited states make the collisional transfer of energy to surrounding oxygen molecules possible.

Type I photochemical reaction, whereby the PS reacts directly with an organic molecule in a cellular microenvironment, leads to the formation of pairs of neutral radicals or radical ions following an electron or hydrogen transfer, with most biological substrates undergoing oxidation. Both the excited PS and the ground state substrate can act as hydrogen donors. The resulting radical species from type I primary processes can subsequently participate in different kinds of reactions. In the presence of oxygen, for example, oxidized forms of the PS or of the substrate readily react with oxygen to give peroxy radicals, thus initiating a radical chain auto-oxidation. Semi-reduced forms of the PS or of the substrate also interact efficiently with oxygen, and the electron transfer generates superoxide anion radical, also producing hydroperoxide by spontaneous dismutation or one-electron reduction, which in turn can undergo one-electron reduction to a potent and virtually indiscriminate oxidant hydroxyl radical.

In type II process, the reaction proceeds via energy transfer from the excited triplet-state PS to the oxygen molecule in its triplet state (eq. 1). Singlet oxygen can only be generated by PSs that possess an energy gap between the ground state and the excited triplet state higher than the energy needed to excite oxygen into its excited singlet state (94 kJ/mol [31]). Theoretically all molecules absorbing light at a wavelength < 1260 nm can mediate generation of 1O_2 . Singlet oxygen is a very reactive species, much more electrophilic than its ground state, and can oxidize biomolecules very rapidly. It is a metastable species with a lifetime varying from about 4 μ s in water to 25-100 μ s in non-polar organic solutions, which can be considered as a model for lipid regions of the cell. The lifetime of singlet oxygen greatly decreases in biological environment

due to the presence of various quenchers, and is calculated to be about 10-330 ns [32]. This short lifetime allows the diffusion of singlet oxygen to a distance from 10 to 55 nm at the sub-cellular [33, 34], thus limiting the photodestructive effect to the immediate intracellular localization of the PS [35].



1.3. Mechanisms of tumor photoeradication: direct, vascular, immune effects

Schematically, the principle of PDT-induced destruction of a tumor is depicted in Fig. 2. The administration of the PS is followed by the irradiation of the tumor site after a certain DLI to allow for PS accumulation.

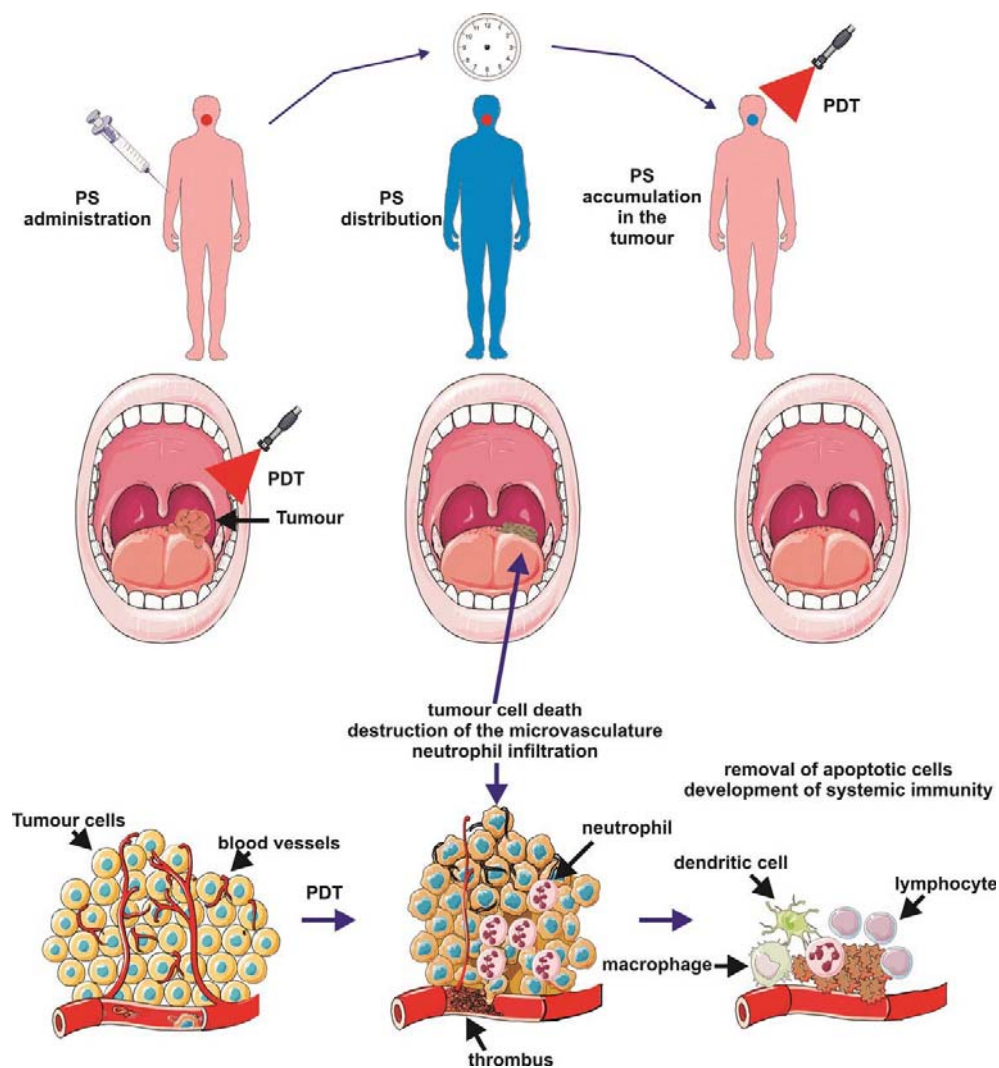


Figure 2. Principle of PDT and tumor photoeradication (from [1]).

There are three interlinked mechanisms of tumor destruction by PDT [36]: direct cytotoxic effects on tumor cells, damage to the tumor-associated vasculature leading to tissue ischemia, and activation of the immune response against tumor cells following inflammatory reaction. The relative importance of each of the mechanisms for the overall tumor response is dependent on a variety of factors, such as the PS used, DLI, tissue oxygenation, and irradiation

settings [1, 37]. However, the combination of all three components is required for long-term tumor control.

Direct tumor cell destruction

In vivo exposure of tumors to PDT has been shown to reduce the number of clonogenic tumor cells through direct photodamage [38]. PDT can provoke the 3 main cell death pathways: apoptotic, necrotic, and autophagy-associated cell death [1].

Apoptosis is morphologically characterized by chromatin condensation, cleavage of chromosomal DNA into internucleosomal fragments, cell shrinkage, membrane blebbing, and the formation of apoptotic bodies without plasma membrane breakdown. Apoptotic cells release the “find me” and “eat me” signals required for the clearance of the remaining corpses by phagocytic cells. Among the subcellular structures mitochondria play an essential role in apoptosis initiation [39]. The damage to mitochondria after PDT results in a cascade of reactions ultimately leading to the apoptosis of cells. Thus, based on the locality of the effect of singlet oxygen-mediated cell damage, the PS (generally hydrophobic [40]) has to be localized in mitochondria to induce the apoptotic cascade [41]. However, the lysosomal localization of the PS may also activate apoptotic cascade [42].

Necrosis is characterized by the vacuolization of the cytoplasm and swelling and breakdown of the plasma membrane, resulting in an inflammatory reaction due to the release of cellular contents and pro-inflammatory molecules. Necrosis is thought to be the result of pathological insults or to be caused by a bioenergetic catastrophe: ATP depletion to a level incompatible with cell survival. The PDT-related necrotic cell death is typically induced by the inhibition or genetic deficiency of caspases in the cell signaling [43]. The localization of the PS (usually hydrophilic) in lysosomes and plasmatic membrane generally leads to necrotic death pathway [41].

Another mechanism of cell death has been described *in vitro*: when a cell dies by direct effect, the adjacent cells present lethal cellular damage that is propagated by means of a chain of adjacent cells. The degree of this phenomenon, called the bystander effect, is higher for cells killed by necrosis than by apoptosis. This effect is thought to be the result of gap-junction communications and diffusion of the reactive oxygen released in the medium [44].

Autophagy is characterized by a massive vacuolization of the cytoplasm. Autophagic cytoplasmic degradation requires the formation of autophagosome, which sequesters cytoplasmic components as well as organelles, and traffics them to the lysosomes. Recent studies describe autophagy as a mechanism to preserve cell viability after photodynamic injury [45]. Photodamage of lysosomal compartment by the PS may compromise completion of the autophagic process.

Complete tumor eradication may not always be obtained through direct tumor cell death. Indeed, non-homogenous distribution of the photosensitizer within the tumor, or distance of tumor cells from the vessels [46] as well as availability of oxygen [47] may hamper the tumoricidal effect. Besides, transformed cells that are deeply seated within the tumor mass can receive suboptimal light doses and survive due to the induction of cytoprotective mechanisms [1]. Thus, other mechanisms are necessary for efficient PDT.

Vasculature photodamage

Tumor cell destruction is also potentiated by damage to the microvasculature if the PS is located near the vessels, which restricts oxygen and nutrient supply. Thus, targeting the tumor vasculature is a promising approach to cancer treatment. Early studies reported initial blanching and vasoconstriction of the tumor vessels, followed by heterogeneous responses including eventual complete blood flow stasis, hemorrhage, and, in some larger vessels, the formation of platelet aggregates [48]. Hypoxia sufficient to preclude direct tumor cell killing was identified at subcurative PDT doses. Moreover, various endothelial cells were shown to be more sensitive to PDT compared to muscle cells, together with increased PS uptake [49, 50]. Interestingly, a study by Synder showed that PDT combined with chemotherapy was significantly more potent compared to either therapies alone due to an increase in tumor vascular permeability and increased doxorubicin accumulation [51].

Immune response

Studies have shown that infiltration of lymphocytes, leukocytes and macrophages into PDT-treated tissue occurs, indicating activation of the immune response [52]. PDT activates both humoral and cell-mediated antitumor immunity. It was reported that the induction of antitumor immunity after PDT is dependent upon the induction of inflammation [53]. A strong acute inflammatory reaction is often observed as localized edema at the target site [36], being a consequence of oxidative stress. The PDT effect is regarded by the host as an acute localized trauma, and it launches protective actions evolved for dealing with a threat to tissue integrity and homeostasis at the affected site [54]. The acute inflammatory response is the principal protective effector process involved in this context. Its main task is containing the disruption of homeostasis and ensuring the removal of damaged cells, and then promoting local healing with the restoration of normal tissue function.

It has been demonstrated that PDT can influence the adaptive immune response in disparate ways, resulting both in potentiation of adaptive immunity and immunosuppression. It appears as though the effect of PDT on the immune system depends on the treatment regimen, the area treated, and the photosensitizer type [55]. PDT efficacy appears to be dependent on the induction of antitumor immunity, since long-term tumor response is diminished or absent in

immunocompromised mice [56, 57]. These results indicate that whereas the direct effects of PDT can destroy the bulk of the tumor, the immune response is required to eliminate the surviving cells [57].

The specific mechanism acting upon PDT depends on several factors [37]:

- Tumor localization of the photosensitizer determined by vascular permeability and interstitial diffusion, which depend on the PS properties as well as the physiological properties of blood vessels [58]. Binding of the drug with various tissue components can also influence its transport and retention in tumors.
- DLI. With a short DLI the PS predominantly accumulates in the vascular compartment, while increasing it leads to tumor accumulation. Thus, different DLIs destroy tumor cells by different mechanisms and have different consequences [59].
- Means to direct the PS to a certain cell type or compartment by specific targeting carriers. The site of action within a cell also contributes to the efficacy of PDT [60]. Mitochondria and lysosomes represent the main subcellular targets of the PS, whereas localization in the Golgi apparatus and endoplasmic reticulum mostly corresponds to a non-specific partition of the PS between the membranes of intracellular organelles.

1.4. Photosensitizers

1.4.1. An ideal photosensitizer

The archetypal photosensitizer is Photofrin® (purified form of HpD), a complex mixture of many different porphyrin molecules derived from blood. Photofrin® possesses a large Soret band around 400 nm and several smaller Q-bands at longer wavelengths, a spectrum structure characteristic of tetrapyrrole PSs. Although it has many disadvantages, it is still widely utilized. The disadvantages include a long-lasting skin photosensitivity and a relatively low absorbance at 630 nm. The drug is an inefficient producer of singlet oxygen at 630 nm, so treatment times are relatively long. Based on the deficiencies of Photofrin®, general guidelines were developed for the properties desired for an ideal PS [8, 61, 1].

Photophysical properties

(a) High absorption (molar extinction coefficient) in the range of 600-800 nm, for maximum light penetration in the tissue. Absorption of photons with wavelengths longer than 800 nm does not provide sufficient energy to excite oxygen to its singlet state and to form a substantial yield of reactive oxygen species; moreover, water will absorb most of the light introduced [62]. At the same time, the penetration of light into the tissue increases with its

wavelength, and wavelengths approaching 700-800 nm will penetrate the tissue to more than 2-3 cm while wavelength closer to 600 nm penetrate to about 0.5 cm [63]. The wavelengths below 600 nm exhibit very poor penetration into the tissue due to absorption by endogenous chromophores and intense scattering.

(b) Sufficient fluorescence quantum yield to facilitate the monitoring of biodistribution and imaging.

Photochemical properties

(a) High singlet oxygen generation quantum yield for high photodynamic efficiency (implying high triplet state yield).

(b) Stability against rapid photobleaching in order to retain efficacy during treatment or, alternatively, rapid photobleaching so that the treatment becomes self-limiting, depending on the treatment protocol.

Chemical properties

(a) High stability.

(b) Single, pure molecular species.

(c) Ease and low cost of synthesis.

Biological properties

(a) Low dark toxicity, absence of metabolic creation of toxic byproducts.

(b) Pharmacokinetics matched to the application (e.g. rapid clearance for vascular targeting).

(c) Selective uptake in target tissues/tissue structures; microlocalization to sensitive cellular/subcellular targets (e.g. mitochondria).

(d) Relatively rapid clearance from normal tissues, minimizing phototoxic side effects (ideally, measured in hours and days, not weeks and months). The tissue or vascular half-life should be amenable to the clinical application.

(e) Versatile and easy administration, depending on the clinical situation.

From the perspective of the end user of the PS, i.e. the patient, several other requirements may be added [64]:

(a) Worldwide commercial availability and approval.

(b) Standardized manufacturing process, batch-to-batch reproducibility.

(c) Drug stability and ease of transportation/preparation.

(d) Reliable and pain-free activation, outpatient treatment.

(e) Forgiving treatment. With limited dosimetry available, a highly active PS may easily lead to treatment overdosage. Less active drugs may be more forgiving of excess illumination.

1.4.2. Distribution of the photosensitizer in the body

Injection of the drug involves a series of events for the PS with their characteristic time lengths. First, the PS will be distributed between the various blood components. This involves the PS disaggregation or dissociation from delivery system, binding to serum proteins and association to the blood cells. The second step is the binding of the PS to the blood vessels wall, with the different characteristics of blood vessels in normal and tumoral tissues, as well as the type of vessels in the various organs governing this association. Third, the PS will penetrate the wall of the blood vessel. After extravasation, the PS will diffuse throughout the extracellular medium of the tissues or organ to which it has been delivered. At this moment, the PS may penetrate the tumoral cells. Finally, the PS will be eliminated from the body by lymphatic drainage and/or organ retention and clearance. The large temporal variability of these events must be emphasized. Studies have shown that the variation in pharmacokinetics reported for different PSs is very significant. The retention of the PS in tumor and its elimination pathways seem to depend on the structure of the PS [65].

The repartition of the PS in blood after IV injection allows to define three classes of PSs. First, most of the relatively hydrophilic PSs are bound to albumin fractions (such as sulfonated tetraphenylporphyrin derivatives). Second, the asymmetric and amphiphilic PSs, such as chlorin e6, can be associated with the lipoproteins. These compounds are primarily partitioned between albumin and high-density lipoproteins. Third, the hydrophobic PSs can be incorporated in the core of lipoproteins and, in particular, are bound to low-density lipoproteins. In the case of the drug incorporated into a delivery system, it may considerably change the plasma behavior and the cellular localization of the PS [66]. The transfer of the drug to different serum proteins [67] influences the *in vivo* pharmacokinetics and biodistribution of the PS.

The properties of the proliferating tissue are important for the PS accumulation. The accumulation may be favored by the high number of LDL receptors and/or by the low interstitial pH of targeted tissues [68]. The increased cholesterol catabolism of proliferating tissues leads to overexpression of LDL receptors, thus LDL, while bound to the PS, could ensure targeting to the tumor cells [69]. At the same time, the tumor microenvironment, in particular, a slightly acid pH of the tumor extracellular medium, could play an important role by governing the physicochemical properties of the PS and facilitating the entry into the intracellular environment [70]. The correlation between the PS accumulation in tumors and their structure, in particular, their lipophilic character, the distribution of their polar and hydrophobic chains around the macrocycle and the electric charges of these chains, has been established [67]. The pH-dependent exchange of the PS between albumin and LDL could play a role in the selective

retention of some of these molecules [42]. It has been suggested that in an acid tumoral environment PS redistribution appears to be in favor of LDL association.

PS-cell interactions and PS subcellular localization are governed by various factors, including hydrophobicity/hydrophilicity balance, charge and structural asymmetry. Relatively hydrophilic PSs, bearing polar or charged side chains, are too polar to cross the biological membranes and are usually internalized by endocytosis. In contrast, hydrophobic compounds with no or few polar groups can diffuse across the membranes and may be distributed freely between the membranes of various organelles [42].

1.4.3. Photosensitizers approved clinically/in trials

PSs that have received clinical approval or are currently in trials are summarized in Table 1. Each of them requires a specific protocol of drug and light dosage, with drug doses varying from 0.1 mg/kg to 5 mg/kg, and light doses from 10 J/cm² to 300 J/cm² to achieve optimal effect [64, 1]. Of special interest is temoporfin, or meta-tetra(hydroxyphenyl)chlorin (mTHPC) [71, 72], which is an extremely potent approved drug. The properties of mTHPC will be described in the section below.

Table 1. Photosensitizers approved for clinics or undergoing clinical trials (from [1]).

PHOTOSENSITIZER	STRUCTURE	WAVELENGTH, nm	APPROVED	TRIALS	CANCER TYPES
Porfimer sodium (Photofrin) (HPD)	Porphyrin	630	Worldwide		Lung, esophagus, bile duct, bladder, brain, ovarian
ALA	Porphyrin precursor	635	Worldwide		Skin, bladder, brain, esophagus
ALA esters	Porphyrin precursor	635	Europe		Skin, bladder
Temoporfin (Foscan) (mTHPC)	Chlorine	652	Europe	United States	Head and neck, lung, brain, skin, bile duct
Verteporfin	Chlorine	690	Worldwide (AMD)	United Kingdom	Ophthalmic, pancreatic, skin
HPPH	Chlorin	665		United States	Head and neck, esophagus, lung
SnEt2 (Purlytin)	Chlorin	660		United States	Skin, breast
Talaporfin (LS11, MACE, NPe6)	Chlorin	660		United States	Liver, colon, brain
Ce6-PVP (Fotolon), Ce6 derivatives (Radachlorin, Photodithazine)	Chlorin	660		Belarus, Russia	Nasopharyngeal, sarcoma, brain
Silicon phthalocyanine (Pc4)	Phthalocyanine	675		United States	Cutaneous T-cell lymphoma
Padoporfin (TOOKAD)	Bacteriochlorin	762		United States	Prostate
Motexafin lutetium (Lutex)	Texaphyrin	732		United States	Breast

Abbreviations: ALA, 5-aminolevulinic acid; AMD, age-related macular degeneration; Ce6-PVP, chlorin e6-polyvinylpyrrolidone; HPD, hematoporphyrin derivative; HPPH, 2-(1-hexyloxyethyl)-2-devinyl pyropheophorbide-a; MACE, mono-(L)-aspartylchlorin-e6; mTHPC, m-tetrahydroxyphenylchlorin; nm indicates nanometers; SnEt2, tin ethyl etiopurpurin.

1.4.4. Photosensitizer generations

The attempt to classify the photosensitizers is based on the development timeline [73]. First generation PSs were porphyrin-based and included Hp, its derivatives HpD and its purified form Photofrin®. Second generation PSs were developed according to ideal PS guidelines and with due regard for the deficiencies of the first generation drugs. These PSs have various

chemical structures including porphyrins, expanded porphyrins, chlorins, and dyes. Third generation PSs contain 1st and 2nd generation PSs covalently attached to various biological modifiers like antibodies, hydrocarbons, amino acids and lipoproteins, or formulated into nanoparticles like liposomes, polymers, emulsions to improve the photosensitizing and pharmacokinetic properties of the drugs [74].

It is noteworthy that, in some cases at least, the claim that newer generation drugs are better than the older ones is unjustified [61, 64]. Premature conclusions regarding novel or investigational photosensitizers, according to which the older drugs should be replaced by the newer ones, may be misleading. In clinical reality few head-to-head comparisons have ever been conducted to prove or disprove this point. Even pre-clinical experiments directly comparing different-generation drugs are scarce.

1.4.5. meta-Tetra(hydroxyphenyl)chlorin

5,10,15,20-Tetra(*m*-hydroxyphenyl)chlorin (mTHPC, Fig. 3) is a second generation PS synthesized by Bonnett in 1989 with the properties of an ideal drug in mind [71]. It was shown to be a promising compound in a set of screening procedures (including an assessment of the PDT efficacy) in mouse tumor models [75]. mTHPC (generic name temoporfin, proprietary name Foscan®) lists several properties of an ideal drug, including pure-compound preparation, efficient red light absorption, hence efficient light tissue penetration, certain selectivity of tumor uptake and a low administration dose [75, 76]. Its major photophysical properties are summarized in Table 2 [77, 75].

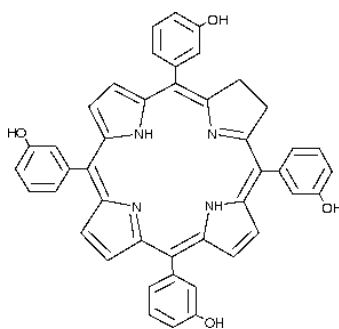


Figure 3. mTHPC chemical structure.

Table 2. Photophysical properties of mTHPC (in methanol)

Property	Value
Absorption maximum, nm	650
Extinction coefficient, M ⁻¹ cm ⁻¹	29600
Fluorescence maximum, nm	652
Fluorescence Q.Y.	0.089
Singlet state lifetime, ns	7.5
Triplet Q.Y.	0.89
Triplet state lifetime, μs	50
Singlet oxygen generation Q.Y. (air-saturated)	0.43

mTHPC, considering total photodynamic doses (light dose x photosensitizer dose), was found to be 100 to 200 times as potent as HpD [78, 79]. In 2001 mTHPC (marketed by Biolitec GmbH) was granted EU approval for palliative treatment of patients with advanced head and neck cancers, and it has been successfully used for the treatment of early squamous cell carcinoma [80, 18], basal cell carcinoma [81], prostate [82] and pancreatic cancer [83]. In general, the dosing of mTHPC is between 0.1 and 0.3 mg/kg and illumination requires only 20 J/cm², thus the treatment time is only a few minutes. Apart from Photofrin®, mTHPC is the only other PS approved for use in systemic cancer therapy.

Cell uptake and cellular localization

mTHPC is a highly hydrophobic compound, which defines its affinity to cell membranes and plasma proteins. Resonance light scattering showed the formation of J-aggregates of mTHPC in aqueous solution [84, 85]. mTHPC seems to be taken up by cells in aggregated form, followed by slow monomerization [86]. Incubation with serum modifies the process, as higher serum concentration diminishes the PDT effect on cells. HDL-mediated endocytosis was proposed as the main mode of drug transport in cells [87]. However, as mTHPC was shown to bind to HDL, LDL and albumin fractions depending on incubation time [88-90], uptake may also be mediated by LDL. The uptake of the compound into cells appears to be pH independent [91]. It is rigidly fixed in model membranes and is strongly retained in cells *in vitro* [92, 93].

The Golgi apparatus and endoplasmic reticulum (ER) were shown to be the preferred sites of mTHPC accumulation in MCF-7 human adenocarcinoma cells [94]. They were also shown to be the primary PDT-induced damage sites as measured by the enzymes photoinactivation technique [94, 95]. A confocal fluorescence microscopy study showed only weak localization in lysosomes and mitochondria [94]. The intratumoral distribution of mTHPC is dependent on the time of circulation and the distance to blood vessels [96].

Mechanism of action

mTHPC exhibits photosensitizing efficacy primarily through the generation of singlet oxygen, which is similar to other porphyrin PSs. The studies on the photodynamic effect in the presence of singlet oxygen scavengers showed a limited reduction in the photoinactivating ability of mTHPC [97].

A study by Kessel showed the release of cytochrome c and activation of caspase-3 resulting in an apoptotic response after mTHPC-PDT *in vitro* [98]. Mitochondrial damage and cytochrome c release has been described for various cancer cells [99, 100]. Combined with the data on mTHPC subcellular localization sites, it appears that ER/Golgi complex damage initiates a death signal for the mitochondrial apoptotic processes, while mitochondria are not

affected directly [75]. Thus, mTHPC acts in a more indirect manner compared to mitochondria-localizing PSs. Both necrosis and apoptosis effects are associated with the action of mTHPC, as well as autophagy [75].

Pharmacokinetic properties

The interaction of mTHPC with plasma is of relevance, as shown both in human and murine plasma *in vivo* [90] and might be responsible for the specific pharmacokinetic behavior of mTHPC. mTHPC displays unusual pharmacokinetics in human and rabbit plasma, with a secondary peak at about 10 h and 6 h after injection, respectively [101, 102]. These phenomena were explained by the initial retention of the PS in the liver or sensitizer aggregates in the vasculature, with subsequent disaggregation, binding to lipoproteins and mTHPC release from the depot. mTHPC has a small initial volume of distribution with important retention in the vasculature together with two peaks of PDT efficacy (2 and 24 h) in mice [103]. The early vascular response appears to be necessary for an efficient mTHPC-PDT response [104], as well as tumor cell accumulation. Indeed, a fractionated double injection (3 and 21 h prior to PDT) was superior to a single dose administration of the drug [105]. The absence of correlation between the mTHPC concentration in tumor and PDT efficiency was observed [106, 107, 105], while the plasma level correlated with the PDT effect in a mouse model [106].

Immune effects

Mouse models showed that mTHPC-PDT of solid tumors results in a strong and lasting induction of systemic neutrophils mediated by complement activation [108]. mTHPC-PDT also activates macrophage-like cells [109].

Side effects

Photosensitivity is a major concern for light-activated drugs. Studies have indicated that mTHPC results in less photosensitivity than Photofrin® [110]. Still, skin photosensitivity persists for up to 6 weeks (usually 2-3 weeks) post-administration [64]. Significant pain was noted to occur during the treatment [64]. Illumination itself must be precise, with a considerable effort required to block light from reaching normal tissues, as even reflected light is potent enough to generate a photodynamic reaction in healthy regions [64]. This indicates that mTHPC in the form of Foscan® is a highly active PS with a significant clinical efficacy, but is far less forgiving of inaccurate dosimetry and sunlight exposure than other PSs.

The side effects of mTHPC, as, indeed, of other PSs, clearly emphasize the need to improve the treatment protocols by decreasing the DLI, drug dose, and increasing selectivity of PS accumulation to reduce the damage to healthy tissues. Significant efforts to create efficient

2nd generation PSs have mostly been aimed at developing photosensitizing drugs that are chemically pure, absorb more strongly at longer wavelengths, with a high singlet oxygen yield, rather than placing a high priority on the development of improved biological properties. Most 2nd generation PSs (i) are hydrophobic drugs, which aggregate upon administration and show reduced efficacy, and/or make IV administration a difficult task [111, 112], (ii) possess a very low selectivity towards the tumor tissue due to poor bioavailability and unfavorable biodistribution, which leaves room for improvement. Thus, current efforts are aimed at the 3rd generation PSs, where additional biological criteria are included in the design principle, and which are expected to improve the pharmacological aspect and tumor selectivity. These drugs generally consist of 2nd generation PSs formulated into a drug delivery system.

2. DRUG DELIVERY SYSTEMS: AN OVERVIEW OF SYSTEMIC NANOCARRIERS

Many new potential therapeutics have poor pharmacokinetics and biopharmaceutical properties [113] such as low aqueous solubility, irritant properties, lack of stability, rapid metabolism and non-selective drug distribution. This leads to a number of adverse consequences, including the lack of or suboptimal therapeutic activity, dose-limiting side effects due to high organ toxicity, and a poor quality of patient's life [114]. Therefore, there is a need to develop suitable drug delivery systems (DDSs) that distribute the therapeutically active drug molecule. Significant efforts have been made toward this goal by developing nanoparticle DDS, having particle diameters of 100-200 nm or less [115].

2.1. A rational design of drug delivery systems and drug suitability

The design of an efficient DDS requires the knowledge of the drug physicochemical properties, specific intended therapeutic application of the drug and the characteristics of interaction of the DDS with the biological structures [116, 115, 117, 118]. One of the more important drug properties to consider is potency: the lower the maximal payload, the more potent the drug must be. If only a few drug molecules can be encapsulated into a particular DDS, drugs with high potencies are needed in order to deliver therapeutically relevant amounts of drug. The use of unreasonably high quantities of the carrier can lead to problems of carrier toxicity, metabolism and elimination, or biodegradability. Additional properties such as stability, solubility, size, molecular weight, and charge of the drug are also important, as they govern the means to entrap the drug into a DDS. The drug must also survive the process of incorporation into the DDS and not be degraded.

If the drug is already in clinical use, the advantages of a particular DDS shall be compared to a free drug. Besides, toxicity profile (not degree) of the free drug is generally similar to its DDS-entrapped form [116], thus facilitating the estimation of the side effects. Hence, in many cases the formulation of the already-approved drug into the DDS is more efficient than the development of entirely new drugs and their DDS formulation.

The mechanism of action of a drug also dictates its suitability for delivery in a particular DDS. If release from the DDS is required, a question arises as to whether the DDS leads to appropriate rates and levels of drug bioavailability. Bioavailability will depend on the release rate. Thus, the methods to measure drug release rates should also be integrated into the development of DDSs, not only the measurements of the total drug level (e.g., in plasma).

2.2. Advantages of drug delivery systems

Although final properties will depend on the particular design of the DDS, there are several general advantages of using a DDS for cancer therapy:

- DDSs can carry a large payload of drug molecules and protect them from degradation and increase drug water solubility. For example, a 110 nm liposome can contain approximately 10,000 mTHPC molecules [119]. Furthermore, drug payloads are generally located within the particle, and their type and number do not affect the pharmacokinetic properties and biodistribution of the nanoparticles (however, premature efflux of the drug outside the action site will change the overall pharmacological parameters of the system).

- The alteration of pharmacokinetics and biodistribution compared to a free drug is a particular strength of the DDS [120, 121]. Generally, with a DDS the drug clearance decreases (increasing plasma half-life), the volume of distribution decreases, and the area under the time-*vs.*-concentration curve increases [122]. For large DDSs (50-200 nm), the size of the carrier confines it mainly to the blood compartment, and the volume of distribution of the carrier associated drug will approach that of the plasma volume if the rate of release of the drug is low. Even with a rapid drug release, the improvement in solubility of the drug and reduction in drug toxicity may be seen [123]. Surface modifications of the DDS, such as PEGylation, may dramatically change the circulation time, as discussed in the next section. Surface characteristics contribute to the DDS solubility, aggregation tendency, ability to traverse biological barriers (such as the cell wall), biocompatibility, and targeting ability [136].

- Changes in the biodistribution of the DDS generally occur through a tumor-specific mechanism known as the enhanced permeability and retention (EPR) effect [124] of the tumor vasculature, also called passive targeting, which will be described in the next section. Alternatively, active targeting may be applied with a particular DDS, using DDS functionalization with molecular conjugates (e.g., conjugation of antibodies, aptamers, peptides, folic acid or transferrin to the DDS surface [125, 126]) to restrict drug delivery to specific sites of action [125]. Either of the mechanisms is intended to increase the drug concentration at the desired site of action, reduce systemic drug levels and toxicity [127, 128], and allow for lower effective drug dose [117].

- Delivery of more than one therapeutic substance within one nanoparticle is possible when using combination therapy [129, 130]. Additionally, visualization of sites of drug delivery by combining therapeutic agents with imaging modalities is available [130].

- The release kinetics of the drug from the DDS can be tuned to match the mechanism of action [129]. Moreover, triggered drug release is possible with either

endogenous or external stimuli [131-133]. Controlled release of loaded drugs from nanoparticles can maintain the therapeutic dose for an extended period of time and avoid the adverse effects induced by the high drug concentration in systemic circulation that are frequent in conventional formulations [128].

- Finally, nanocarriers composed of biocompatible materials are safe alternatives to existing vehicles, such as Cremophor®, that may cause severe adverse effects [139]. Biodegradability implies that the unloaded carrier is degraded or metabolized into nontoxic components and cleared from the circulation [127]. Thus, toxicities associated with the carrier molecules *per se* tend to be mild.

2.3. Types of drug delivery systems

Rapid advances in nanotechnology allowed for the incorporation of drugs into a variety of nano-DDSs with a size range from several nanometers up to several hundred nanometers. These agents have offered new exciting opportunities for detection, prevention and treatment of oncological diseases. The family of nanocarriers includes drug-polymer conjugates, polymeric nanoparticles, lipid-based carriers such as liposomes and micelles, dendrimers, protein-based nanoparticles, carbon nanotubes, and gold nanoshells (Fig. 4) [118, 115], as well as drug-antibody conjugates [140] and quantum dots [141]. Each of them is based on the unique properties of the structural components of the DDS, while accommodating the pharmaceutical agent. Examples of clinically approved DDSs, DDSs in clinical trials, as well as several DDSs studied *in vivo* are listed in Table 3.

Table 3. Examples of DDS and their clinical applications in cancer therapy.

Type of DDS (diameter, nm)	Entrapped drug	Stage of development	Disease	References
Drug-polymer conjugates (6-15)	Doxorubicin, Paclitaxel, Platinate	Phases I-III, <i>in vivo</i>	Various tumors	[118, 142]
Polymeric nanoparticles (50-200)	Doxorubicin, Paclitaxel, platinum-based drugs, Docetaxel	Phases I-III, <i>in vivo</i>	Adenocarcinoma, metastatic breast cancer, acute lymphoblastic leukemia	[143, 144]
Polymerosomes (100)	Doxorubicin, Paclitaxel	<i>In vivo</i>	-	[118]
Liposomes (85-100)	Lurtotecan, platinum-based drugs, anamycin	Phases I-III, <i>in vivo</i>	Solid tumors, renal cell carcinoma, mesothelioma, ovarian and acute lymphoblastic leukemia	[145]
Liposomes, PEGylated (100)	Doxorubicin	Approved	Metastatic ovarian cancer, ovarian cancer, refractory Kaposi's sarcoma	[118, 146]

Micelles (10-several hundred)	Doxorubicin	Phase I	Metastatic or recurrent solid tumors refractory to conventional chemotherapy	[118]
“	Paclitaxel	Phase I	Pancreatic, bile duct, gastric and colon cancers	[118]
Dendrimers (5)	Methotrexate, indometacin	<i>In vivo</i>		[139, 147]
Albumin-based particles (130)	Paclitaxel	Approved	Metastatic breast cancer	[118, 148]
Gold nanoshells (130)	No drug	<i>In vivo</i>	Photothermal therapy	[118]

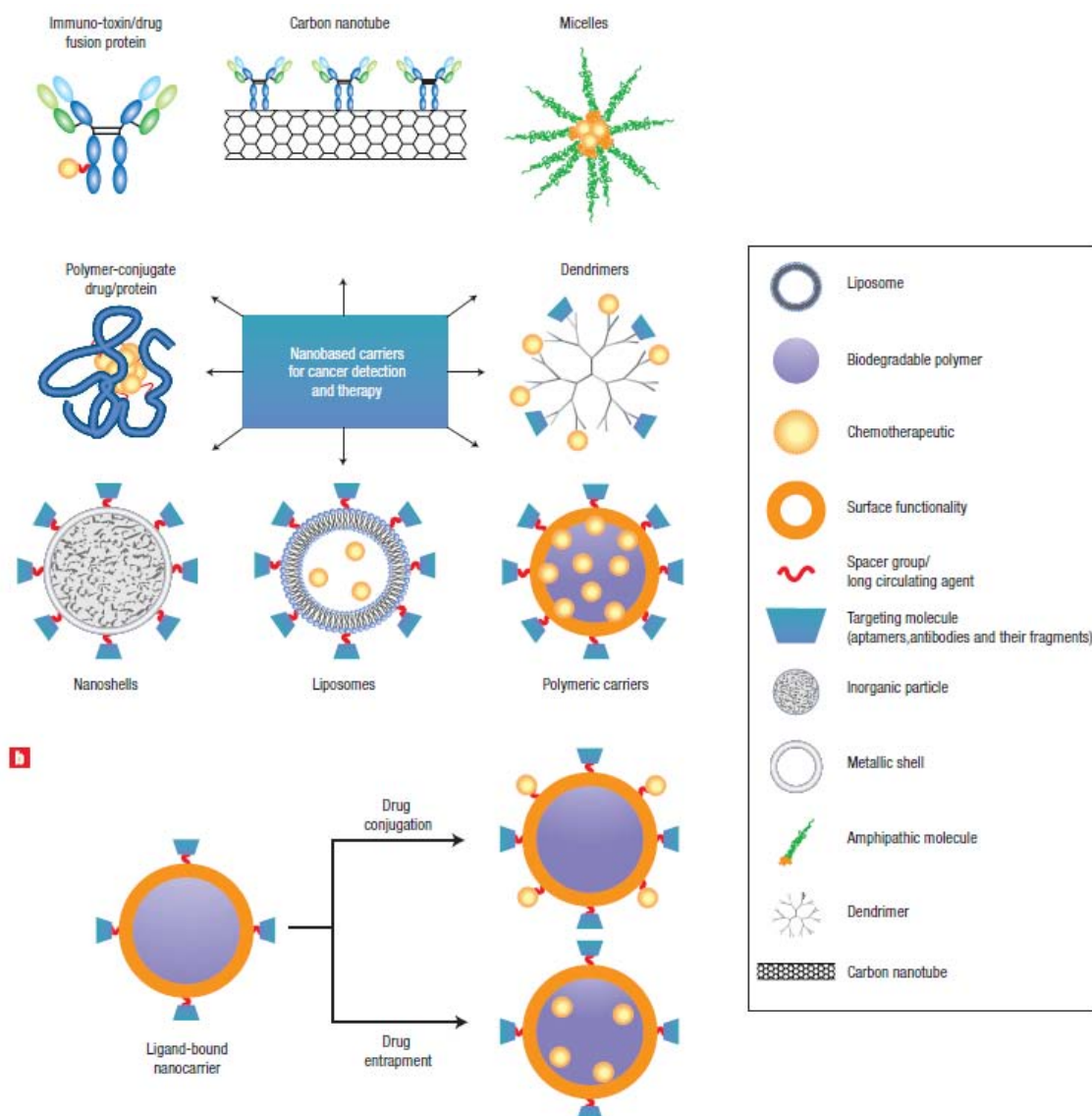


Figure 4. Schematic structures of DDS (from [118]).

Drug-polymer conjugates

Several polymer-drug conjugates have entered clinical trials [126]. They are especially useful for targeting blood vessels in tumors. Examples include anti-endothelial immunoconjugates, fusion proteins, and polymer-angiogenesis inhibitor conjugates [118].

Polymer-drug conjugates present pharmacokinetic profiles distinct from that of the free drug. Only four polymers – (N-(2-hydroxypropyl)methacrylamide copolymer, poly-*L*-glutamic acid, poly(ethylene glycol), and dextran – have been repeatedly used to develop polymer-drug conjugates [142, 118]. Apart from polymers, there are several ways to functionalize drugs (specifically, PS), including conjugation to saccharides, peptides and proteins, which leads to improved bioavailability and specificity [111].

Polymeric nanoparticles

Polymeric nanoparticles can be made from synthetic polymers, including poly(lactic acid) and poly(lactic co-glycolic acid) [149], or from natural polymers such as chitosan and collagen, and may be used to encapsulate drugs without chemical modification. Polymeric nanoparticles may have functional moieties intercalated into the backbone structure for active targeting [127]. The drugs can be released through surface or bulk erosion, by diffusion through the polymer matrix, or in response to the local environment. However, these particles are characterized by high polydispersity and inherent structural heterogeneity [118].

Micelles

Micelles can be considered amphiphilic colloids, having a particle diameter within the range of 10-100 nm. They consist of self-assembled lipid monolayers with a hydrophobic core and hydrophilic shell. Among drug carrier systems, micelles provide considerable advantages, since they can solubilize and increase the bioavailability of poorly soluble drugs, and offer long blood circulation [150, 151].

Dendrimers

Dendrimers are a unique class of repeated tree-like branched polymeric macromolecules with a nearly perfect 3D geometric pattern, formed of an apolar core and a polar shell. Polyamidoamine dendrimers [151] are promising for biomedical applications due to the ease of conjugation with drugs, high water solubility, biocompatibility and fast clearance due to their small size (~5 nm). The dendritic core can act as a reservoir encapsulating the drug molecules while the free functional groups can form complexes or conjugates with drug molecules or ligands [152]. An important application of dendrimers as a DDS is the transport of DNA drugs (genes or genes inhibitors) into the cell nucleus [153]. A disadvantage of dendrimers is that they require a complicated multi-step synthesis procedure.

Protein-based nanoparticles

Albumin, a plasma protein with a molecular weight of 66 kDa, has been extensively investigated as a drug carrier, with promising results [127]. It is soluble in both water and ethanol, non-toxic and well tolerated by the immune system, being the most abundant plasma protein. Albumin has favorable pharmacokinetics owing to its long half-life in plasma, making it attractive for passive targeting. An albumin nanoparticle-bound paclitaxel formulation was recently approved (Table 3)

Liposomes

Liposomes, spherical vesicles with a lipid bilayer membrane structure (formed by one or several concentric bilayers with an inner aqueous core), can encapsulate both hydrophilic and hydrophobic agents, protecting the cargo during the circulation in the body [155]. Liposomes, together with drug-polymer conjugates, have historically provided the foundation for DDS based on polymeric nanoparticles [126].

The focus of the following sections will be on liposomes as one of the most widely spread delivery systems

3. LIPOSOMES FOR ANTICANCER THERAPY

Liposomes, discovered by Alec Bangham in 1965 [156], are spherical self-closed structures formed by one or several concentric lipid bilayers with an aqueous phase inside and between the lipid bilayers (Fig. 5). Liposomes were suggested as drug carriers in cancer chemotherapy by Gregoriadis *et al.* [157] more than 35 years ago. Since then, the interest in liposomes has widely grown, and liposomal systems are currently being extensively studied as drug carriers.

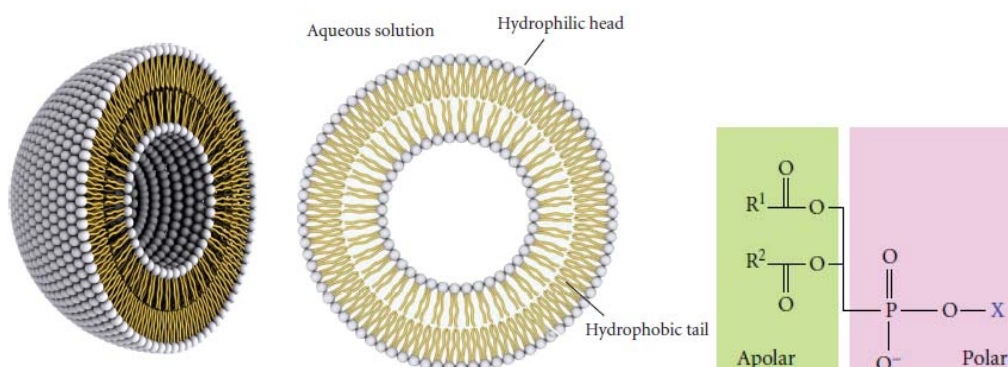


Figure 5. Steric and fundamental organization of a liposome with one lipid bilayer and the general structure of lipid (from [158]).

3.1. Liposome classification, structure and basic properties

Liposomes may be classified according to their size and lamellarity (number of lipid bilayers) [145, 159]:

- Multilamellar vesicles, consisting of multiple (5-25) bilayers, with a diameter from 500 to 5000 nm
- Oligolamellar vesicles, approximately 5 bilayers, diameter 100-1000 nm
- Giant unilamellar vesicles with a single bilayer and diameter > 1000 nm
- Large unilamellar vesicles, with a single bilayer and diameter from 200 to 800 nm
- Small unilamellar vesicles, with a single bilayer and diameter from 20 to 100-150 nm (these liposomes are currently most widely used for the delivery of macromolecules).

Other classifications distinguish the presence of a steric stabilizing agent like PEG on the liposomal surface (conventional and PEGylated liposomes), surface target-modifications (active- or passive-targeted liposomes [145]), and the preparation method [151].

Liposomes possess unique properties due to the amphiphilic character of the lipids composing the lipid bilayer, which make them suitable for drug delivery. Lipids used in the liposome preparation consist of charged or neutral polar headgroup and at least one hydrophobic hydrocarbon chain. Liposomes are mainly composed of phospholipids that have two

hydrophobic chains (Fig. 5). Two hydrocarbon chains are usually esterified to a glycerol backbone (glycerolipids), or they constitute the hydrophobic ceramide moiety (sphingolipids). This hydrophobic part is linked to a hydrophilic headgroup containing either a phosphate (phospholipids) or some carbohydrate units (glycolipids). Biologically relevant lipid headgroups are either zwitterionic (phosphatidylcholine, phosphatidylethanolamine, sphingomyelin), negatively charged (phosphatidic acid, phosphatidylglycerol, phosphatidylserine, phosphatidylinositol), positively charged or entirely uncharged (unsubstituted glycolipids). Saturated acyl chains typically vary in length from 10 carbons (lauryl), 12 (myristoyl), 14 (palmitoyl) to 16 (stearoyl), and the longer 18-carbon chains are usually unsaturated with one (oleoyl), two (linoleyl) or three (linolenyl) *cis*-double bonds [160]. Depending on their composition, liposomes can possess a positive, negative, or neutral surface charge.

A polar environment, such as water solution, promotes the spontaneous aggregation of lipid molecules and the formation of a variety of microstructures aiming to minimize the interactions between the hydrophobic chains and water molecules [161]. While single-chain lipids spontaneously assemble into micelles, two-chained lipids tend to be driven into bilayers.

The strong tendency of lipids to form membranes is due to their structural characteristics. Their polar heads promote aqueous interactions, while long nonpolar acyl chains prefer to interact with each other, stacking themselves side by side. The simplest formation serving both types of interactions is the formation of a lipid bilayer consisting of two lipid sheets [158]. The self-closing of a bilayer into a liposome is a competition between two effects, the bending or curvature energy and the edge energy of a bilayer [162]. Drug molecules, either hydrophobic or hydrophilic, can thus be encapsulated inside the lipid bilayer or inside the liposomal core, provided that they are present during the formation process.

The presence of negatively or positively charged lipids leads to a greater overall volume for aqueous entrapment and reduces the likelihood of aggregation after the preparation of the liposomes [163]. The physical stability of a liposome formulation is determined by its colloidal behavior and its ability to retain the cargo for long periods during storage.

The physical properties of lipid bilayer, such as permeability and fluidity, greatly influence the performance of liposomes *in vitro* and *in vivo*, and these properties can be specifically tailored by choosing different combinations of lipid mixtures [164]. One of the most significant properties of structurally-organized lipids is the effect of temperature on their mobility, known as the phase behavior of lipids. With increasing temperature, lipids pass from the ordered gel to a disordered liquid-crystalline phase, which greatly increases the molecular motions of the lipids (lateral diffusion and trans-gauche fluctuations) and fluidity of the bilayer. The encapsulated contents may thus permeate easier through the bilayer. Stability against

leakage may be promoted by using phospholipids that remain in the solid phase at physiological temperatures or by adding cholesterol [159].

Lipid bilayers in the fluid liquid-crystalline state readily accommodate hydrophobic drugs, whose solubility correlates with their octanol-water partition coefficients. In the gel state, on the other hand, hydrophobic compounds are less soluble in membranes and tend to be expelled to the surface, which will minimize the packing defects of the lipids [160].

3.2. Properties and behavior of liposomes as a drug delivery system

Liposomes possess attractive biological properties, including biocompatibility, biodegradability, protection of the host from any undesirable effects of the encapsulated drug, and the ability to entrap both hydrophilic and hydrophobic drugs. They generally do not provoke antigenic, pyrogenic, allergic or toxic reactions (however, some liposome-specific adverse effects such as various skin reactions, and hypersensitivity reactions, were reported [165]). Liposomes provide a unique opportunity to deliver pharmaceuticals into cells or even inside individual cellular compartments, since they present an interface to the biological milieu that is similar to the cell surface. Through the addition of agents to the lipid membrane or by the alteration of the surface chemistry, properties of lipid-based carriers, such as their size, charge, and surface functionality, can easily be modified [166].

Liposomes have been studied as carrier in anticancer therapy, with good results particularly in terms of efficacy, improvement of the therapeutic index, and higher intratumoral retention. The advantages of liposome-mediated drugs include greater solubility, longer circulation times, greater exposure, and focused delivery for the enclosed drug [167]. Historically, one of the first clinically approved liposomal drugs was the formulation of doxorubicin, a cytotoxic drug used for cancer chemotherapy. This formulation, branded Doxil®, was approved by the US FDA in 1995 for the treatment of Kaposi's sarcoma and later for other cancer types [168].

3.2.1. Effects of liposomal formulation on drug pharmacokinetics

It is important to understand liposome pharmacokinetics (PK) and drug pharmacodynamics in order to develop liposomal DDSs that can release drugs specifically in the tumor tissue with a release rate that matches the efficacy profile of the carried drug. PK changes influence the toxicity and efficacy of the liposome-delivered drugs [169]. Liposomal formulations can affect drug PK by a number of mechanisms, including decreased volume of distribution (and a shift in distribution in favor of diseased tissues with increased capillary permeability), delayed metabolism, and delayed clearance [170].

There are two major sources of factors that influence the PK of liposomal drugs. One source is host-associated factors like age, gender and physiological factors. The other source is liposome-associated factors, including the physicochemical properties of liposomes, such as size, surface charge, and membrane composition.

Particle size

When a liposomal drug is introduced into the body, the distribution mainly depends on its particle size. The general trend for liposomes of similar compositions is that increasing size leads to a more rapid uptake by the reticuloendothelial system (RES) [171]. Particles of > 250-300 nm in diameter exhibit shorter circulation times as compared to smaller particles, and seem to accumulate to a great extent in the spleen (exceeding 40% of the administered dose) [172, 173]. For drug delivery applications, liposomes of ~100 nm in diameter are most frequently used, this value being an empirical optimum between acceptable circulation times and an adequate encapsulation volume that is available for drug loading [174].

Surface charge

In general, uncharged liposomes have a slower clearance from the circulation than either positively or negatively charged liposomes [175]. The surface charge can also affect the biodistribution of liposomes. High concentrations of anionic lipids increase accumulation of liposomes in the liver and spleen [174, 176]. However, this relationship between the presence of charged lipids and circulation lifetimes is extremely complex and cannot be readily explained with simple models [174].

Lipid composition

The lipid composition has a major impact on the PK of liposomal drugs. First, it can affect the drug release rate, as the permeability of the drug through the lipid bilayer is controlled by the lipid composition. Second, the properties of the lipid bilayer are also controlled by the lipid composition. The bilayer fluidity has a considerable impact on the clearance of the liposome and thus of the associated drug by inhibiting the penetration and binding of serum proteins [177]. The presence of cholesterol in the liposome composition probably has one of the more important roles in maintaining bilayer stability and long circulation times *in vivo* [176].

Ligand conjugation

The conjugation of a specific targeting ligand to the surface of a liposome can affect its PK and biodistribution [175]. This so-called active targeting to cancer cells will be discussed in the sections below.

3.2.2. Liposomal clearance

The PK and biodistribution of liposome-encapsulated drugs are controlled by the interplay of two variables: the rate of plasma clearance of the liposome carrier, and the stability of the liposome-drug association in the circulation.

Unlike small-molecule drugs, which are cleared by enzymes and transporters in the liver and filtration and secretion in the kidneys, the clearance of IV-injected liposomes is governed by the mononuclear phagocyte system (MPS), or RES, which includes monocytes, macrophages, and dendritic cells located primarily in the liver and spleen [178]. In addition, depending on the size and composition of the liposomes, the parenchymal cells of the liver (hepatocytes) may also play a dominant role in the elimination of liposomes from the blood [179]. Clearance depends on the endothelial fenestral size [180].

The propensity for accumulation of liposomes in cells of the MPS is determined and mediated by specific proteins (opsonins) that are adsorbed *in vivo* to the particle surface [181], and can be influenced through modification of surface characteristics [182]. The process of protein adsorption, known as opsonization, begins immediately after the liposomes contact with plasma. The exact nature of the types and quantities of proteins, and their conformations, govern the reaction. Immunoglobulins (IgA, IgG) and complement proteins are the predominant contributors to the recognition of foreign particles by the cells of the RES [183]. A schematic illustration of the opsonins-mediated liposome uptake by liver macrophages and hepatocytes, implying specific protein-receptor interaction on the surface of cells, is provided in Fig. 6. Uptake by the MPS usually results in the irreversible sequestering of the encapsulated drug in the MPS, where it can be degraded. Moreover, the capture of the liposomes by the MPS can result in acute impairment of the MPS and toxicity.

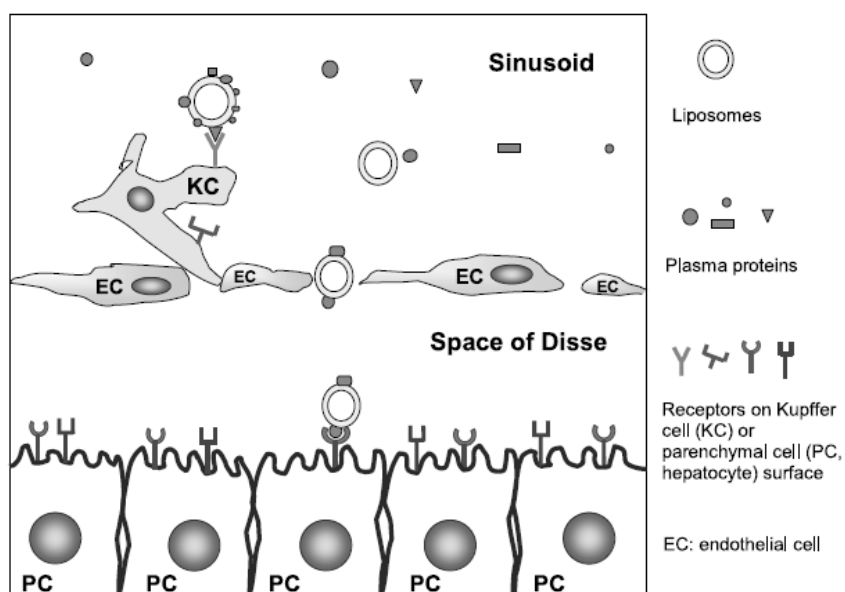


Figure 6. Opsonin-mediated liposome uptake by Kupffer cells and hepatocytes (from [184]).

The administered dose can also play a significant role in the circulation lifetime of a carrier. Conventional liposomes are removed from the circulation in a dose-dependent manner, indicating the saturation of the mechanisms responsible for their uptake [171, 185]. Circulation lifetimes typically increase as a function of the increasing liposomal dose. This effect is likely due to a decreased phagocytic capacity of RES macrophages after the ingestion of high lipid doses, or to the saturation of plasma factors that bind to circulating liposomes and cause their opsonization [185]. Alternatively, liposomes have been shown to bind serum proteins in a manner inversely proportional to their blood clearance rates [186], giving rise to the hypothesis that the depletion of plasma opsonins at high lipid doses results in an increase in blood circulation half-lives [187]. Liposomes that bind more than 50 g of proteins/mol lipid were shown to be cleared from the circulation in less than 2 min, while liposomes with less than 20 g protein/mol lipid binding had circulation times of more than 2 h [186]. With the increase in the surface charge of liposomes (either positive or negative) as well as the size of vesicles, interactions with the RES increase and lead to greater clearance of the particles [129].

Current methods for addressing the negative attributes associated with opsonization have focused on slowing the process by rendering the liposome surface more hydrophilic or by neutralizing the surface charge. The predominant strategy has been to adsorb or graft a hydrophilic polymeric coating, such as PEG, to the surface of the particle [188]. However, the PEG effect may be transient, so eventual opsonization and macrophage clearance still occurs.

3.2.3. Liposome destruction in circulation

Upon entering the blood circulation via IV injection, the complex interactions between liposomes and serum proteins begin. There are three major types of liposome-protein interactions that play a critical role in liposomal clearance as well as drug release *in vivo*: (1) serum protein surface binding to the liposome with limited effect on the phase transition temperature of the bilayer, (2) serum protein surface binding to the liposome followed by penetration across its bilayer with a decrease in the phase transition temperature and alteration in the bilayer permeability properties, and (3) serum protein insertion of its proteolipid into the phospholipid bilayer of the liposome with limited effect on the phase transition temperature but with an increase in the phospholipid bilayer permeability [189]. Protein binding can lead to liposome disintegration and release of the encapsulated drug into the blood stream.

The question of liposomal disintegration has been widely addressed both *in vivo* and *in vitro*. The release of lipids from the liposomes has a highly destructive influence on the liposomal structure [190]. A molecular mechanism of phospholipids transfer is envisioned as the phospholipids-apolipoprotein substitution in HDL particles, together with the incorporation of

additional phospholipids molecules in HDL without apolipoprotein loss [193]. Serum apolipoproteins (A1 and E) are the most potent liposome-disrupting agents, however, various serum proteins, including complement components [194], may interact with lipid vesicles. LDL was shown to transfer lipid from vesicles [195]. The phospholipid transfer protein facilitates transfer to HDL [196] by desorbing phospholipids molecules from the liposome surface [197].

Liposome stability in plasma was shown to depend on the relative concentrations, liposome size, lamellarity, charge and fluidity, and incubation temperature [198]. Improved plasma stability of liposomes has been found to correlate with increased delivery to tumors [199].

3.2.4. Drug release from liposomal formulation

Successful delivery to the target organ requires stable retention of the drug by the carrier while in circulation. The rate of *in vivo* drug release is an extremely important parameter because it can influence the rate of clearance of the drug from the general circulation, the bioavailability, and thus the activity of the drug at its site of action, the targetability of the drug, and the observed toxicities [174, 2]. After the drug is released from the carrier, the PK disposition of the drug will follow the PK of the non-liposomal form of the drug.

The rate of leakage or efflux of drug from liposomes should be lower than the rate of liposome clearance from the blood, otherwise there will be little gain in drug targeting from prolonged liposome circulation time. For drugs which are very slowly released from liposomes (compared to liposome destruction rate), their PK will be very similar to that of the liposomes themselves and will be characterized by a low volume of distribution (approximately the plasma volume), a slow rate of clearance and a low tendency for distribution into normal tissues with the exception of the MPS. For drugs with intermediate rates of release, the kinetics will be a combination of the pharmacokinetics of the free drug and that of the carrier [116]. Ideally, drug leakage should be kept to a minimum while the liposomes are in circulation, but after extravasation in the tumor tissue the liposome contents should be released and made bioavailable. In a study by Charrois and Allen [200] three PEGylated liposomal doxorubicin formulations with different drug release rates were compared for antitumor efficiency. The best therapeutic response, as well as the highest drug accumulation, was obtained for the formulation with the slowest release rate.

The release of the drug at the target site is an important step, because generally only the released drug is active. In most instances a compromise has to be worked out, enabling a reasonable stability in the circulation and an effective drug release at the target. The drug release will mostly depend on the rate of drug efflux from liposomes, and the rate of liposome

breakdown. Drug release at the target site may proceed by different mechanisms, including diffusion, pH-influenced release, release by tumor specific enzymes, release by phospholipase A₂, release by matrix metalloproteinases or oxidizing agents [201], as well as with the help of external stimuli, such as heat, light or ultrasound [202]. For example, local hyperthermia of tumor was applied to dramatically increase the release of doxorubicin from liposomes, showing high antitumor efficacy of the developed liposomal form of the drug, ThermoDox [203].

Since hydrophobic compounds are readily accommodated in the fluid hydrocarbon region of the bilayer, liposomes might be intuitively considered to be excellent carriers for the lipophilic cargo. However, it has been noted that hydrophobic solutes are often rapidly (within minutes) depleted from their carriers by exchange mechanisms, leading to their equilibration amongst all other lipidic structures in the circulation (lipoproteins, erythrocyte membranes, etc.) [204]. Drug release from liposomes was shown to depend on the size and multilamellarity of the liposomes, being faster in unilamellar liposomes than in multilamellar ones. The release can be dependent on the kind of drug: the release of cations is slower than that of anions [156], the same applies to small molecules as opposed to macromolecules.

The ability to control drug release rates, combined with the ability to protect associated drugs from degradation, allows properly formulated liposomes to function as sustained release systems, continually releasing their store of drugs over several hours to several days. The properties affected by rapid or sustained drug release from liposomal formulation are summarized in Table 5.

Table 4. Properties of rapid release and sustained release lipidic DDS (from [2])

Property	Rapid release formulations	Sustained release formulations
Structure	may be liposome, micelle, complex or aggregate	normally liposome
Function of lipid	excipient	Carrier
Drug solubility	low (hydrophobic)	- high - if the drug is weak acid or weak base, solubility may be low, with the drug remotely loaded into the liposome aqueous interior
Effect on PK and PD of the drug relative to the free drug	little or none	- proportional to drug release rate - the drug is biologically inactive as long as it is entrapped in liposomes - the drug is protected from metabolism and degradation while entrapped in liposomes - for drugs that are well retained by the carrier, the PK of the drug approaches the PK of the carrier

Effect on the therapeutic outcome compared to the free drug	little or none	- complex relationship depending on the physical properties of the drug and the carrier - increases in the therapeutic effect are often seen
Alterations in toxicity profile compared to traditional excipients	substantial reductions in toxicity may occur	N/A
Alterations in side effects of the drug compared to the free drug	little or none	- side effects are often reduced compared to the free drug - new side effects may appear that are similar to those seen for the free drug given by infusion

3.2.5. Liposome-cell interaction

Anticancer drugs displaying a poor cancer cell uptake in their free form are not suitable for extracellular release, and have to be taken up in the liposomal form by various endocytosis mechanisms, and subsequently released inside the cancer cells [201]. Generally, the interactions of liposomes with cells are categorized into five types:

(1) adsorption, or binding of liposomes to cells specifically or nonspecifically, where the lipid bilayer of the carrier is degraded by factors like enzymes, lipases, or mechanical strain, which usually takes long. That may result in the liberation of the drug to the extracellular fluid, where it can be diffused towards the cytoplasm;

(2) fusion of the adsorbed or bound liposomes with the cell membrane, causing the liberation of the entire liposomal content directly into the cytoplasm;

(3) exchange of lipid components and the drug content of liposomes with the cell membrane directly or through the mediation of transfer proteins, including the transfer of a usually lipophilic active ingredient from the liposomes to the plasma lipoproteins;

(4) specific or nonspecific endocytosis of liposomes [145];

(5) phagocytosis, accomplished by specific cells of the immune system, such as monocytes, macrophages, and Kupffer cells.

The internalization pathways of intact nanocarriers are summarized in Fig. 7. Phagocytosis is an actin-based mechanism occurring primarily in specific phagocytes, and is closely associated with opsonization. Clathrin-mediated endocytosis is a widely shared pathway of nanoparticle internalization, associated with the formation of a clathrin lattice and depending on the GTPase dynamin. Caveolae-mediated endocytosis occurs in typical flask-shaped invaginations of the membrane coated with caveolin dimers, also depending on dynamin. Macropinocytosis is an actin-based pathway, engulfing nanoparticles and the extracellular milieu with a poor selectivity. Other endocytosis pathways can be involved in the nanoparticle internalization, independent of both clathrin and caveolae [205].

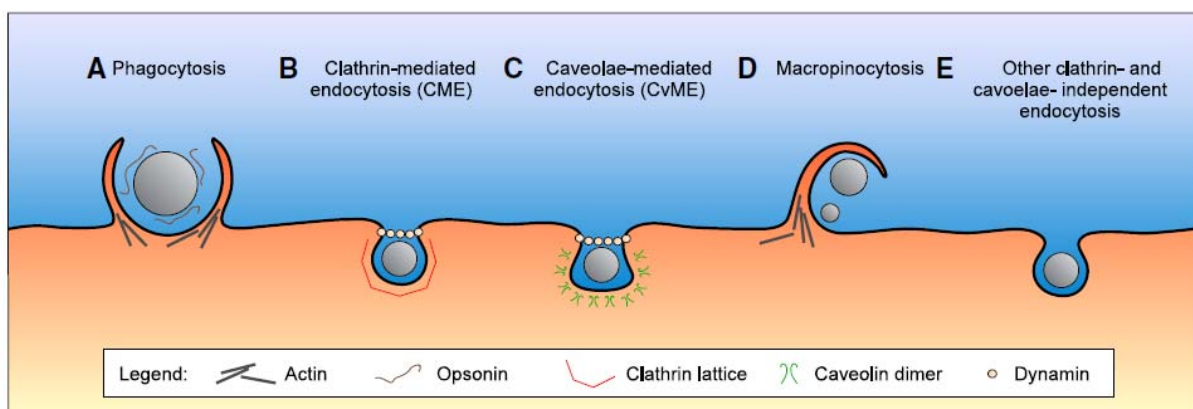


Figure 7. Principal nanocarrier internalization pathways in cells (from [205]).

3.2.6. Long-circulating liposomes

The rapid elimination of liposomes from the blood circulation by means of opsonization and sequestration by RES (usually within 15-30 min) [206], along with their predominant uptake by the liver and spleen, hindered early attempts to deliver liposomal drugs to tissues outside the MPS. Effective anti-cancer liposomal drug carriers have to be long-circulating to maintain the required level of a pharmaceutical agent in the blood for an extended time interval [167]. This allows long-circulating liposomes to slowly accumulate in pathological primary tumor sites [124] and improve or enhance drug delivery in those areas [207].

In the late 1980s, liposomes possessing long-circulating properties in mice were developed through incorporation of glycolipids (monosialoganglioside GM1) [208]. However, in rats these liposomes failed to display long-circulating properties [209]. Subsequent studies have led to the development of a second generation of long-circulating liposomes carrying surface-grafted hydrophilic polymers, principally PEG coupled to phosphatidylethanolamine [210]. The grafting of PEG to the surface of a liposome (PEGylation) has been clearly shown to extend the circulation lifetime of the DDS [211] in all mammalian species investigated, including mice, rats, dogs, and humans [211, 184, 212]. Circulation times of conventional liposomes (typically minutes) have been increased this way up to many hours [160]: in mice and rats, half-lives of as long as 20 h can be attained [213] whereas in humans, half-lives of even up to 45 h have been reported [214]. Under non-pathological conditions, the PEG-liposomes are ultimately uptaken, as conventional liposomes, by the cells of the MPS in the liver and spleen.

PEG is a neutral, crystalline, thermoplastic linear polyether diol. Its ability to fulfill the role of circulation-prolonging agent has been mostly attributed to its properties [215, 167] which include good biocompatibility (absence of toxicity, low stimulation of the immune system, lack of accumulation in the RES cells), a very high solubility both in aqueous and organic solutions, a large excluded volume and a high degree of conformational entropy [216]. The unique high degree of water solubility of PEG is believed to be due to its good structural fit with water [217].

PEG polymeric chains are flexible and have been noted to extend approximately 5 nm (for PEG-2000) from the liposomal surface [158], although this value may be variable depending on PEG packing density. From the practical perspective, PEG is commercially available in a variety of molecular weights. PEGs that are used for the modification of drug and drug carriers have a molecular weight from 350 to 20000 Da [167].

The behavior of PEGylated liposomes depends on the characteristics and properties of the specific PEG linked to the surface. Fig. 8 represents the PEG conformation regimens that depend on the graft density, when the polymer is attached to the liposome surface [218]. The molecular mass of the polymer, as well as the graft density, determine the degree of surface coverage and the distance between graft sites. If the PEG grafting density is low, the polymer is said to be in the mushroom regimen. When the graft density is high, the polymers are said to be in the brush regimen [211]. Generally, the flexibility of the PEG structure allows a relatively small number of surface-grafted polymer molecules to create an impermeable layer over the liposome surface. Optimum stabilization is typically achieved with 5-10% PEG-phosphatidylethanolamine with a molecular mass in the range of 1000-2000 Da. At lower concentrations the polymer chain configuration changes from an optimal extended brush- to a mushroom-regimen, in order that the surface remains fully covered, but rendering less steric protection [160].

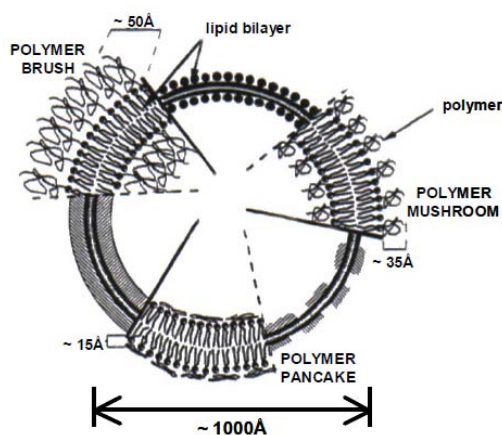


Figure 8. Schematic diagram of PEG configuration regimens (mushroom, brush and pancake) for the polymer grafted to the surface of the lipid bilayer (from [219]).

In liposomes composed of phospholipids and cholesterol, the ability of PEG to increase the circulation lifetime of the vehicles has been found to depend on both the amount of grafted PEG and the length or molecular weight of the polymer [178]. In most cases, the longer-chain PEGs have produced the greatest improvements in the blood residence time. It was reported [178] that blood levels were higher for liposomes with longer PEG (PEG-1900 and PEG-5000) than for liposomes containing PEG-lipid with a shorter chain PEG (PEG-750 and PEG-120).

The most widely held belief regarding the mechanism of increased circulation time is that PEG grafted to the liposome surface creates a steric barrier (protective layer) that prevents the

adsorption of opsonins to the liposome surface (Fig. 9) [167, 201]. However, a conclusive link has not been established between the chemical and physical properties of PEG and its ability to extend the circulation lifetime. The notion that PEG increases the circulation time by decreasing protein binding is supported by both *in vitro* studies that have demonstrated a screening effect of PEG against protein adsorption to liposome surfaces [220], and some *in vivo* studies where low protein binding in the bloodstream has been correlated with longer circulation times [221].

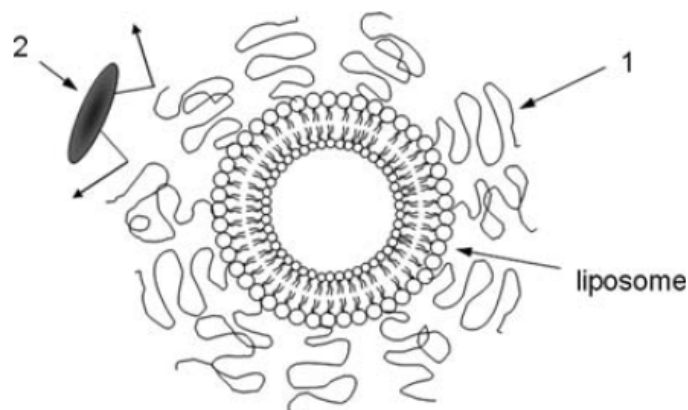


Figure 9. Mechanism of steric protection by PEG. PEG chains (1) prevent opsonins (2) from being absorbed on the liposome surface (from [167]).

By contrast, results from other studies have shown that the presence of bound serum proteins did not result in increased macrophage uptake, and that pre-incubating the PEG-liposomes with serum actually lowered the macrophage uptake [222]. The alternative explanation for the ability of PEG to extend the blood circulation time of liposomes is that, rather than minimizing the adsorption of all serum proteins, certain serum proteins adsorb to the liposome surface despite the PEG coating, and subsequently act as nonspecific dysopsonins that, along with the PEG polymers, prevent the adsorption of opsonin proteins and mask the liposome. Besides, other studies have shown that the steric barrier provided by PEG prevents aggregation of liposomes into larger structures while in the circulation, and thus enhances their stability *in vivo* [223]. This reduces MPS uptake, which is known to increase with increasing carrier size.

It has been demonstrated that, because of their long-circulation properties, PEG-liposomes have a relatively high probability to extravasate and accumulate at sites that are characterized by increased vascular permeability. This passive targeting of tumors will be discussed in the following section.

It is noteworthy that a general drawback of PEGylated liposomes is their reduced ability to approach the target membrane and undergo fusion [160]. To circumvent this limitation, various liposome formulations have been designed to shed their PEG coat. After PEG-liposomes accumulation at the target site, the PEG coating is detached under the influence of local pathological conditions (decreased pH in tumors). Detachable PEG conjugates have been

described, in which the detachment process is based on the mild thiolysis of the dithiobenzylurethane linkage between PEG and an amino-containing substrate [145].

3.2.7. Tumor targeting of liposomes

An important question concerning the liposomal DDS is whether it may lead to appropriate rates and levels of drug bioavailability. For optimal efficacy, a drug must reach tumors in amounts sufficient to kill cancer cells but at the same time should not have adverse effects in normal tissues.

The advantages of drug targeting include simplified drug administration protocols, reduced drug quantity required to achieve a therapeutic effect, and a possible decrease in the cost of therapy [167]. Targeting has been achieved using two predominant strategies that rely on either passive or active modes of action (Fig. 10). The first approach exploits the characteristic features of the tumor, and is based on spontaneous penetration of liposomes into the interstitium through the leaky tumor vasculature. This is considered to be passive targeting [224]. The second targeting mechanism is based on attaching specific ligands to the surface of liposomes, such as antibodies, that bind to overexpressed antigens or receptors on the target cells. This approach corresponds to the active targeting strategy [225].

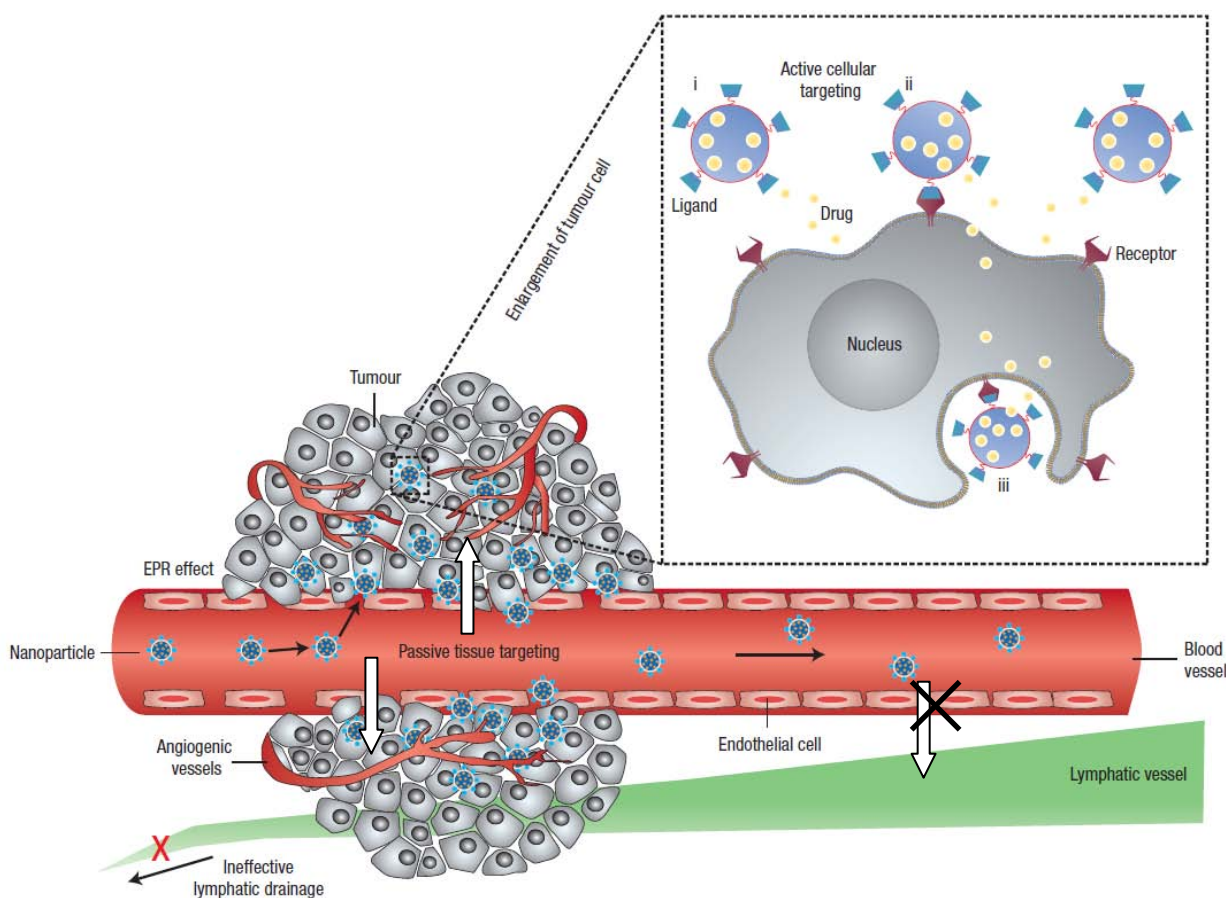


Figure 10. Schematic representation of passive and active mechanisms of liposomal drug accumulation in tumor (from [118]).

3.2.7.1. *Passive targeting*

Delivery of therapeutic agents differs dramatically between tumor and normal tissues because of physiological differences in their structure. Whereas free drugs may diffuse nonspecifically, a nanocarrier can extravasate into the tumor tissues via the leaky vessels and be retained there by the enhanced permeability and retention (EPR) effect [226, 227], first described in 1986 [228].

Unlike normal vessels, the tumor vasculature lacks an orderly branching hierarchy from the larger into successively smaller vessels that feed a regularly spaced capillary bed [116]. Instead, the tumor vessels are heterogeneous in their spatial distribution, dilated and tortuous, leaving avascular spaces of various sizes. In addition, the vessel-wall structure is abnormal, with wide interendothelial junctions, large number of fenestrae, and large maximum pore diameters [129]. The pore size ranges from 200 nm to 1.2 μm and varies with both the tumor type and tumor location. Most of the tumor models have a pore size between 380 and 780 nm [201]. The pore sizes in the solid tumor vasculature are much larger than the junctions in the normal tissue where the gaps are less than 6 nm [229]. The threshold liposome diameter for extravasation into tumors is ~ 400 nm, but several studies have shown that particles with diameters < 200 nm are more effective [230].

The normal lymphatic network drains excess fluid from the tissue in order to maintain the tissue interstitial fluid balance. In the tumor tissue, the proliferating cancer cells compress lymphatic vessels, particularly at the center of the tumor, causing their collapse [231]. Therefore, functional lymphatic vessels exist only in the tumor periphery. The lack of functional lymphatic vessels and the vascular hyperpermeability inside the tumors result in interstitial hypertension. The uniformly elevated interstitial fluid pressure reduces convective transport, while the dense extracellular matrix hinders nanoparticle diffusion [129]. The inefficient drainage of fluid from the tumor allows the retention of liposomes and release of incorporated drugs into the vicinity of the tumor cells [118]. Local tumor drug concentrations are up to 10-fold or higher when liposomes are administered when compared to free drug [116].

Vascular permeability in tumors is heterogeneous with respect to the tumor type and microenvironment. The permeability in tumor models depends on the transplantation site and varies with time and in response to treatment [129]. It was observed that the EPR effect is present in tumors of more than ~ 100 mm^3 in volume, which hinders its use for targeting small or unvascularized metastases [232]. The EPR effect is a progressive phenomenon that requires many passages of nanoparticles through the tumor vasculature to achieve a substantial tumor accumulation. For this reason, long-circulating liposomes are most suitable for passive-targeted drug delivery, as conventional liposomes cannot show sufficient liposomal drug accumulation

levels [201]. The drug should reside in the carrier until the accumulation by EPR has occurred, otherwise the effect of the liposomal system will be but small.

3.2.7.2. Active targeting

Although the passive targeting approach forms the basis of clinical therapy, it suffers from several limitations, such as inability to ubiquitously target cells within a tumor, lack of process control, and even the absence or heterogeneity of the EPR effect [118]. A possible way to overcome these limitations is to program the nanocarriers to actively bind to specific cells after extravasation. This binding may be achieved by attaching targeting agents such as ligands to the surface of the nanocarrier. The DDS will recognize and bind to target cells through ligand-receptor interactions. It is imperative that the agent binds with high selectivity to molecules that are overexpressed on the surface of rapidly dividing cancer cells [118]. For example, because of the high metabolic demands due to rapid proliferation, many types of cancer cells overexpress transferrin and folate receptors, which makes conjugation of transferrin, folic acid or antibodies to these receptors to liposome surface a successful targeting approach [233]. However, because these receptors are expressed to some degree on many types of non-target cells, toxic off-target effects are not totally eliminated [126]. Moreover, for solid tumors, there is evidence that high binding affinity of targeted liposomes can reduce penetration of nanocarriers due to a binding-site barrier, where the nanocarrier binds to its target so strongly that penetration into the tissue is prevented [118].

Recent work comparing non-targeted and targeted lipid-based DDSs has shown that the primary role of the targeting ligands is to enhance cellular uptake into cancer cells rather than increase the accumulation in the tumor. This behavior suggests that the colloidal properties of liposomes will determine their biodistribution, whereas the targeting ligand serves to increase the intracellular uptake in the target tumor [125]. Active targeting may be crucial in some cases, such as transport across specific barriers like the blood-brain barrier [234].

Targeting agents can be broadly classified as proteins (mainly antibodies and their fragments), nucleic acids (aptamers), or other receptor ligands (peptides, vitamins, and carbohydrates) [118, 126].

The current development of liposomal carriers often involves an attempt to combine the properties of long-circulating liposomes and targeted liposomes in one preparation [235]. To achieve better selectivity of PEG-coated liposomes, it is advantageous to attach the targeting ligand via a PEG spacer arm, so that the ligand extends outside of the dense PEG brush, excluding steric hindrances for the ligand binding to the target. Generally, the active-targeting strategy is very difficult to fulfill, partially due to the lack of specific receptors for cancer cells,

synthesis complications, and sometimes the lack of expected improvement of the therapeutic index compared to non-targeted DDSs [236].

4. LIPOSOMES FOR PHOTODYNAMIC THERAPY OF CANCER

Most photosensitizers that are in clinical use or preclinical development are hydrophobic and tend to aggregate in an aqueous environment, while the monomer state is required to maintain their photophysical, chemical, and biological properties for efficient PDT [74, 237]. This limits their delivery and photosensitizing efficiency [238, 239]. Additionally, an insufficient affinity of most PSs to tumor sites also results in some damage to the normal tissue following PDT in patients [20].

To resolve these issues and avoid potential side effects, drug formulations for PSs are required to achieve greater solubility and selective delivery to tumor sites. During the continuous search for improving the efficacy and safety of PDT, liposomes with their high loading capacity and flexibility to accommodate PSs with variable physicochemical properties came into focus as a valuable DDS. Liposomes have the ability to encapsulate the hydrophobic PS molecules and avoid aggregation in an aqueous environment, thus increasing the PS photoactive portion [240, 241]. As it turned out, the PDT efficacy and safety of various PSs can be substantially improved by using liposomal formulations [242-244].

4.1. Photophysical properties and localization of photosensitizers in liposomes

The photophysical properties of porphyrins as typical PSs strongly depend on their aggregation state: for large self-associated supramolecular structures, the porphyrin absorption coefficient decreases, the Soret band is shifted and the fluorescence yields and lifetimes become very low [112, 245]. Aggregation, moreover, reduces the yield and the lifetime of the porphyrin triplet state, thus reducing their ability to generate reactive oxygen species efficiently [112, 67]. Two modes of porphyrin aggregation are described in literature: face-to-face aggregation (H-aggregates) and edge-to-edge interaction (J-aggregates) [246], but only monomeric species and possibly planar aggregates, observed in liposomal and mitochondrial membranes, are endowed with a significant photosensitizing ability [112, 245].

Formulation of hydrophobic PSs into liposomes maintains them in the monomeric state for the efficient production of singlet oxygen. For instance, the formulation of the hydrophobic photosensitizer hypocrellin A in egg phosphatidylcholine liposomes induced almost complete monomerization of the aggregated species, as compared to a suspension of the PS in dimethyl sulphoxide-solubilized saline [247]. Also, monomerization was demonstrated for azaphthalocyanines loaded into dioleoylphosphatidylcholine liposomes [248]. The lipid bilayer

of liposomes can prevent aggregation between monomeric molecules for purified porphyrins, Zn(II)-phthalocyanine, pyropheophorbide-a methyl ester and mTHPC [249].

Generally, after incorporation of the PS into liposomes, the corresponding absorption and fluorescence emission bands are usually red-shifted, and fluorescence intensity and fluorescence anisotropy are increased [112, 250, 251]. Hematoporphyrin and deuteroporphyrin exhibit a red shift of the absorption and emission maxima of about 10-20 nm after incorporation into a liposomal matrix [250]. Incorporation of a porphyrin PS into the lipid bilayer affects the conformational dynamics of the molecule in the ground and excited singlet states. These changes influence the Stokes shift [252]. Interactions between PS molecules in the lipid bilayer can contribute to specific photochemical and photophysical photosensitizer properties, including concentration-dependent fluorescence quenching, previously reported for liposome-embedded benzoporphyrin derivative mono-acid ring A (BPD-MA, verteporfin) [253].

4.1.1. Localization of photosensitizers in liposomes

The amphiphilic PS molecules are assumed to remain more or less parallel to the hydrocarbon chains. By varying the lengths of hydrocarbon chains between the tetrapyrrole ring and the carboxylate groups of modified porphyrins, it was shown that the hydrophobic part of the molecule tends toward a deeper position in the bilayer [254, 255]. Bronshtein *et al.* used iodide fluorescence quenching and the parallax method to demonstrate that the vertical localization of a PS in a lipid membrane can be modulated by inserting spacer moieties into the molecular structure, while anchoring one end of the molecule at the lipid/water interface [255]. The depth of the porphyrin core insertion into the membrane is not affected by the temperature when the membrane is in the liquid phase. However, changing to the solid phase by lowering the temperature expels the PS toward the water interface.

This tendency was argued to be valid for any hydrophobic PS [256]. Moreover, a model of hydrophobic porphyrin distribution into lipid bilayer was proposed, where the drug is located within the membrane at two distinguishable sites. One site is between the two lipid layers, and the other site is along the hydrocarbon chains [256].

4.1.2. Singlet oxygen generation by liposomal photosensitizers

Several studies have demonstrated a direct correlation between the location depth and photosensitizing activity [254, 255], and PSs incorporated deeper in the membrane were found to be more efficient. In a study comparing three PSs, mTHPC, chlorin e6 and sulfonated tetraphenylchlorin, the efficacy of singlet oxygen generation correlated with the relative position of the PS within the lipid bilayer, tetraphenylchlorin and chlorin e6 being anchored by their negative chains nearer to the water-lipid interface compared to deep-located mTHPC [257].

mTHPC showed the highest efficacy, while chlorin e6 – the lowest. At the same time, in ethanol solution, the apparent quantum yield was the same for the three chlorins. It has been pointed out that singlet oxygen can diffuse rapidly out of membranes and reach the aqueous medium, where its lifetime is considerably shortened. Accordingly, the deeper the PS was inserted into the hydrophobic core of the lipid bilayer, the longer the path of singlet oxygen diffusion in the membrane and the greater the photodamage to the lipidic structure [257].

The production of singlet oxygen by a liposome-bound sensitizer is controlled by many factors, often acting against each other. An increase in the quantum yield of singlet oxygen formation in the presence of liposomes can be attributed to the monomerization effect of the vesicles. A study has shown that the incorporation of bacteriochlorin-a in dimyristoylphosphatidylcholine liposomes increased oxygen consumption 9-fold compared to the value in the phosphate buffer, solely by promoting the monomerization of the photosensitizer [241]. Usually, a decrease in the quantum yield of singlet oxygen formation can be ascribed to aggregation occurring in liposomes due to the concentration effect [252]. The local concentration of the sensitizer inside a vesicle is larger, by several orders of magnitude, than in a solvent. High local concentrations can even lead to a structurally controlled aggregation process in liposomal bilayers [258]. The structure of a porphyrin, the local microenvironment, including the solvent used and the dye concentration, will determine the contribution from monomers, dimers, and higher order aggregates to the net spectroscopic properties.

4.2. Liposomal photosensitizers in biological systems

4.2.1 Phototoxicity of liposomal photosensitizers *in vitro*

The incorporation of PS molecules in liposomes was previously reported to significantly enhance their phototoxicity [259, 260]. Damoiseau *et al.* in *in vitro* studies on WiDr cells found a four-fold improvement of PDT when bacteriochlorin-a was encapsulated in dimyristoylphosphatidylcholine liposomes [241]. The sulfonated aluminum phthalocyanine PS, loaded into the liposomes, was found to be substantially more phototoxic to KB cells than the free PS [261]. Liposome-bound Hp accumulated in the cells in an amount twice as large as the water-dissolved Hp, resulting in a more efficient photosensitization [262]. Liposomal formulations may, at least *in vitro*, alter the subcellular distribution of a PS. Liposomal Hp appeared to induce early and extensive endocyttoplasmic damage, leading to the swelling of mitochondria and vesiculation, while the water-dissolved Hp predominantly photosensitized the plasma membrane. The different patterns of cell photodamage reflect a different subcellular distribution of the photosensitizing compounds [262].

As mentioned in the previous section, long-circulating liposomes, with their hydrophilic interface, do not interact effectively with cells. This is critical since the cytotoxic singlet oxygen generated by the irradiated PS shows an extremely short migration radius. Gijssens *et al.* demonstrated that sterically stabilized liposomes containing hydrophilic sulfonated aluminum phthalocyanine did not display any *in vitro* phototoxicity on malignant cells, while the free compound did [263]. It was concluded that the liposomal PS was not phototoxic because it was retained tightly in the liposomal formulation, and since the liposomes did not display any interaction with the cells, the PS was denied cellular access. This underlines the requirement for the PS to be released from liposomes as one of the modes of PDT action, if the liposomes are not uptaken by the cells efficiently.

4.2.2 Photodynamic therapy with liposomal photosensitizers *in vivo*

A release of the PS from the liposomes, as well as the disintegration of liposomes during the circulation, leads to association of the drug with plasma proteins. The final protein association pattern of the released PS might differ substantially from the pattern seen after injection of the free PS. The fact that a released PS is present in the blood in its non-aggregated form, while a non-liposomal PS is administered in an aggregated state, could explain this variable association pattern. The PDT outcome might be dramatically different upon association with different lipoproteins [264]. Selective accumulation of liposome-encapsulated PSs has already been explained by the fact that the liposomes may serve as donors of PS molecules to lipoproteins [74, 243]. This was demonstrated by liposome-delivered BPD-MA, which only slightly increased the photosensitizer accumulation in the tumor tissue as compared to an aqueous preparation of the free PS [264]. Nevertheless, the PDT efficiency was substantially improved, suggesting that the intratumoral localization of the liposomal PS was more advantageous for photodynamic destruction. Research has consistently showed that most of the liposome-released BPD-MA was associated with HDL, LDL and very low density lipoproteins, whereas the free PS was distributed evenly between albumin and HDL [264]. It was found that the delivery vehicle influenced the plasma distribution immediately post injection, while afterwards the PS partitions according to the plasma concentration of the lipoproteins [265].

A number of reports comparing the PDT outcome of liposomal *vs.* non-liposomal PSs under identical conditions provide strong evidence that a liposomal formulation can be advantageous [75, 243, 242, 244]. PDT with Photofrin® proved to be significantly more efficient against a human glioma implanted in the rat brain when the PS was formulated in liposomes [266]. Accordingly, Photofrin® uptake in the tumor tissue was significantly enhanced with the liposomal formulation. In a different study, mice implanted with a human gastric cancer

xenograft were injected with multilamellar liposomal or free-form Photofrin® [267]. The liposomalization of the PS increased its tumor accumulation, with a resulting enhancement of the therapeutic effect of PDT. A higher PDT damage was caused by the liposomal form of Photofrin® in gliosarcoma and U87 glioma xenografts in rats [266]. A dramatic increase in PDT efficacy was achieved for liposomal HpD, which was explained by a reduced release of cell-bound porphyrin into the extracellular medium [268]. Liposomal formulations were also used for the delivery of pheophorbide PSs. The tumor response to PDT was significantly better for liposomal drugs compared to Tween solution of methylpheophorbide-a [269], although no difference in the tumor uptake was evident.

In a study comparing different liposomal formulations of BPD-MA, it was noted that tumor accumulation of the PS after injection within PEG-liposomes in Meth A sarcoma-bearing mice was significantly higher than that observed after injection with non-PEGylated liposomes [270]. However, significant tumor growth suppression after PDT was only observed for conventional but not for PEGylated formulation, explained by the absence of drug release and inefficient interaction of PEGylated liposomes with cells.

4.3. Release of photosensitizers from liposomes

An essential point in the evaluation of drug delivery systems is the rate at which the drug is released from the carrier. In order to rationally design liposomal drug delivery systems, it is necessary to fully characterize their drug retention and release properties both *in vitro* and *in vivo* [271]. The rate of *in vivo* drug release can influence the rate of clearance of the drug from the general circulation, its bioavailability and tumor accumulation. Liposomes that display dramatic differences in PK generally show superior efficacy for the longer circulating constructs, while liposomal drugs that display comparable PK and drug release rates will have similar antitumor activities [175].

It is worth noting that the targeting of liposomes to the diseased tissue does not automatically lead to increased drug activity in the target tissue, if drug release is not considered. This is particularly important for PEGylated liposomes, which offer long circulation times enabling passive targeting via the EPR effect, but activity may be hampered by insufficient drug release and ineffective cell uptake of liposomes [203]. It would be ideal to design liposomes that have little or no drug leakage in the circulation and increased release rate at the diseased site.

Although the correlation between the circulation lifetime and antitumor activity is relatively strong, the correlation between the antitumor activity and *in vivo* drug release rate is more complex [175]. In order to maximize the benefits of using liposomal carriers, a balance between liposome delivery and drug release must be achieved. It is important to consider the

effects of liposomes on all aspects of the drug delivery process, like the *in vivo* drug release rates, rather than just the PK of the carrier.

4.3.1. Mechanisms of drug release from liposomes

There are two mechanisms of drug transfer from liposomes that, in general, may act simultaneously [273]. The first mechanism is the transfer of drugs upon collisions between the donor liposome and the acceptor structure. In this case, the drug molecules directly migrate from the liposome to the acceptor with a minimal exposure to the aqueous phase. Collisions require two structures to come to close proximity. The second mechanism refers to the transfer of drugs via diffusion through the aqueous phase, without the need of collisions between the donor and the acceptor. In this case the transfer steps are: (1) departure of the drug from the donor membrane into the aqueous phase, (2) association of the drug component in the aqueous phase with the acceptor structure, followed by (3) dissolution of the drug in the acceptor membrane.

In some cases, both mechanisms were suggested to contribute to the transport of lipophilic drugs from oil-in-water emulsions to cells [274] and from plasma proteins to lipid vesicles [87]. In a study investigating mTHPC redistribution between liposomes, it was found that above a certain concentration the transfer was dominated by collisions, while for smaller concentrations transport through diffusion was prevalent [275].

In a recent simulation study on the drug release rate from liposomal formulations [276], a high drug load was found to increase the transfer rate of the PS. Besides, the presence of attractive interactions between drug molecules within the liposomes (aggregation) was expected to slow down the transfer kinetics, as the energy barrier to remove a drug molecule from the bilayer increased.

4.3.2. Methods of drug release measurement

The methods for determining release profiles can be broadly divided into four groups [277]: (1) membrane diffusion methods; (2) sample-and-separate methods; (3) continuous flow methods and (4) *in situ* methods.

One of the most common membrane diffusion techniques relies on dialyzing the formulation against large volumes of buffer (possibly supplemented with serum to mimic *in vitro* conditions) at physiological temperatures. The method has been reported to be of limited value and to possess poor correlation in predicting the *in vivo* behavior of colloidal carriers intended for IV administration [277].

In the sample-and-separate method, the carrier is diluted with buffer, and samples are taken at intervals. The carrier is then separated by filtration or centrifugation, and the quantity of the released drug is calculated. Considering liposomal carriers, the problem is how to achieve a

rapid and clean separation [278]. Commonly reported problems are clogging of filters by small particles, drug binding to the filter material or instabilities of the investigated formulations.

An interesting example of this method was reported by Shabbits *et al.* [271]. Drug-encapsulated unilamellar 100-nm liposomes were incubated with an excess of multilamellar vesicles that served as acceptors, and separated by centrifugation. The amount of the drug in multilamellar liposomes sedimented in a pellet reflected the degree of drug leakage from the donor liposomes. The results indicated that that release assay was a better predictor of *in vivo* drug transfer than dialysis-based systems, although it lacked the lipoproteins during the incubation, which significantly hindered the interpretation of physiological conditions.

A study by Fahr *et al.* proposed using a mini ion exchange column to investigate the transfer of mTHPC between two different types of liposomes [279]. The column separates the donor from acceptor liposomes and thus allows the time dependence of the drug transfer to be monitored. However, this was only applicable to model membrane systems requiring preparation of specifically designed acceptors, thus hindering its use in *in vivo* conditions.

Continuous-flow methods utilize flow-through cells containing the particle formulation under investigation which is circulated with a release medium. Flow cytometry may also be added to the continuous-flow methods. In a recent study it was applied to monitor the transfer of mTHPC from donor liposomal carriers to acceptor oil/water emulsion droplets simulating cell-like structures [280]. The major advantage of this method, compared to techniques like ultrafiltration or centrifugation, was the absence of any procedures of separating the donor and acceptor particles. One limitation was the minimal size requirement for the acceptor particles in the lower μm range. Therefore, a transfer into nanosized blood components like serum proteins and platelets could not be measured, which represents a major disadvantage considering the IV administration route of liposomal PSs.

In situ methods offer a possibility to directly analyze the drug within the particle containing release medium by distinguishing between the released and non-released drug. Thus, these methods are sensitive only to either the released or the non-released drug. For example, the drug can be analyzed spectroscopically (UV/vis, fluorescence, phosphorescence), which limits the number of potential drug candidates. One example of *in situ* method is the combination of fluorimetry (PS fluorescence) and radioactive counters (radioactive lipids) to measure the release of anticancer drugs from liposomes by comparing the signal of fluorescence and radioactivity in the blood. However, a known problem is the stability of radioactive markers in *in vivo* conditions [116]. An assay to estimate the release of BPD-MA was developed that made use of concentration-dependent fluorescence quenching of the PS in liposomes [253]. By applying this

fluorescence assay in blood, the transfer of the PS out of the liposomes to serum proteins was found to be almost instantaneous (less than 2 min).

Of all the methods described above, *in situ* ones probably offer the best opportunity of direct *in vivo/ex vivo* measurements. However, if drug release from liposomes *in vivo* can be estimated by measuring the drug-to-lipid ratio of liposomes in the blood compartment, it is important to recognize that two events are being monitored as a function of time after IV administration. Liposomes are being eliminated from the plasma, and the drug is being released from liposomes, which provides a *relative* concentration of the blood-borne liposomal PS, and additional methods of quantifying the drug in plasma have to be employed.

In the design and development of a therapeutic liposomal agent, an *in vitro* release study has been considered as one of the key standards to evaluate and optimize the formulation [281]. The *in vitro* results reveal the structure-function relationship of the materials, contribute to the tailoring of material for optimal controlled release and also provide insights into the performance of the formulation *in vivo*. However, a major concern is the lack of direct correlation between *in vitro* and *in vivo* release profiles. Currently, attention has been focused on the *in vivo* release studies and the correlation between *in vitro* and *in vivo* release data. The physiological conditions are much more complex than the buffer solutions that are commonly employed for *in vitro* evaluations. It is highly desirable to develop a single method that could be applied to estimate drug release both in model and *in vivo* conditions.

4.4. Liposomal formulations of meta-tetra(hydroxyphenyl)chlorin

A second generation sensitizer mTHPC (Foscan®) is one of the most potent drugs, since only relatively small drug and light doses are required to achieve treatment response. Possessing a water/octanol partition coefficient of 9.4 [282], it is highly hydrophobic. Following the trend of overcoming problems of 2nd generations PSs, the focus in the development has been shifted to liposomal formulations of mTHPC. Two formulations are currently under intensive investigation. Foslip® is a conventional liposomal formulation based on DPPC/dipalmitoylphosphatidylglycerol (DPPG) (9:1 w/w), with an mTHPC load of 1:12 drug:lipid molar ratio. The other formulation, Fospeg®, consists of DPPC/DPPG liposomes with the addition of PEG-2000 distearoylphosphatidylethanolamine. The degree of PEGylation of the surface varies, depending on the preparation and the study, from 2 to 8%.

4.4.1. Photophysical properties of mTHPC in liposomes

Incorporation into liposomes significantly changes the properties of mTHPC [283]. As noted in the previous sections, incorporation into liposomes gives mTHPC a high efficacy of

singlet oxygen generation [257]. Spectral properties also undergo changes, including an increase in fluorescence and the position of the Soret absorption band. The fluorescence lifetime measurements indicate that the mTHPC fluorescence is strongly quenched in the high-drug load liposomes, compared to a monomer drug [284]. The results were found to be consistent with the occurrence of fluorescence self-quenching due to dimerization in combination with energy-transfer between adjacent mTHPC monomers and weakly fluorescent aggregates within the liposomes. However, the studies on the aggregation state of mTHPC in liposomes were not carried out within the range of mTHPC loads in the studied PEGylated liposomes [284].

As the PS molecules are mostly restricted to the lipid phase of liposomes, this results in high local concentrations of the drug in the bilayer (up to 0.1 M for Foslip® [119]), suggesting strong PS interactions contributing to the PS photophysical properties. This may imply the presence of concentration quenching, as previously noted for other PSs like BPD-MA [253]. However, the concentration effect was found to be small in liposomes loaded with mTHPC up to the limit of the loading capacity [119]. Meanwhile a very small distance between mTHPC molecules in Foslip® (ca 2.6 nm), being less than the Förster radius, implies a high probability of energy migration between the PS molecules in the lipid bilayer, confirmed by fluorescence polarization measurements. mTHPC fluorescence in high-drug load formulations like Foslip® was shown to be completely depolarized, hence strong interactions between mTHPC molecules are likely to be present [119].

An unusual phenomenon, termed by the authors the ‘photoinduced quenching effect’, was described on the basis of energy migration [119]. Exposure of Foslip® suspensions to small light doses ($<50 \text{ mJ/cm}^2$) resulted in a substantial drop in fluorescence, which was completely restored after addition of a non-ionic detergent disrupting liposomal structure. This effect depended strongly on the molar mTHPC:lipid ratio and was only revealed for high local mTHPC concentrations. The results were interpreted assuming energy migration between closely located mTHPC molecules with its subsequent dissipation by the molecules of the photoproduct acting as excitation energy traps, which were formed upon irradiation. The authors showed that the phenomenon could not be attributed to the photobleaching of mTHPC in liposomes, as fluorescence was completely restored after liposome disruption, and the absorption spectra remained unchanged. However, a formation of a very small quantity of non-fluorescent mTHPC photoproducts, insignificant for marked spectral properties, but sufficient to quench the fluorescence of the whole mTHPC population in a liposome in the conditions of efficient energy transfer, was likely.

The phenomenon was shown to be applicable as a method of estimating local mTHPC in liposomes [119]. Indeed, changes in local mTHPC concentration would be consistent with

changes in photoinduced fluorescence quenching amplitude. Monitoring variations in the relative fluorescence intensity immediately after irradiation and after liposomal destruction by the detergent could be explored to assess the redistribution of mTHPC from liposomes to a biological substrate. This method may be related to *in situ* methods, and the major advantage of it is the applicability both for *in vitro* systems (model liposomes, serum) and *in vivo* blood sampling, as it makes use of intrinsic mTHPC properties in the lipidic environment regardless of the surrounding milieu. The application of the photoinduced quenching technique to the release of mTHPC *in vitro* constitutes a major part of this thesis.

4.4.2. mTHPC release from liposomes

The interliposomal transfer kinetics of conventional liposomal mTHPC with a very low drug load (70 times less than in Foslip®) was recently studied by Fahr and co-authors [275] using a mini ion exchange column technique. The transfer was noted to occur by both diffusion and collision mechanisms, and the process was entropically controlled. Positively charged donor liposomes showed higher transfer rates than negatively charged, while the maximum amount transferred was almost the same. The rate of transfer depended strongly on the incubation temperature, increasing when the liposomes were heated. This was ascribed to a decrease in the hydrophobic interaction strength between the lipids and the drug when the temperature was increased, thus resulting in a higher aqueous solubility of mTHPC [275]. The total lipid dose also augmented the transfer rate. A more rigid structure of the donor liposomes (lipid bilayer phase) increased the transfer rate of mTHPC by expelling the drug from the membrane interior.

The influence of mTHPC liposomal localization on the release was hypothesized in a study of PEGylated PLGA nanoparticles, where a burst release of more than 30% of mTHPC was noted after incubation in the medium complemented with 10% serum. It was suggested that the fast release could be a consequence of localization of a fraction of mTHPC on the particle surface and low compatibility with hydrophilic PEG chains [285]. Thus, as conventional and PEGylated liposomal formulations of mTHPC possess different surface characteristics, the study of mTHPC localization is an important step to characterize the behavior of the liposomal drug.

It should be taken into account that not only liposomes influence the behavior of the incorporated hydrophobic drug, but also the drug may influence the physicochemical properties and biological behavior of the carrier, especially at high drug loads. The morphology and thermal properties of conventional and PEGylated liposomes with a varying mTHPC load were studied by Kuntsche *et al.* [283]. It was found that the phase transition temperature of Foslip® and Fospeg® (8 mol% drug load) was shifted to below-physiological values, 34-36 °C, while

corresponding drug-free liposomes underwent phase transition at 41-43 °C. A decrease of the mTHPC content to 3 mol% raised the phase transition temperature to values above 37 °C.

4.4.3. *In vitro* studies

The study by Kiesslich *et al.* investigated the photodynamic characteristics of mTHPC in a solvent-based formulation and Foslip® in an *in vitro* model system consisting of two biliary cancer cell lines [286]. Foslip® was shown to possess 50 times less dark toxicity to cells. At the same time, a somewhat lower Foslip® phototoxicity was noted, due to a lower cell uptake. It was found that the incubation with serum resulted in a lower cell uptake for both forms. The authors concluded that mTHPC from both forms binds to serum proteins present in the cell medium; however, the protein binding pattern of neither Foslip® nor Fospeg® has been studied to date.

Dark toxicity and phototoxicity were compared for Foscan® and Fospeg® in a human epidermoid carcinoma cell line [287]. Fospeg® showed a strongly reduced dark toxicity and a similar phototoxic efficiency compared to Foscan®. Both mTHPC formulations showed similar *relative* uptake kinetics with a plateau phase of the intracellular PS concentration after 20 h incubation time and comparable kinetics for PS release from the cells.

A very recent study reported the effects of density and thickness of PEG coating on *in vitro* cell uptake and dark- and phototoxicity of PEGylated mTHPC liposomal formulations in human normal fibroblasts and lung cancer cells [284]. In the dark all PS formulations were less cytotoxic than solvent-based mTHPC, and cytotoxicity decreased with increasing PEGylation degree and length. The cell uptake of Fospeg® was slower and reduced by 30-40% compared to Foscan®, which, however, led to only a slight reduction in the phototoxicity. The study reported a biphasic uptake of mTHPC from Fospeg®, which suggested a difference in the modality of internalization compared to the free drug form.

The lower cell uptake of mTHPC in the form of Fospeg® but similar phototoxicity could imply a higher photosensitizing efficiency of the chlorin delivered (at least, initially) with nanoparticles compared to that in the standard solvent. It is known [88] that solvent-based mTHPC associates with the serum proteins partly as aggregates. Ma *et al.* reported that such aggregates are taken up by the cells together with the monomer PS molecules, but they are characterized by a much lower photosensitization efficiency [97]. In contrast, mTHPC embedded in the nanoparticles is, presumably, mostly monomer, and it is thus transferred to serum proteins essentially in a monomer form. The absence, or a very low level of mTHPC aggregates in cells, when incubated with the nanoparticles, may explain the higher phototoxicity. This has already been noted for silica particles-entrapped mTHPC, from which mTHPC released and was bound to the proteins in the cell incubation medium [288]. Hence, data on the release of mTHPC from

liposomal formulations is required to adequately estimate the behavior of the liposomal drug in cellular systems.

4.4.4. *In vivo* studies

To date, both Foslip® and Fospeg® have been investigated as delivery systems for mTHPC for systemic PDT in a small number of preclinical studies [289-293].

Foslip®

The first animal study with Foslip®, conducted in 2007 on HT-29 grafted mice [294], reported a rapid tumor uptake and higher tumor/muscle ratio in comparison with Foscan®.

PDT efficiency with Foslip® in EMT6-grafted mice, studied by Lassalle *et al.* [289], was found to be maximal at a DLI of 6 h, significantly shorter than the 24 h DLI optimal for Foscan® [103]. The optimal efficacy was linked to the presence of mTHPC in both endothelial cells and the tumor parenchyma at 6 h, as shown by microscopy of the intratumoral spatial drug distribution. The study indicated that Foslip® resided in the plasma compartment of the tumor up to 1 h post-injection and diffused to the first cell layers at 3 h interval, while at long intervals of 15 and 24 h mTHPC was localized far from the tumor blood vessels. Thus, the best Foslip®-PDT effect at 6 h DLI indicated the presence of both direct and vascular PDT effects. The PDT efficacy did not correspond to plasma or tumor pharmacokinetics, as observed with Foscan® studies. Foslip®-induced mTHPC was uptaken by the tumor and reached plateau as early as after 15 h, in contrast to Foscan® with a 24-48 h plateau. Pharmacokinetics indicated a 4 times higher volume of distribution compared to the one observed for Foscan®, as well as 3-fold increase in the initial volume of distribution. While the first value was considered to indicate a preferential accumulation of Foslip®-induced mTHPC in certain tissues, the second one implied that the initial retention of Foslip® in the blood compartment was low [289], indicating a high RES uptake, as confirmed by the biodistribution analysis.

A study by D'Hallewin *et al.* has shown the importance of the sufficient Foslip®-induced mTHPC bioavailability in tumor for optimal PDT efficacy [291]. The highest cure rates in mice were obtained at 24 h post intratumoral injection, in spite of the significant mTHPC efflux from the tumor. This points out that the 24 h DLI provided the highest mTHPC accumulation in tumor cells, which correlates with the *in vitro* results of Foslip® uptake by tumor cells [287]. Fluorescence macroscopy experiments have shown that the maximal fluorescence of mTHPC in the tumor was registered also 24 h post-injection. This unexpected result may be explained by the presence of the photoinduced quenching effect of mTHPC in Foslip® immediately after intratumoral injection, which resulted in low fluorescence intensity upon macroscopy laser

excitation. In time, upon mTHPC release from liposomes, the quenching effect was diminished, and the tumor fluorescence build-up was registered. The decrease of the photoinduced quenching implies increased bioavailability of mTHPC, as the presence of the drug-drug interactions in liposomes inhibits efficient photosensitization process (V.Reshetov, unpublished results).

Fospeg®

The first animal studies of Fospeg®-PDT [293, 295] showed advantageous PDT outcome compared to Foscan®. A clinical trial on cats with spontaneous squamous cell carcinoma of the nose showed a 75% 1-year cure rate without general adverse effects [295]. In contrast, the recurrence rate for Foscan® was 75%. Fospeg®-PDT was optimal with the DLI of 16 h vs. 48 h for Foscan®. The liposomal mTHPC concentration in the tumor reached a maximum at 4 h post-injection, in sharp contrast to Foscan® (16 h, maximal measured time point) [293]. Tumor fluorescence intensities, fluorescence tumor/skin ratios and bioavailability in the tumor were 2, 3.5 and 4 times higher, respectively, with Fospeg® compared to Foscan®.

A related study in cat patients reported vascular effects following Fospeg®-PDT at a DLI of 16 h [296]. By using Doppler ultrasonography, the vascularity and blood volume of the tumor vasculature were measured. A significant decrease in vascularity and blood flow was noted already 5 min after PDT, with the lowest values at 24 h post-treatment reflecting vessel occlusion, indicating that mTHPC was present in endothelial cells at the time of PDT.

PEGylated liposomal mTHPC formulations (Fospeg® 2% and 8%) were found to be more efficient than Foscan® in a recent study in tumor-bearing rats by Bovis *et al.* [290]. The authors concluded that the total light and the administered mTHPC dose may be reduced with Fospeg® to induce the same PDT effect as with Foscan®. The percentage of induced tumor necrosis, as well as pharmacokinetic parameters, depended on the degree of PEGylation.

Elimination half-life was the shortest for Foscan® and the longest for Fospeg® 8%, indicating the influence of both the liposomes themselves, and the degree of liposome surface PEGylation on pharmacokinetics. A significantly smaller volume of distribution was observed for PEGylated liposomal mTHPC than for Foscan®. The peak tumor concentration of Fospeg®-induced mTHPC was 5 times higher than in the free-drug form. Maximal tumor/normal tissue ratios were observed 6 h post-injection irrespective of the drug form, being the highest for Fospeg® 8% and the lowest for Foscan®. The authors proposed that the vascular damage makes a significant contribution to the overall efficacy of Fospeg®, based on the longevity in blood.

Foslip®/Fospeg® comparison

The comparison of Foslip®/Fospeg® behavior was studied in window-chamber model in tumor-bearing rats [297] and in chick embryo chorioallantoic membrane model (CAM) [298].

Fospeg® has shown a marked difference from Foslip® and Foscan® in tumor accumulation kinetics in rats [297]. Maximum tumor fluorescence was reached at 8 h for Fospeg® (as previously observed in [293]) and at 24 h for Foscan® and Foslip®. Tumor fluorescence intensity was the highest for Fospeg® and the lowest for Foscan®. Both liposomal formulations showed enhanced bioavailability of mTHPC in the vasculature, as the vascular mTHPC fluorescence after IV injection increased for Foslip® and Fospeg®, but decreased for Foscan®.

The study in CAM model evaluated the ability of Foslip®- and Fospeg®-PDT to occlude neovascularization [298]. Fospeg® exhibited a significantly higher photothrombic activity, while the kinetics of extravasation was similar to the kinetics of Foslip®. Fospeg® required a twice lower light dose to induce the same vascular damage. The authors hypothesized that the PEGylation of liposomes provided a higher concentration of mTHPC in endothelial cells due to increased circulation times compared to Foslip®, however, neither the cell uptake nor the drug release rate were estimated, which could both influence the PDT efficacy.

Objectives

OBJECTIVES

Application of liposomal nanocarriers has become one of the major directions of research in the field of phototherapy. Significant advantages that liposomes offer for PDT have inspired research into the preclinical and clinical efficacy of nanoformulated photosensitizers. Deep characterization of these systems is essential to achieve an adequate understanding of the system-target interactions responsible for the *in vivo* results, and to formulate a reliable system that can be proposed for the therapy. The incorporated drug may take part in the microstructure of the system and influence it, and it is for this reason that there is a need for investigating the physicochemical, photophysical and biological properties of the ultimate system.

It is not clear from the studies of anticancer drugs, what is the critical parameter to consider when optimizing liposomal anti-cancer therapy. Drug release is considered to be a crucial property of the liposomal drug formulation. Investigations of the release properties *in vitro* and *in vivo* provide data on the basic efficacy of the system, its interaction with biological substrates and tumoricidal capability of the drug, and its efficient use. Meanwhile, the results of drug release *in vitro* obtained with current methods of investigation are usually difficult to correlate with *in vivo* results. The question of developing a method applicable in both cases is, therefore, of great importance. Finally, a detailed picture of liposome trafficking, release, interaction with the blood components is also needed.

The large number of photosensitizing drugs and liposomal carriers developed to date raises the question of direct comparison between different formulations of the same drug, in order to understand its properties and choose the optimal liposomal formulation. However, the number of studies addressing this issue is rather small.

The general objects of study in this work are two liposomal formulations of mTHPC – Foslip® (conventional liposomes) and Fospeg® (PEGylated liposomes).

The objective of the work was to determine the properties of mTHPC in two liposomal formulations and estimate its release from the carriers. To this end, the following studies were conducted:

- Developing an assay to estimate the mTHPC release from liposomes to serum proteins and model cell membranes *in vitro* and *in vivo* during the blood circulation.
- Determining the localization of mTHPC in Foslip® and Fospeg® and its influence on drug release properties.
- Estimating the photophysical properties of mTHPC in liposomes and its aggregation state.

These tasks are addressed in the first research chapter (Chapter II, section 1).

- Comparing the fluorescence-based methods suitable for mTHPC release studies.

This is addressed in the second research section (Chapter II, section 2).

- Determining the binding pattern of liposomal mTHPC to serum proteins.

- Developing a method to evaluate the rate of liposome destruction in serum. Evaluating the stability of mTHPC-loaded liposomes in serum, determining the influence of mTHPC on the structural stability of the carriers.

- Estimating the input of the drug efflux and liposome destruction into the overall release kinetics of mTHPC from conventional and PEGylated liposomes.

These points are addressed in the third research section (Chapter II, section 3).

Results

CHAPTER II. RESULTS

1. mTHPC PHOTOPHYSICAL PROPERTIES AND LOCALIZATION IN LIPOSOMES. RELEASE FROM LIPOSOMES TO BLOOD SERUM PROTEINS

The first part of the results is described in the article published in 2011 on the photophysical properties and localization of mTHPC within conventional and PEGylated liposomes, as well as its release from the carriers to serum proteins.

Redistribution of meta-tetra(hydroxyphenyl)chlorin (m-THPC) from conventional and PEGylated liposomes to biological substrates

***Vadzim Reshetov**, Dzmitry Kachatkou, Tatiana Shmigol, Vladimir Zorin, Marie-Ange*

D'Hallewin, François Guillemin and Lina Bezdetnaya

Photochem. Photobiol. Sci.; 2011. 10:911-919

Photophysical properties of mTHPC in conventional and PEGylated liposomes with varying drug:lipid ratios were investigated. It was shown that the spectral characteristics and the relative yield of mTHPC fluorescence depend on the drug load. Using the technique of resonance light scattering, the presence of mTHPC aggregation in high-drug load liposomes was shown. PEGylated liposomes possessed more aggregated mTHPC than conventional ones. Fluorescence quenching of mTHPC in liposomes by iodide indicated that a part of mTHPC in PEGylated liposomes was localized in the PEG shell, while the rest was bound to the lipid bilayer. In conventional liposomes, mTHPC is heterogeneously distributed within the lipid bilayer.

The phenomenon of photoinduced fluorescence quenching, previously described by our group, was studied in liposomes with different drug loads. This data served as a means to quantify the mTHPC release from the liposomes to serum proteins. A substantial percentage of mTHPC is released from Fospeg® much faster than from the conventional liposomal formulation Foslip®, and is then followed by a much slower release of the drug. Drug release pattern from Fospeg® was explained by the presence of the two molecule pools in PEG shell and in the lipid bilayer. The release of mTHPC from the lipid bilayer was found to depend on the temperature. Thermodynamic characteristics of the release process were estimated, and the release was estimated to proceed by both the collision and diffusion mechanisms.

Cite this: *Photochem. Photobiol. Sci.*, 2011, **10**, 911

www.rsc.org/pps

PAPER

Redistribution of *meta*-tetra(hydroxyphenyl)chlorin (m-THPC) from conventional and PEGylated liposomes to biological substrates

Vadzim Reshetov,^{a,b} Dzmitry Kachatkou,^{a,b} Tatiana Shmigol,^c Vladimir Zorin,^b Marie-Ange D'Hallewin,^a Francois Guillemin^a and Lina Bezdetsnaya^{a*}

Received 14th October 2010, Accepted 23rd December 2010

DOI: 10.1039/c0pp00303d

We used the phenomenon of previously described photoinduced fluorescence quenching and fluorescence polarization to evaluate the transfer of *meta*-tetra(hydroxyphenyl)chlorin (m-THPC) from commercial high-drug load liposomes to plasma proteins and model membranes. Fluorescence quenching of m-THPC in liposomes by iodide indicates that part of m-THPC in PEGylated liposomes is localized in the PEG shell, while the rest is bound to the lipid bilayer. It was shown that the two molecule pools in the commercial PEGylated liposomal formulation Fospeg® condition the characteristics of the m-THPC release kinetics. A substantial percentage of m-THPC from Fospeg® is released much faster than from the conventional liposomal formulation Foslip®. Using the technique of resonance light scattering, it was shown that partial m-THPC aggregation is present in liposomes with very high drug loads, higher in PEGylated liposomes compared to conventional ones.

Introduction

Photodynamic therapy (PDT) is an effective modality in the curative and palliative treatment of malignant tumors and other diseases,¹ which is based on the administration of a photosensitizer followed by irradiation to produce cytotoxic molecular species. Porphyrins (including chlorins) are the most frequently used photosensitizers, possessing high efficacy *in vivo*. A substantial limitation for clinical applications is their low water solubility, which impairs drug administration and efficacy.

Liposomes are popular carriers for poorly soluble drugs,²⁻³ which can be solubilized in the hydrophobic lipid bilayer. Incorporation into lipid vesicles maintains a monomeric state of the drug, providing a high photosensitizing activity.⁴ In this perspective, a clinically approved photosensitizer, *meta*-tetra(hydroxyphenyl)chlorin (m-THPC, commercial formulation Foscan®) has been loaded into dipalmitoylphosphatidylcholine/dipalmitoylphosphatidylglycerol liposomes. The resulting compound, Foslip®, was recently tested in xenografted tumors⁵⁻⁷ and demonstrated favourable pharmacokinetic properties, consisting of a better tumor/healthy tissue selectivity and rapid plasma clearance, at least 2 to 3 times faster as compared to

pure m-THPC.⁷ Liposomes modified with poly(ethylene glycol) (PEG) represent a longer-circulating delivery system⁸ compared to conventional liposomes, which have a shorter plasma half-life.⁹ Fospeg®, a PEGylated derivative of Foslip®, was evaluated for photothrombic activity in chick chorioallantoic membrane model, showing a higher efficacy than Foslip®.¹⁰ Fospeg® was also shown to possess superior pharmacokinetics as compared to Foscan® in feline spontaneous squamous cell carcinoma.¹¹

Upon intravenous administration the liposomal drug is likely to be transferred to target sites by the blood flow in the vascular system, implying the interaction with blood components, including cells and serum proteins. A proper understanding of interaction of liposomal drug with blood serum proteins and cell membranes and the knowledge of the rates of drug release from the carrier is a prerequisite for the assessment of drug efficacy.

A novel approach to analyze drug transfer to large oil-in-water emulsion droplets by flow cytometry was suggested by Petersen *et al.*¹² Although inapplicable to drug release to nano-sized blood components, it estimated the characteristic release times of m-THPC to cell-sized acceptors. In a very recent publication by the group of Fahr¹³ the kinetics of m-THPC transfer between liposomal membranes using radiolabelled [¹⁴C]m-THPC were investigated with regard to the mechanism of transfer and physicochemical characteristics of the lipid. The study from the same group on physicochemical properties of m-THPC liposomal formulations¹⁴ revealed a drug concentration dependence of phase transition behaviour of liposomes. This implies that not only the liposomal delivery system influences the drug behaviour, but the drug properties may influence the delivery system and the characteristics of drug release, especially at high drug concentrations.

^aCentre de Recherche en Automatique de Nancy, Nancy-Université, CNRS, Centre Alexis Vautrin, Avenue de Bourgogne, 54511, Vandœuvre-les-Nancy, France. E-mail: l.bolotine@nancy.fr; Fax: +33 3834 4607 1; Tel: +33 3835 9835 3

^bLaboratory of Biophysics and Biotechnology, Physics Faculty, Belarusian State University, 4 Nezavisimosti pr., 220030, Minsk, Belarus. E-mail: vyzorin@mail.ru; Fax: +375 1720 9544 5; Tel: +375 1722 6594

^cDepartment of Biological and Medical Physics, Russian State Medical University, 1 Ostrovityanova str., 117997, Moscow, Russian Federation; Fax: +7 4953 3662 52; Tel: +7 4954 3466 76

The aim of the present study was the comparison of the kinetics of m-THPC redistribution from high drug-load PEGylated and conventional liposomal formulations, Fospeg® and Foslip®, to plasma proteins and liposomes using fluorescence polarization and the recently described¹⁵ technique of photoinduced m-THPC fluorescence quenching. The influence of incubation temperature, acceptor concentration, and the presence of PEG coating of liposomes on release kinetics was investigated. Dye localization in liposomes was evaluated using fluorescence quenching by iodide.

Experimental

m-THPC and its liposomal formulations

The photosensitizer m-THPC and its liposomal formulations Foslip® and Fospeg® were provided by Biolitec AG (Jena, Germany). A stock solution of m-THPC was prepared by dissolving m-THPC powder in 99.6% ethanol. m-THPC liposomal formulation Foslip® was reconstituted from lyophilized powder in distilled water. Foslip® is based on L- α -dipalmitoylphosphatidylcholine (DPPC), dipalmitoylphosphatidylglycerol (DPPG) and m-THPC, with a dye : lipid molar ratio of 1:12. Fospeg® formulation was supplied in aqueous solution. Fospeg® has the same composition as Foslip®, with addition of distearoylphosphatidylethanolamine-mPEG 2000 (DSPE-PEG) and has a dye : lipid ratio of 1 : 13.

Preparation and characterization of liposomes

Two techniques of liposome preparation were used in the present study. Unilamellar liposomes containing different amounts of m-THPC were made by filter extrusion.¹⁶ Briefly, 18 mg ml⁻¹ of DPPC (Avanti, Alabaster, USA) and 2 mg ml⁻¹ of DPPG (Avanti, Alabaster, USA) were dissolved in 1 ml of 99.6% ethanol, m-THPC being added to ethanol solution to obtain the required dye to lipid molar ratio. A thin film was obtained by removal of the solvent by rotary evaporation at 60 °C. The film was hydrated in 1 ml of phosphate buffered saline (PBS, pH 7.4, Invitrogen, USA) and underwent 3 freeze-thaw cycles. The suspension was extruded 21 times through 100 nm polycarbonate Nuclepore® membranes using Avanti Mini-Extruder (Avanti, Alabaster, USA) at 50 °C. After extrusion the liposomes were stored at 4 °C in a light-protected tube. PEGylated liposomes were prepared using a similar protocol, with 2 mg ml⁻¹ DSPE-PEG (Avanti, Alabaster, USA) added to an ethanol solution.

Dye-free acceptor unilamellar liposomes were prepared using the ultrasonic method.¹⁷ 40 mg of DPPC was dissolved in 1 ml of ethanol, which was afterwards evaporated to form a lipid film on the flask walls. Upon addition of 4 ml of PBS, the lipid film was hydrated, removed from the flask walls by vortexing for 15 min and sonicated in a UZDN-2T ultrasonic dispersator (Ukrrospribor, Sumy, Ukraine) for 5 min. The final suspension was stored at 37 °C.

The concentration of m-THPC in the lipid suspension was estimated by a spectrophotometric method using an m-THPC molar extinction coefficient of 30 000 M⁻¹ cm⁻¹ at 650 nm after dissolution of the sample aliquot in ethanol.

The diameter of liposomes was measured by the dynamic light scattering technique on a Malvern ZetaSizer Nano (Malvern

Instruments, UK) at 25 °C in distilled water. For Foslip® and extruded conventional liposomes the z-average diameter was 111 ± 8 nm (polydispersity index 0.113 ± 0.01), Zeta-potential -49.7 mV, while Fospeg® and extruded PEGylated liposomes were characterized by a diameter of 114 ± 7 nm and a polydispersity index of 0.108 ± 0.01, indicating a narrow size distribution, and Zeta-potential of -47.1 mV.

Encapsulation efficiency of m-THPC was estimated by the ultracentrifugation technique. Liposomes were centrifuged at 100 000 g for 30 min at 4 °C in Sorvall RC-M120GX centrifuge (ThermoScientific, St Herblain, France) to separate free and liposome-encapsulated m-THPC. The m-THPC amount was estimated using a spectrophotometric method. Encapsulation efficiency in all samples was determined to be more than 85%.

Spectroscopic measurements

Absorption spectra were measured on PerkinElmer Lambda 35 (PerkinElmer, Waltham, USA) and Solar PV 1251A (Solar, Minsk, Belarus) spectrophotometers using 1 cm optical path quartz cuvettes. Fluorescence spectra were recorded on PerkinElmer LS55B and Solar SFL 1211A spectrofluorimeters equipped with polarizers, thermostated cuvette compartments (PTP-1 Peltier temperature controller in the case of LS55B) and magnetic stirring. In m-THPC fluorescence polarization measurements, samples were excited at 435 nm and fluorescence was registered at 650 nm.

Resonance light scattering measurements

Resonance light scattering (RLS) spectra were recorded on a PerkinElmer LS55B fluorimeter with a custom-built cuvette compartment scheme as suggested by Tikhomirov *et al.*¹⁸ Simultaneous scanning of excitation and emission monochromators was employed, with $\Delta\lambda = 0$ between them. RLS spectra were corrected for fluorimeter sensitivity and inner filter effects by the method described by Collings *et al.*¹⁹

Photoinduced fluorescence quenching

As previously shown,¹⁵ irradiation of m-THPC liposomal formulations at low light doses induces a significant fluorescence decrease, followed by its restoration after the addition of a detergent. We attributed this behaviour to photoinduced fluorescence quenching. The effect of photoinduced fluorescence quenching arises from energy migration between closely located m-THPC molecules in liposomes, the energy probably being dissipated by non-fluorescent photoproducts acting as energy traps.

Samples containing liposomal m-THPC were subjected to irradiation by coupling an optical fiber with a frontal diffuser to a 660 nm semiconductor laser ILM-660-0.5 (LEMT, Minsk, Belarus). The irradiance rate was set to 50 mW cm⁻², and irradiation was carried out under continuous stirring at room temperature for 10 s, corresponding to an irradiance of 0.5 J cm⁻². Normalized fluorescence was defined as the (I/I_{X-100}) ratio, where (I) is the m-THPC fluorescence intensity measured immediately after irradiation and (I_{X-100}) is the m-THPC fluorescence intensity measured after addition of 0.2% Triton® X-100 (Sigma-Aldrich, Lyon, France) to the same sample. The value of normalized fluorescence was used as an indicator of photoinduced quenching.

All photoinduced fluorescence quenching measurements were done in triplicate.

m-THPC fluorescence quenching by iodide

Potassium iodide (Sigma–Aldrich, Lyon, France) was used to quench m-THPC fluorescence in liposomes. Potassium iodide was added from the 6 M stock solution to the sample containing liposomes in consecutive steps under constant stirring. 0.005 M of sodium thiosulfate (Sigma–Aldrich, Lyon, France) was also added to the sample to prevent the production of I_2 . After each addition of the quencher, the sample was incubated for 1 min at set temperature, and the m-THPC fluorescence was measured ($\lambda_{\text{ex}} = 419 \text{ nm}$, $\lambda_{\text{em}} = 654 \text{ nm}$). Fluorescence quenching parameters were calculated using at least 8 quencher concentrations. Experiments were performed in duplicate with different liposomal preparations. The results were corrected for sample dilution.

In the experiments on m-THPC fluorescence quenching in buffer, 10^{-3} M of PEG-2000 (Sigma–Aldrich, Lyon, France) and $2 \times 10^{-7} \text{ M}$ of m-THPC were used. Fluorescence intensity measurements indicated that the major part of m-THPC molecules in these conditions was in a monomer state.

The fluorescence quenching data were analyzed using the modified Stern–Volmer equation:²⁰

$$\frac{I_0}{I_0 - I} = \frac{1}{fK_Q[\text{KI}]} + \frac{1}{f}$$

which gives the Stern–Volmer quenching constant (K_Q) and the fraction of iodide-accessible m-THPC ($1/f$). There, I_0 is the intensity of m-THPC fluorescence before the addition of the quencher, I is the m-THPC fluorescence intensity in the sample with a concentration $[\text{KI}]$ of iodide.

Blood serum

Human blood was collected from healthy donors and coagulation was carried out according to established protocols.²¹ Venous blood was precipitated in a glass test-tube without anticoagulants at room temperature ($20 \text{ }^\circ\text{C}$) for 30 min until clot formation. The clot was separated from the test-tube walls and the sample was centrifuged for 10 min at 1000–1200 g. The serum obtained was stored in plastic test tubes at $-18 \text{ }^\circ\text{C}$ until use. Immediately before the experiment, the serum was centrifuged at 400 g for 5 min and the supernatant was collected.

Redistribution of m-THPC from liposomal formulations

Foslip® or Fospeg® was added to a suspension of drug-free acceptor DPPC liposomes (donor : acceptor liposomes ratio 1 : 50, acceptor liposomes final concentration 0.5 mg mL^{-1} of lipid ($6.8 \times 10^{-4} \text{ M}$) or to 5% (v/v) human blood serum. m-THPC final concentration in sample was $1.1 \times 10^{-6} \text{ M}$. Samples were analyzed immediately after addition of Foslip® or Fospeg® and after incubation for 0.5, 1, 2, 3, 4, 6 and 24 h.

The photosensitizer content in the donor liposomes was estimated by the degree of photoinduced fluorescence quenching. The experimental normalized fluorescence value obtained during Foslip® or Fospeg® incubation in the serum solution ($\Delta_{\text{exp}}(t)$) corresponds to the sum of normalized fluorescence values in donor

liposomes ($\Delta_{\text{donor}}(C(t)/C_0)$) and acceptor structures (Δ_{acceptor}) with appropriate weighting factors:

$$\Delta_{\text{exp}}(t) = C(t)/C_0 \times \Delta_{\text{donor}}(C(t)/C_0) + (C_0 - C(t))/C_0 \times \Delta_{\text{acceptor}}$$

where C_0 is the initial m-THPC concentration in Foslip® or Fospeg®, $C(t)$ stands for the m-THPC concentration in Foslip® or Fospeg® liposomes during incubation. $\Delta_{\text{donor}}(C(t)/C_0)$ is derived from independent measurements of normalized fluorescence of liposomes with different dye : lipid ratios. Therefore, the $C(t)/C_0$ ratio may be calculated as follows:

$$C(t)/C_0 = (\Delta_{\text{acceptor}} - \Delta_{\text{exp}}(t))/(\Delta_{\text{acceptor}} - \Delta_{\text{donor}}(C(t)/C_0)) \quad (1)$$

Eqn (1) was solved using a numerical method, taking into account that Δ_{acceptor} is equal to 1 (as no photoinduced fluorescence quenching was attributed to m-THPC in acceptor structures due to their excessive amount).

This approach allowed us to calculate the amount of m-THPC residing in liposomes at each time point as well as the percentage of m-THPC released from the carriers. Approximating the plots of log(amount of m-THPC released from liposomes for the first 4 h incubation) vs. incubation time with linear function, we calculated the rate constants of m-THPC release, defined as the slopes of the linear fits.

Activation energy (E_a) of m-THPC release was calculated from the slope of Arrhenius plot of rate constants over a temperature range of $35\text{--}50 \text{ }^\circ\text{C}$. The Eyring theory²² was used to calculate enthalpy (ΔH) and entropy (ΔS) of m-THPC release from liposomes. Enthalpy was determined from the equation $\Delta H = E_a - RT$, entropy $\Delta S = 2.3R \log(hNk_e^{-\Delta H/RT}/RT)$. Here R is the gas constant, T temperature, h Planck's constant, N Avogadro's number, k release rate constant.

Results

Spectral properties of m-THPC in liposomes

Spectral properties of m-THPC in liposomal formulations differ from those in reference ethanol solution, as expressed by bathochromic shift of the Soret band maximum (5 nm for Foslip® and 8 nm for Fospeg®) and lower relative fluorescence yields (0.79 for Foslip® and 0.72 for Fospeg®) (Tables 1, 2).

A decrease of m-THPC content in liposomes leads to a smaller shift of the Soret peak as compared to Foslip® and Fospeg®, with a maximum at 419 nm at the dye : lipid ratios below 1 : 80 (Tables 1, 2). The relative fluorescence yield increases with decreasing m-THPC local concentration, and from dye : lipid ratio of 1 : 45 it exceeds that of m-THPC in ethanol, thus indicating the influence of microenvironment on dye characteristics.^{4,23}

The parameters strongly related to the m-THPC content in liposomes appeared to be fluorescence polarization and normalized fluorescence. Inclusion of low amounts of m-THPC in liposomes yields very high m-THPC fluorescence polarization values. An increase in the dye content is accompanied by a decrease in polarization, with almost complete depolarization at ratios above 1 : 100 (Tables 1, 2). The pattern of normalized fluorescence (the indicator of photoinduced fluorescence quenching) in function of dye content in liposomes matches that of polarization. For Foslip® and Fospeg® the values of normalized fluorescence are 0.11 and 0.12. A decrease of the dye content to 1 : 600 dye : lipid

Table 1 Spectral characteristics of m-THPC in conventional liposomes

Dye : lipid ratio	1 : 12 (Foslip®)	1 : 17	1 : 45	1 : 85	1 : 150	1 : 250	1 : 600	m-THPC in ethanol
$\lambda^{\text{Soret}} / \text{nm}$	421	421	421	419	419	419	419	416
F.Y.	0.79	0.81	1.16	1.33	1.35	1.36	1.37	1
p	0.043	0.068	0.073	0.085	0.128	0.172	0.235	0
$I/I_{X=100}$	0.11	0.17	0.30	0.49	0.69	0.84	0.96	—

λ^{Soret} – absorbance maximum of the Soret band; F.Y. – fluorescence yield, relative to the fluorescence of m-THPC in ethanol; p – fluorescence polarization; $I/I_{X=100}$ – normalized fluorescence (exposure 500 mJ cm⁻²). The polarization and normalized fluorescence experimental error did not exceed 7%.

Table 2 Spectral characteristics of m-THPC in PEGylated liposomes

Dye : lipid ratio	1 : 13 (Fospeg®)	1 : 17	1 : 45	1 : 80	1 : 200	1 : 450	1 : 600
$\lambda^{\text{Soret}} / \text{nm}$	424	421	421	419	419	419	419
F.Y.	0.72	0.82	1.07	1.24	1.29	1.35	1.36
p	0.053	0.069	0.072	0.093	0.193	0.239	0.274
$I/I_{X=100}$	0.12	0.19	0.34	0.56	0.92	0.99	0.99

λ^{Soret} – absorbance maximum of the Soret band; F.Y. – fluorescence yield, relative to the fluorescence of m-THPC in ethanol; p – fluorescence polarization; $I/I_{X=100}$ – normalized fluorescence (exposure 500 mJ cm⁻²). The polarization and normalized fluorescence experimental error did not exceed 7%.

ratio leads to the disappearance of the photoinduced response (normalized fluorescence values approaching 1).

No changes of Soret band extinction coefficient higher than 5% were present in liposomes compared to ethanol solution within the studied range of m-THPC concentrations, with Soret band width at half height $1900 \pm 30 \text{ cm}^{-1}$ compared to 1930 cm^{-1} in ethanol.

Aggregation state of m-THPC in Foslip® and Fospeg® was assessed by RLS. m-THPC liposomal formulations possess a strong RLS signal in the 400–500 nm region (Fig. 1, curves 1, 2), indicating the presence of aggregates. RLS maxima are red-shifted from the Soret absorption peak to 430 nm for both types of liposomes. Fospeg® exhibits a 2.5 times higher RLS signal than Foslip®. Our experiments showed a strong dependency of RLS on the m-THPC concentration in liposomes, decreasing with

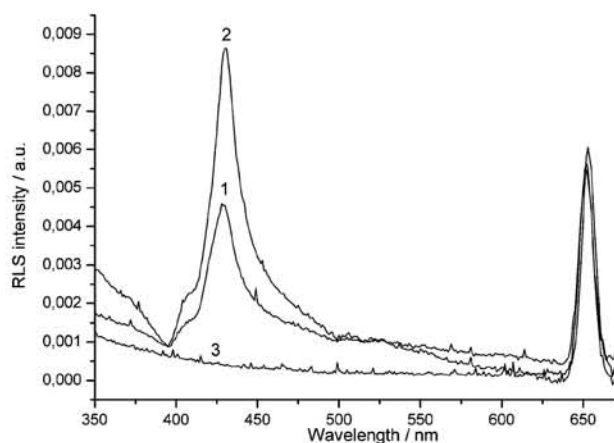


Fig. 1 Resonance light scattering spectra of m-THPC in ethanol and liposomal formulations. 1 – RLS in Foslip®, 2 – RLS in Fospeg®, 3 – RLS in samples after addition of the neutral detergent. Samples containing $5 \times 10^{-6} \text{ M}$ m-THPC were incubated at 20 °C.

a lower dye local concentration, almost no signal being registered below the dye : lipid ratio of 1 : 100 (data not shown).

m-THPC fluorescence quenching in liposomes

We applied the technique of fluorescence quenching with the low membrane permeability collisional²⁰ quencher iodide, to characterize the localization of m-THPC in liposomes. To avoid the influence of a high dye concentration on the m-THPC fluorescence properties, we used conventional and PEGylated liposomes with a dye : lipid ratio of 1 : 600.

Fig. 2 shows the results of fluorescence quenching of m-THPC in both types of liposomes. The quenching plots in direct Stern–Volmer coordinates are non-linear and exhibit downward curvature (Fig. 2A, curves 1, 2). Plotting the quenching data in modified Stern–Volmer coordinates yields a linear fit (Fig. 2B), which was used to calculate the quenching constant and the fraction of quencher-accessible dye in liposomes. K_Q in PEGylated liposomes is higher than in conventional ones (2.31 M^{-1} and 2.05 M^{-1} , respectively), with iodide-accessible fractions of 36% and 28%.

We also evaluated m-THPC fluorescence quenching in PEG-2000/PBS solution used as a model of water bulk. According to quenching data, all m-THPC molecules were accessible to iodide, and fluorescence quenching in such system at 20 °C yielded the K_Q value of 3.85 M^{-1} .

The characteristics of m-THPC fluorescence quenching in liposomes were found to depend on the temperature. The quenching constant decreases with increasing temperature (Fig. 3A), and in PEGylated liposomes there is a larger difference in K_Q at 20 and 50 °C (Fig. 3A, curve 2) compared to conventional ones (Fig. 3A, curve 1). The increase in the temperature from 20 to 33 °C is accompanied by 5% lowering of the values of the accessible fraction (Fig. 3B). Further heating leads to a sharp increase of accessibility to iodide, so that at temperatures above 40 °C, 100% of m-THPC is accessible to the quencher.

Kinetics of m-THPC release from Foslip® and Fospeg®

The fluorescence and polarization properties of m-THPC in liposomes depend on the local dye concentration (Tables 1 & 2) and may therefore be used to monitor m-THPC release from Foslip® and Fospeg® to biological substrates.

Fig. 4 reports the behaviour of normalized fluorescence for Foslip® and Fospeg® incubated in suspension of DPPC lipid vesicles. When Foslip® was incubated with acceptor dye-free liposomes, we observed a slow increase in normalized fluorescence (Fig. 4, curve 2), while incubation in PBS for over 24 h did not provoke any changes (Fig. 4, curve 1).

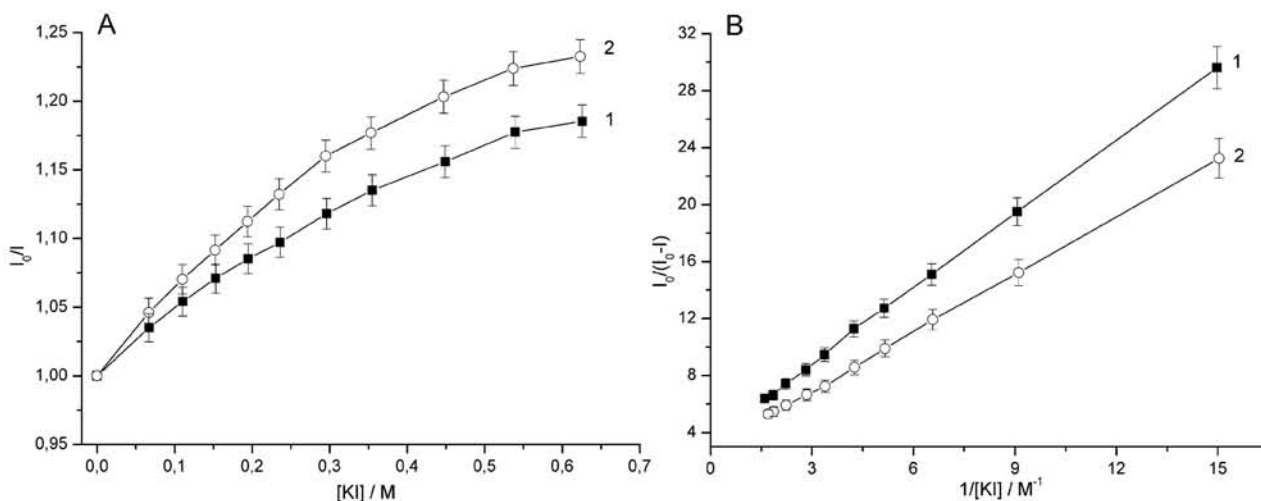


Fig. 2 Fluorescence quenching of m-THPC in liposomes at 20 °C. A – in direct Stern–Volmer coordinates, B – in modified Stern–Volmer coordinates. 1 – in conventional liposomes, 2 – in PEGylated liposomes. Dye : lipid ratio 1 : 600, m-THPC concentration 5×10^{-7} M.

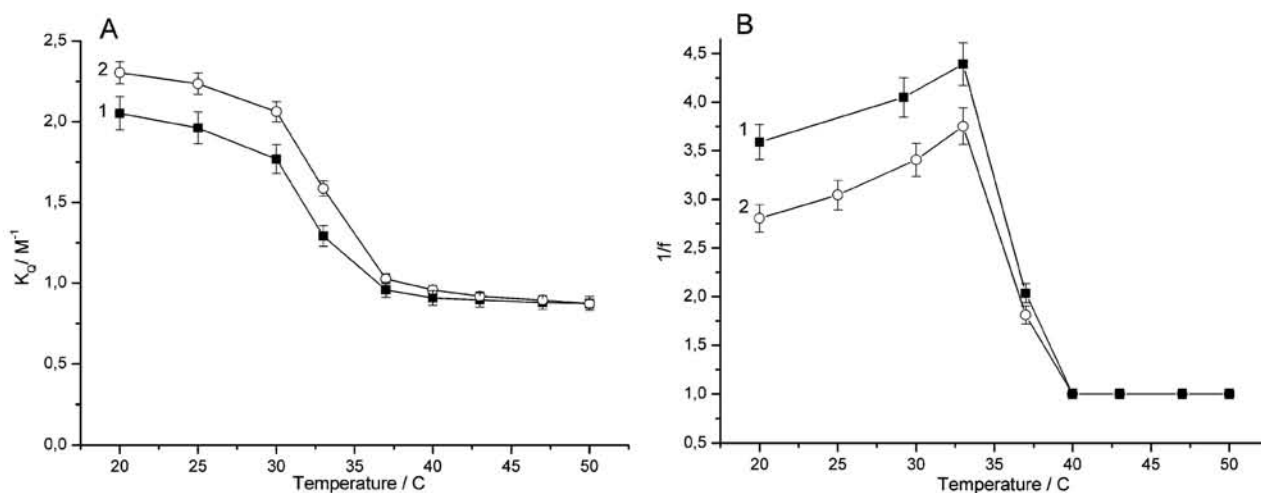


Fig. 3 Fluorescence quenching characteristics of m-THPC depending on temperature. A – m-THPC quenching constant. B – Accessibility of m-THPC to quencher. 1 – in conventional liposomes, 2 – in PEGylated liposomes. Dye : lipid ratio 1 : 600, m-THPC concentration 5×10^{-7} M.

Different kinetics pattern was observed during incubation of Fospeg® with acceptor liposomes (Fig. 4, curve 3). A very fast increase of normalized fluorescence is observed at the onset of incubation, which is then followed by a slow growth.

The release kinetics showed an identical profile when assessed by polarization measurements (data not shown), owing to the similarity in the dependence of both parameters on dye local concentration.

The release of m-THPC from Foslip® and Fospeg® incubated in a 5% human blood serum solution is displayed in Fig. 5. Since the values of normalized fluorescence are directly related to the m-THPC concentration in liposomes (Tables 1, 2), we calculated the dye : lipid ratio at each incubation time point, using the method described in Experimental. These ratios were used to plot the kinetics of m-THPC release from liposomes (Fig. 5 insets). For Foslip®, the release is described by a linear function at least during

3 h incubation (Fig. 5A inset), indicating that the redistribution process follows the 1st order kinetics.

For Foslip® the amount of dye released within 30 min incubation was 11%, and increased to 47% within 4 h. m-THPC release from Fospeg® shows the two-phase kinetics with 20% of m-THPC released within the first 5 min incubation (Fig. 5B inset), increasing to 38% after 30 min. Between 30 min and 4 h of incubation, only an additional 10% of m-THPC is released from the liposomal formulation.

Influence of temperature on m-THPC redistribution from liposomes

Kinetics measurements allowed us to quantify the rate constants of m-THPC release from liposomal formulations. Fig. 6 represents the rate constants of m-THPC release to serum proteins in function of temperature. At low temperatures, the rate of m-THPC release

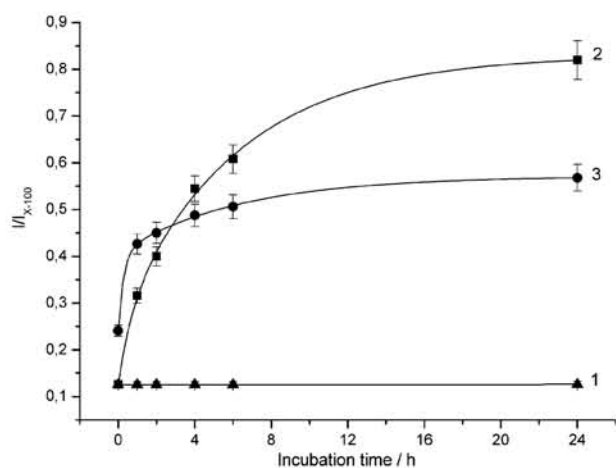


Fig. 4 m-THPC release from liposomal formulations to acceptor liposomes estimated by photoinduced quenching. 1 – reference curve for Foslip® (Fospeg®) incubated in PBS, 2 – redistribution from Foslip®, 3 – redistribution from Fospeg®. Foslip® (Fospeg®) : acceptor liposomes ratio 1 : 50, incubation temperature 37 °C.

from Foslip® is slow, followed by a sharp acceleration of the redistribution process (Fig. 6, curve 3) above 30 °C.

The slow-phase rate constant of m-THPC release from Fospeg® (Fig. 6, curve 2) shows roughly the same dependence as the rate constant for Foslip®, although the absolute values are much smaller. The rate constant of the fast phase (Fig. 6, curve 1) weakly depends on temperature, steadily increasing from 0.71 h⁻¹ to 0.85 h⁻¹.

The activation parameters of m-THPC transfer from Foslip® and Fospeg® to serum were calculated from the slope of the Arrhenius plot of release rate constants (see Experimental, last subsection). E_a of m-THPC release from Foslip® is 11.2 kcal mol⁻¹. The release from Foslip® is enthalpy- and entropy-dependent ($\Delta H = 10.6$ kcal mol⁻¹, $T\Delta S = -7.7$ kcal mol⁻¹). In the fast phase ($E_a = 0.51$ kcal mol⁻¹) of m-THPC release from

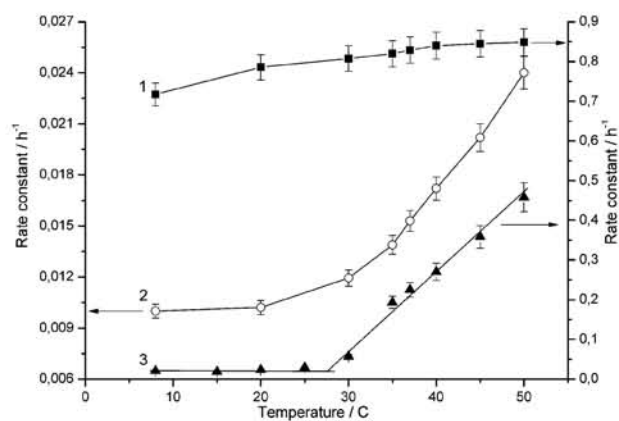


Fig. 6 Rate constant of m-THPC release from liposomes upon incubation with 5% blood serum as a function of temperature. 1, 2, m-THPC release from Fospeg®: 1 – rate constant describing the release during the first 30 min of incubation, 2 – rate constant describing the release from 30 min to 4 h of incubation. 3 – m-THPC release from Foslip® during 4 h of incubation.

Fospeg® the process is entropy-controlled ($T\Delta S = -30.5$ kcal mol⁻¹, $\Delta H = -0.1$ kcal mol⁻¹), while in the slow phase ($E_a = 6.86$ kcal mol⁻¹) both entropic and enthalpic factors are significant ($T\Delta S = -20.2$ kcal mol⁻¹, $\Delta H = 6.25$ kcal mol⁻¹).

The effect of the acceptor concentration on the release rate may serve as indicator of the mechanism of redistribution. In our experimental conditions, the concentration of acceptor proteins considerably exceeded that of donor liposomes. Thus, at the initial stage of redistribution the contribution of m-THPC back transfer from proteins to donor lipid vesicles is negligible. Our experiments show that the serum concentration only slightly affected the redistribution rate of m-THPC, since a decrease in the protein content from 50% to 2% resulted in a 6% decrease in m-THPC release from Foslip®, and 11% in release from Fospeg® after 2 h incubation in serum.

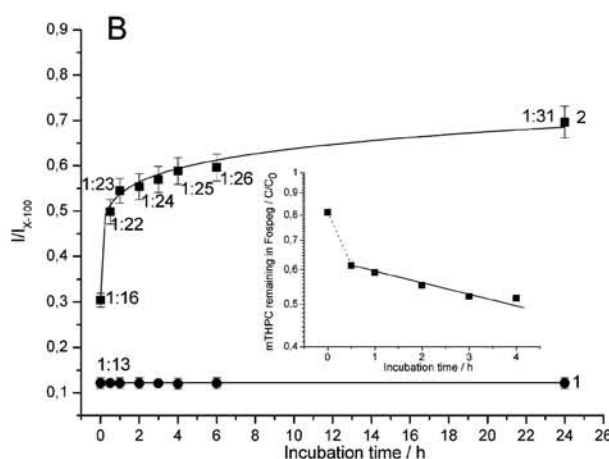
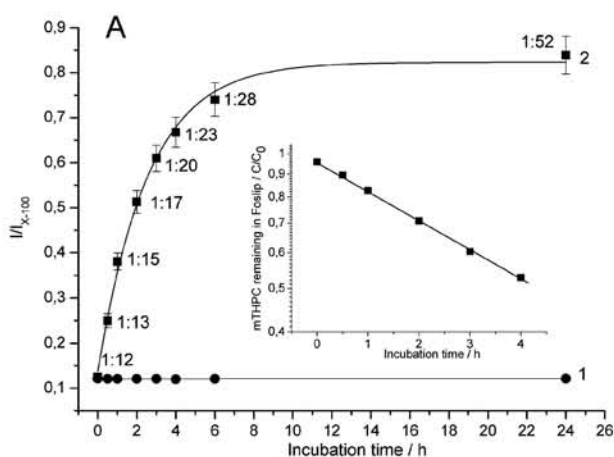


Fig. 5 Redistribution of m-THPC from Foslip® and Fospeg® to blood serum proteins. A. Redistribution kinetics from Foslip®: 1 – reference curve (Foslip® in PBS), 2 – Foslip®-based m-THPC incubated with serum. B. Redistribution kinetics from Fospeg®: 1 – reference curve (Fospeg® in PBS), 2 – Fospeg®-based m-THPC incubated with serum. Values at the curves stand for the calculated dye : lipid ratios. Insets display the kinetics of m-THPC remaining in liposomes. Serum concentration 5%, incubation temperature 37 °C.

Discussion

Characterization of m-THPC in liposomes

Spectroscopic characteristics of m-THPC in different liposomes with varying m-THPC : lipid ratios (Tables 1, 2) clearly demonstrate an impact of dye-dye interactions at high liposomal dye loads, opposed to low ones (ratios below 1 : 250). A decrease in the distance between dye molecules increases the probability of resonance energy transfer,¹⁵ which leads to significant depolarization and appearance of photoinduced fluorescence quenching (Tables 1, 2). Increasing the dye load above 1:45 results in noticeable red Soret band shift and a lower fluorescence yield, thus pointing out to probable m-THPC aggregation.²⁴ However, considering that Soret band width and extinction coefficient are unaffected, we can deduce that only a minor part of m-THPC embedded in lipid vesicles is in aggregated state. The strong RLS signal in dye-loaded liposomes is red-shifted compared to absorption, which could indicate the presence of J-aggregates²⁵ in liposomes, more pronounced for Fospeg® than for Foslip® (Fig. 1, curves 1, 2). m-THPC aggregation in liposomes is clearly concentration dependent, since dye ratios above 1:100 do not provoke a detectable RLS signal. Monomerization of m-THPC by neutral detergent destruction of liposomes is accompanied by a complete disappearance of the RLS signal in the Soret band region (curve 3).

m-THPC localization in liposomes

The localization of the dye molecules within the lipid bilayer affects the pharmacokinetics of the formulation, and differs according to the intrinsic properties of both the lipid components and the active molecule. In dynamic quenching, K_Q is proportional to the probability of collision of the dye with the quencher, thus the apparent quenching constant also characterizes the partition of m-THPC in liposomes. Quantitatively, the deeper the location of dye in lipid bilayer, the larger the difference between K_Q in liposomes and in solution. In the present study, we obtained a K_Q value in PEG-2000/PBS solution (3.85 M^{-1}) approximately two times higher than in conventional liposomes, comparable to the values obtained by Bronshtein *et al.*²⁶ for hematoporphyrins in the outer layer of DMPC liposomes and by Lavi *et al.* for protoporphyrins.²⁷ Our data indicate that m-THPC is incorporated within the lipid bilayer and is partially shielded from iodide.

Considering the quenching pattern of m-THPC in conventional liposomes (Fig. 2B, curve 1), the dye is heterogeneously distributed within the lipid bilayer,²⁰ and only 28% of m-THPC molecules are accessible to iodide. Higher K_Q and the accessible fraction of 36% in PEGylated liposomes indicate that a larger percentage of m-THPC molecules is located in a more suitable environment for interaction with the iodide quencher (Fig. 2B, curve 2). Since m-THPC can be solubilized to a certain extent in a PEG solution, it is probable that part of m-THPC resides in the PEG shell, hence the more efficient iodide quenching. The relative amount of m-THPC located in the PEG shell depends on the liposomal m-THPC content, increasing with higher dye load, albeit the correct quantitative measurements with fluorescence quenching technique are hindered due to the presence of aggregation in high drug load liposomes.

Temperature affects the m-THPC localization within the liposomal membrane. Following the fluidization of the membrane by heating, K_Q decreases for both conventional and PEGylated liposomes (Fig. 3), suggesting a progressive inward displacement of m-THPC molecules into the lipid bilayer as proposed by Lavi *et al.*²⁷ Notably, above the phase transition temperature all m-THPC molecules are equally accessible to iodide (Fig. 3B). This correlates with the findings of Bombelli *et al.*,²⁸⁻²⁹ where an increase in the fraction of m-THPC accessible to iodide was noted after the phase transition. This effect could also be partly attributed to the enhanced permeation of iodide within the lipid membranes after heating.²⁶

Redistribution of m-THPC from liposomes

We evaluated m-THPC release rate from liposomal carriers to biological substrates (liposomes and serum proteins). Upon addition of DPPC liposomes there is a progressive transfer of m-THPC towards the acceptor structures, indicated by the increase in normalized fluorescence (Fig. 4).

It appears that redistribution of m-THPC from Foslip® to lipid membranes is a very slow one-phase process, and the final distribution is only achieved after approximately 8 h of incubation at 37 °C. This kinetics is consistent with the recently described findings,¹³ where the intermembrane m-THPC release from conventional liposomes with low drug load was studied, as well as our own previous study following Foslip® intratumoral injection.⁶

In the case of Fospeg®, a very different two-phase pattern of redistribution is observed. A significant amount of m-THPC (more than 20%) is released after several minutes of incubation. During the slow phase (from 30 min onward) the rate of release is much lower compared to the fast phase.

A similar pattern is observed when liposomal formulations are incubated in serum (Fig. 5). The amount of m-THPC released from liposomes during the first 30 min of incubation in the presence of serum differs by a factor of 3.5 for Fospeg® and Foslip®, being 38% and 11%, respectively. During further incubation, the release from Fospeg® proceeds significantly slower, so that after further 3.5 h of incubation only an additional 12% is released, *versus* 46% in Foslip®.

Inclusion of PEGylated lipids into lipid vesicles usually prevents interaction with serum proteins and cells, which leads to increased drug retention time in lipid carriers, described both in *in vivo*³⁰⁻³² and *in vitro* studies.³³⁻³⁵ In the present study the m-THPC release from Fospeg® does not follow this pattern directly. According to our data, about 40% of the dye is released 4 times faster than from Foslip®, whereas the remaining photosensitizer redistributes much slower. These release kinetics tend to confirm the above-mentioned suggestion regarding two m-THPC pools in Fospeg® with a different localization. Slow-releasing molecules are localized in the lipid bilayer similar to Foslip®, while a percentage of m-THPC is likely to be present in the PEG shell with an easy access to acceptor structures.

The release process is likely to be different for two liposomal m-THPC formulations. The redistribution from Foslip® is a one-step process, involving the interaction with acceptors or release into the media. The relocation of lipid bilayer-bound m-THPC from Fospeg® can be envisioned as the transfer from the lipid

bilayer to the polymer shell, followed by the redistribution from it to acceptors. Release of m-THPC molecules confined to PEG shell occurs similarly to Foslip®-bound dye.

The aggregated fraction of m-THPC, mostly present in PEG shell, is unlikely to exert a significant influence on release kinetics given its low contribution to total m-THPC content.

m-THPC molecules localized in different sites in Fospeg® exhibit distinct dependence of the release rate on the temperature (Fig. 6). The release of m-THPC residing in lipid bilayer is very slow at temperatures below 30 °C, and sharply accelerates at higher temperatures. A phase transition of the lipid bilayer facilitates the process of sensitizer release from liposomes,³⁶⁻³⁷ which was observed for m-THPC.¹³ Due to very high load of m-THPC in donor liposomes, the phase transition temperature is shifted below physiological temperatures (35.7 °C for conventional liposomes and 37 °C for PEGylated liposomes) compared to pure DPPC/DPPG liposomes (41.5 °C),¹⁴ thus leading to a rapid release of m-THPC. In contrast to the dye in the lipid bilayer, m-THPC release from the PEG shell is hardly influenced by temperature changes from 20 to 50 °C.

Thermodynamic parameters may provide useful information on the mechanism of drug redistribution. High activation energy value for Foslip® confirms the slow rate of the drug release from liposomes. Comparable activation energy was obtained for m-THPC release from proteins³⁸ (11.3 kcal mol⁻¹) and from low-drug load liposomes¹³ (10.5 kcal mol⁻¹). Both enthalpic and entropic processes contribute substantially to the free energy of activation for Foslip®, indicating combined collisional and aqueous transfer to serum proteins.³⁸⁻³⁹ This was shown for m-THPC interliposomal release.¹³ Combined mechanism of m-THPC transfer to serum proteins is supported by the study of the effect of acceptor concentration on m-THPC release. A 25-fold decrease in the serum concentration results only in a slight decrease in the release rate, much lower than expected from pure collision model.⁴⁰ Much lower activation energy for fast phase of Fospeg® (0.51 kcal mol⁻¹) is consistent with very fast release of PEG-bound m-THPC. This process is entirely entropy-controlled, indicating the aqueous transfer route.³⁹⁻⁴⁰

Conclusions

Summarizing the results of our study, we conclude that PEGylation of high m-THPC load liposomes results in altered drug localization in the formulation, with a portion of m-THPC residing in the PEG shell. This leads to distinct differences in drug release kinetics in model system of blood serum components. Further studies will be focused on the behaviour of liposomal m-THPC in *in vivo* models with regards to drug release.

Acknowledgements

This work was supported by Centre Alexis Vautrin research funds, French Ligue Nationale contre le Cancer, ECO-NET program (18815ZE) of the Ministry of Foreign and European Affairs of France and by the Belarusian Foundation for Fundamental Research (grant B09K-035). We thank the Ministry of Foreign and European Affairs of France for awarding fellowships to V.R. and D.K., and Biolitec (Jena, Germany) for providing us

with m-THPC, Foslip® and Fospeg®. T.S. acknowledges the FEBS Collaborative Experimental fellowship. We are grateful to Prof. Michel Linder and Ms. Behnoush Maherani of ENSAIA, INPL, France, for their kind help with DLS; to Prof. Alexander Potapenko of the Russian State Medical University, Russian Federation, for his valuable input.

Notes and references

- 1 S. B. Brown, E. A. Brown and I. Walker, The present and future role of photodynamic therapy in cancer treatment, *Lancet Oncol.*, 2004, **5**, 497–508.
- 2 D. K. Chatterjee, L. S. Fong and Y. Zhang, Nanoparticles in photodynamic therapy: an emerging paradigm, *Adv. Drug Delivery Rev.*, 2008, **60**, 1627–1637.
- 3 D. C. Drummond, O. Meyer, K. Hong, D. B. Kirpotin and D. Papahadjopoulos, Optimizing liposomes for delivery of chemotherapeutic agents to solid tumors, *Pharmacol. Rev.*, 1999, **51**, 691–743.
- 4 K. Lang, J. Mosinger and D. M. Wagnerová, Photophysical properties of porphyrinoid sensitizers non-covalently bound to host molecules; models for photodynamic therapy, *Coord. Chem. Rev.*, 2004, **248**, 321–350.
- 5 J. Svensson, A. Johansson, S. Gräfe, B. Gitter, T. Trebst, N. Bendsoe, S. Andersson-Engels and K. Svanberg, Tumor selectivity at short times following systemic administration of a liposomal temoporfin formulation in a murine tumor model, *Photochem. Photobiol.*, 2007, **83**, 1211–1219.
- 6 M. A. D'Hallewin, D. Kochetkov, Y. Viry-Babel, A. Leroux, E. Werkmeister, D. Dumas, S. Gräfe, V. Zorin, F. Guillemain and L. Bezdetnaya, Photodynamic therapy with intratumoral administration of lipid-based mTHPC in a model of breast cancer recurrence, *Lasers Surg. Med.*, 2008, **40**, 543–549.
- 7 H.-P. Lassalle, D. Dumas, S. Gräfe, M.-A. D'Hallewin, F. Guillemain and L. Bezdetnaya, Correlation between *in vivo* pharmacokinetics, intratumoral distribution and photodynamic efficiency of liposomal mTHPC, *J. Controlled Release*, 2009, **134**, 118–124.
- 8 D. D. Lasic, F. J. Martin, A. Gabizon, S. K. Huang and D. Papahadjopoulos, Sterically stabilized liposomes: a hypothesis on the molecular origin of the extended circulation times, *Biochim. Biophys. Acta, Biomembr.*, 1991, **1070**, 187–192.
- 9 A. S. Derycke and P. A. de Witte, Liposomes for photodynamic therapy, *Adv. Drug Delivery Rev.*, 2004, **56**, 17–30.
- 10 B. Pegaz, E. Debeve, J. P. Ballini, G. Wagnieres, S. Spaniol, V. Albrecht, D. V. Scheglmann, N. E. Nifantiev, H. Van Den Bergh and Y. N. Konan-Kouakou, Photothrombotic activity of m-THPC-loaded liposomal formulations: pre-clinical assessment on chick chorioallantoic membrane model, *Eur. J. Pharm. Sci.*, 2006, **28**, 134–140.
- 11 J. Buchholz, B. Kaser-Hotz, T. Khan, C. Rohrer Bley, K. Melzer, R. A. Schwendener, M. Roos and H. Walt, Optimizing photodynamic therapy: *in vivo* pharmacokinetics of liposomal meta-(tetrahydroxyphenyl)chlorin in feline squamous cell carcinoma, *Clin. Cancer Res.*, 2005, **11**, 7538–7544.
- 12 S. Petersen, A. Fahr and H. Bunjes, Flow Cytometry as a New Approach To Investigate Drug Transfer between Lipid Particles, *Mol. Pharmaceutics*, 2010, **7**, 350–363.
- 13 H. Hefesha, S. Loew, X. Liu, S. May and A. Fahr, Transfer mechanism of temoporfin between liposomal membranes, *J. Controlled Release*, DOI: 10.1016/j.jconrel.2010.09.021.
- 14 J. Kuntsche, I. Freisleben, F. Steiniger and A. Fahr, Temoporfin-loaded liposomes: Physicochemical characterization, *Eur. J. Pharm. Sci.*, 2010, **40**, 305–315.
- 15 D. Kachatkou, S. Sasnouski, V. Zorin, T. Zorina, M. A. D'Hallewin, F. Guillemain and L. Bezdetnaya, Unusual photoinduced response of mTHPC liposomal formulation (Foslip), *Photochem. Photobiol.*, 2009, **85**, 719–724.
- 16 M. J. Hope, R. Nayar, L. D. Mayer and P. R. C. Cullis, Reduction of liposome size and preparation of unilamellar vesicles by extrusion techniques, in *Liposome Technology, Volume I*, ed. G. Gregoriadis, CRC Press, Boca Raton, 1993, pp. 123–139.
- 17 E. G. Finer, A. G. Flook and H. Hauser, Mechanism of sonication of aqueous egg yolk lecithin dispersions and nature of the resultant particles, *Biochim. Biophys. Acta, Lipids Lipid Metab.*, 1972, **260**, 49–58.

- 18 A. Tikhomirov, T. Shmigol, E. Kozhinova, A. Kyagova, L. Bezdetnaya and A. Potapenko, Correction of spectra for studying dye aggregates by resonance light scattering, *Biophysics*, 2010, **54**, 584–589.
- 19 P. J. Collings, E. J. Gibbs, T. E. Starr, O. Vafek, C. Yee, L. A. Pomerance and R. F. Pasternack, Resonance light scattering and its application in determining the size, shape, and aggregation number for supramolecular assemblies of chromophores, *J. Phys. Chem. B*, 1999, **103**, 8474–8481.
- 20 J. R. Lakowicz, *Principles of Fluorescence Spectroscopy*, Springer, Berlin, 2006.
- 21 V. V. Menshikov, *Laboratory research techniques in clinics*, Moscow: Nauka, 1987.
- 22 H. Eyring, The Activated Complex in Chemical Reactions, *J. Chem. Phys.*, 1935, **3**, 107–115.
- 23 F. Ricchelli and S. Gobbo, Porphyrins as fluorescent probes for monitoring phase transitions of lipid domains in biological membranes. Factors influencing the microenvironment of haematoporphyrin and protoporphyrin in liposomes, *J. Photochem. Photobiol., B*, 1995, **29**, 65–70.
- 24 S. Sasnouski, V. Zorin, I. Khludeyev, M. A. D'Hallewin, F. Guillemain and L. Bezdetnaya, Investigation of Foscan interactions with plasma proteins, *Biochim. Biophys. Acta, Gen. Subj.*, 2005, **1725**, 394–402.
- 25 J. Parkash, J. H. Robblee, J. Agnew, E. Gibbs, P. Collings, R. F. Pasternack and J. C. de Paula, Depolarized resonance light scattering by porphyrin and chlorophyll a aggregates, *Biophys. J.*, 1998, **74**, 2089–2099.
- 26 I. Bronshtein, M. Afri, H. Weitman, A. A. Frimer, K. M. Smith and B. Ehrenberg, Porphyrin depth in lipid bilayers as determined by iodide and parallax fluorescence quenching methods and its effect on photosensitizing efficiency, *Biophys. J.*, 2004, **87**, 1155–1164.
- 27 A. Lavi, H. Weitman, R. T. Holmes, K. M. Smith and B. Ehrenberg, The depth of porphyrin in a membrane and the membrane's physical properties affect the photosensitizing efficiency, *Biophys. J.*, 2002, **82**, 2101–2110.
- 28 C. Bombelli, G. Caracciolo, P. Di Profio, M. Diociaiuti, P. Luciani, G. Mancini, C. Mazzuca, M. Marra, A. Molinari, D. Monti, L. Toccaceli and M. Venanzi, Inclusion of a photosensitizer in liposomes formed by DMPC/gemini surfactant: correlation between physicochemical and biological features of the complexes, *J. Med. Chem.*, 2005, **48**, 4882–4891.
- 29 C. Bombelli, A. Stringaro, S. Borocci, G. Bozzuto, M. Colone, L. Giansanti, R. Sgambato, L. Toccaceli, G. Mancini and A. Molinari, Efficiency of liposomes in the delivery of a photosensitizer controlled by the stereochemistry of a gemini surfactant component, *Mol. Pharmaceutics*, 2010, **7**, 130–137.
- 30 D. Goren, A. T. Horowitz, S. Zalipsky, M. C. Woodle, Y. Yarden and A. Gabizon, Targeting of stealth liposomes to erbB-2 (Her/2) receptor: in vitro and in vivo studies, *Br. J. Cancer*, 1996, **74**, 1749–1756.
- 31 T. Yang, F. D. Cui, M. K. Choi, J. W. Cho, S. J. Chung, C. K. Shim and D. D. Kim, Enhanced solubility and stability of PEGylated liposomal paclitaxel: in vitro and in vivo evaluation, *Int. J. Pharm.*, 2007, **338**, 317–326.
- 32 P. Crosasso, M. Ceruti, P. Brusa, S. Arpicco, F. Dosio and L. Cattel, Preparation, characterization and properties of sterically stabilized paclitaxel-containing liposomes, *J. Controlled Release*, 2000, **63**, 19–30.
- 33 P. Panwar, B. Pandey, P. C. Lakhera and K. P. Singh, Preparation, characterization, and in vitro release study of albendazole-encapsulated nanosize liposomes, *Int. J. Nanomed.*, 2010, **5**, 101–108.
- 34 C. Celia, M. G. Calvagno, D. Paolino, S. Bulotta, C. A. Ventura, D. Russo and M. Fresta, Improved in vitro anti-tumoral activity, intracellular uptake and apoptotic induction of gemcitabine-loaded pegylated unilamellar liposomes, *J. Nanosci. Nanotechnol.*, 2008, **8**, 2102–2113.
- 35 Y. Sadzuka, K. Tokutomi, F. Iwasaki, I. Sugiyama, T. Hirano, H. Konno, N. Oku and T. Sonobe, The phototoxicity of photofrin was enhanced by PEGylated liposome in vitro, *Cancer Lett.*, 2006, **241**, 42–48.
- 36 A. Fahr, P. v. Hoogevest, S. May, N. Bergstrand and M. L. S. Leigh, Transfer of lipophilic drugs between liposomal membranes and biological interfaces: Consequences for drug delivery, *Eur. J. Pharm. Sci.*, 2005, **26**, 251–265.
- 37 K. Kuzelova and D. Brault, Kinetic and equilibrium studies of porphyrin interactions with unilamellar lipidic vesicles, *Biochemistry*, 1994, **33**, 9447–9459.
- 38 S. Sasnouski, D. Kachatkou, V. Zorin, F. Guillemain and L. Bezdetnaya, Redistribution of Foscan from plasma proteins to model membranes, *Photochem. Photobiol. Sci.*, 2006, **5**, 770–777.
- 39 K. T. Hsu and J. Storch, Fatty acid transfer from liver and intestinal fatty acid-binding proteins to membranes occurs by different mechanisms, *J. Biol. Chem.*, 1996, **271**, 13317–13323.
- 40 H. K. Kim and J. Storch, Mechanism of free fatty acid transfer from rat heart fatty acid-binding protein to phospholipid membranes. Evidence for a collisional process, *J. Biol. Chem.*, 1992, **267**, 20051–20056.

2. COMPARISON OF FLUORESCENCE METHODS SUITABLE FOR MTHPC RELEASE STUDIES

The second part of the results is presented in the article published in 2011 on the methods of mTHPC release measurement.

Fluorescence methods for detecting the kinetics of photosensitizer release from nanosized carriers

V.A. Reshetov, T.E. Zorina, M.-A. D'Hallewin, L.N. Bolotine, and V.P. Zorin
Journal of Applied Spectroscopy; 2011. 78(1):103-109

Three methods to evaluate the mTHPC release from liposomes were compared: fluorescence energy transfer from the lipid probe, anisotropy, and photoinduced fluorescence quenching of mTHPC. The interliposomal release of mTHPC was estimated in the conditions of excess of acceptor vesicles, which allowed not to take into account the back transfer of mTHPC from acceptor to donor liposomes. The temperature was found to significantly affect the drug release rate from the liposomes. Each method was sensitive within a certain range of mTHPC concentrations in donor liposomes. Photoinduced fluorescence quenching possessed the widest range of sensitivity.

FLUORESCENCE METHODS FOR DETECTING THE KINETICS OF PHOTOSENSITIZER RELEASE FROM NANOSIZED CARRIERS

V. A. Reshetov,^{a,b*} T. E. Zorina,^a M.-A. D'Hallewin,^b
L. N. Bolotina,^b and V. P. Zorin^a

UDC 577.352.2:615.011.3

Three approaches to analyzing the rate of release of the photosensitizer meta-tetrahydroxyphenylchlorin (mTHPC) from unilaminar lipid vesicles (ULV) in model biological systems are studied: by excitation energy transfer from probe diphenylhexatriene to mTHPC, by the fluorescence anisotropy of mTHPC, and by photoinduced quenching of the fluorescence of mTHPC. Each of these methods has its characteristic range of sensitivity for measurements of the local concentration of mTHPC in ULV. Fluorescence anisotropy can be used for quantitative determination of the mTHPC yield from ULV for mTHPC:lipid ratios of 1:100 to 1:1000, determining the efficiency of fluorescence quenching of diphenylhexatriene for ratios <1:200, and photoinduced quenching for ratios of 1:10–1:500.

Keywords: lipid vesicles, meta-tetrahydroxyphenylchlorin, drug redistribution, energy transfer, fluorescence anisotropy.

Introduction. Nanosized unilaminar lipid vesicles (ULV) are one of the most widespread ways of delivering water insoluble drug compounds [1, 2]. ULV are closed spherical structures formed by a unilaminar bilayer of natural or synthetic lipids with sizes of 50–1000 nm. Liposomal delivery systems represent a significant change in the pharmacokinetics of drug compounds, since the processes by which they are biologically distributed depends in this case on both the properties of the compound itself and on the properties of the ULV. This makes it necessary to develop methods for nondestructive monitoring of the drug yield from lipid carriers. When the drug compound has fluorescence spectral techniques can be used to monitor the biodistribution.

This paper evaluates the feasibility of using various spectral techniques for detecting the kinetics (time dependence) of the release of meta-tetrahydroxyphenylchlorin (mTHPC), a second generation photosensitizer currently in use in clinical practice for photodynamic cancer therapy, from the composition of classical unilaminar lipid vesicles. This compound has a low polarizability and is essentially insoluble in aqueous media [3]. In order to improve the bio-distribution characteristics when mTHPC is introduced into an organism, various liposomal forms are used, including classical and steric stabilized unilaminar lipid vesicles composed of synthetic lipids. For detecting the yield kinetics of the photosensitizer from ULV we have used several characteristics of the fluorescence of mTHPC which depend on its concentration in the carrier composition: the efficiency with which excitation energy is transferred between the lipid-bound fluorescence probe diphenylhexatriene (DPHT) and mTHPC, the fluorescence anisotropy of mTHPC, and the recently described photoinduced quenching of mTHPC in liposomes [4].

Materials and Methods. *Reagents.* mTHPC provided by the Biolitec company (Jena, Germany) was dissolved in 99% ethyl alcohol to a concentration of 10^{-3} M. Dimyristoylphosphatidylcholine (DMPC), dipalmitoylphosphatidylcholine (DPPC), and the neutral detergent t-octylphenoxypolyethoxyethanol (Triton® X-100) manufactured by Sigma Aldrich (Lyon, France) were used and 2-(3-(diphenylhexatrienyl)propanoyl)-1-hexadecanoyl-sn-glycero-3-phosphocholine (DPHT) was obtained from Molecular Probes (Eugene, USA). All the other reagents were at least chemically pure grade.

*To whom correspondence should be addressed.

^aBelarusian State University, 4 Nezavisimosti Ave., Minsk 220030, Belarus; e-mail: vadim.reshetov@gmail.com;

^bCentre de Recherche en Automatique de Nancy, Nancy-University CNRS, Centre Alexis Vautrin, Vandoeuvre-Les-Nancy, France. Translated from Zhurnal Prikladnoi Spektroskopii, Vol. 78, No. 1, pp. 114–120, January–February, 2011. Original article submitted August 27, 2010.

ULV preparation. (Donor) ULV loaded with mTHPC were prepared using an injection method [5]. A standard solution containing DMPC or DPPC was injected into 3 mL of phosphate-salt buffer at a rate of 1 $\mu\text{L/s}$ with constant mixing and incubated for 30 min at 45°C. The final concentration of the lipid was 0.2 mg/mL; the suspension was stored at 37°C. mTHPC and DPHT were included in the ULV during the stage when a dilipid was added to the standard solution in order to obtain the required lipid:dye molar ratio. The concentration of mTHPC in the dilipid suspension was measured with a Solar PV 1251A (Minsk, Belarus) spectrophotometer using a molar extinction coefficient of $\epsilon = 30,000 \text{ M}^{-1}/\text{cm}$ for the mTHPC at $\lambda = 650 \text{ nm}$.

(Acceptor) ULV without dye were prepared by an ultrasonic method [6]: 40 mg of DMPC or DPPC was dissolved in 1 mL of the standard and evaporated to form a lipid film on the walls of the spherical flask. The dried lipid film was wetted with 2 mL of phosphate-salt buffer for 15 min and irradiated in a UZDN-2T (Ukrrospribor, Sumi, Ukraine) ultraviolet disperser for 5 min. The resulting ULV were stored at 37°C.

Fluorescence measurements. The fluorescence characteristics were measured using a Solar SFL 1211A (Minsk, Belarus) equipped with polarizers and a thermostated cell with magnetic stirring. Fluorescence of DPHT was excited at $\lambda = 354 \text{ nm}$ and of mTHPC at $\lambda = 420 \text{ nm}$. For measuring the fluorescence anisotropy (r) of mTHPC the samples were excited at $\lambda = 435 \text{ nm}$ and the fluorescence was detected at $\lambda = 652 \text{ nm}$. The fluorescence anisotropy was evaluated using the formula $r = (I_{\parallel} - kI_{\perp}) / (I_{\parallel} + 2kI_{\perp})$, where I_{\parallel} and I_{\perp} are the fluorescence intensities with the polarizers in parallel and perpendicular positions, and k is a coefficient that accounts for the polarizing properties of the monochromators. The optical density of all the samples at the excitation and fluorescence detection wavelengths the optical densities of all the samples were at most 0.15.

Photoinduced quenching of fluorescence of mTHPC. The samples were irradiated at $\lambda = 660 \text{ nm}$ by an ILM-660-0.5 semiconductor laser. The energy flux of the light was 50 mW/cm^2 and the irradiation took place with constant stirring at room temperature for 10 s. Irradiation at these doses involves negligible (<1%) changes in the concentration of mTHPC, but does cause photoinduced quenching of the fluorescence of a sort to be examined below. For quantitative description of the photoinduced quenching, we used the normalized fluorescence intensity, defined as the ratio I/I_{X-100} , where I is the fluorescence intensity of a ULV sample in the emission band of mTHPC measured immediately after irradiation and I_{X-100} is the fluorescence intensity measured after adding 0.2% Triton® X-100 to the sample.

Analysis of the redistribution kinetics of mTHPC. For studying the photosensitizer redistribution kinetics, donor ULV loaded with mTHPC in the proportion phospholipid:mTHPC=400:1 were mixed with excess acceptor ULV of DMPC or DPPC (concentrations of the donor and acceptor vesicles in a ratio $\geq 1:10$) and incubated at a given temperature. Samples of the resulting suspension were analyzed immediately after mixing or after incubation for a fixed amount of time (from 1 to 24 h). The concentration of mTHPC in the analyzed samples was $3 \cdot 10^{-7} \text{ M}$.

Results and Discussion. Because of its low polarization, mTHPC has a high affinity for the lipid bilayer. It was shown by ultracentrifuging and gel chromatography that in the lipid vesicles mTHPC is in a bound state and does not enter the water phase. Because of the relatively small volume of the lipid phase, the local concentration of mTHPC in the ULV is high even for low loading of the vesicles with the photosensitizer [4]; this leads to a high probability of interactions of the mTHPC molecules among themselves and with other chromophores contained in the ULV.

Transfer of excitation energy between lipid-bound DPHT and mTHPC. The first approach for studying the redistribution of mTHPC between the ULV examined here is based on determining the efficiency of energy transfer between the probe DPHT bound covalently to lipid molecules and the photosensitizer. The DPHT, conjugated with a lipid in the ULV, has intense fluorescence with a peak at $\lambda = 431 \text{ nm}$ (Fig. 1, curve 1). The fluorescence spectrum of DPHT overlaps the absorption spectrum of mTHPC (curve 4), so adding mTHPC to the vesicles with DPHT ensures a high probability of nonradiative transfer of excitation energy from DPHT to mTHPC. In fact, the Foerster radius for this donor-acceptor pair is comparable to the thickness of the lipid bilayer ($\sim 4.5 \text{ nm}$) and the average distances between chromophore molecules in the ULV (3.2 nm for DMPC:mTHPC) [7]. Adding mTHPC to ULV at DMPC:mTHPC=400:1 leads to quenching of the fluorescence probe by 60% (curve 3). Here the fluorescence excitation spectrum of mTHPC contains bands belonging to DPHT. Destruction of the lipid vesicles by a neutral detergent restores the fluorescence of the DPHT.

The efficiency of energy transfer depends on the local concentration of mTHPC in the ULV and, therefore, varies significantly as molecules of it emerge from the donor vesicles. We have studied the kinetics of the changes in intensity of the fluorescence of DPHT following the addition of excess acceptor ULV (Fig. 2). Incubating the

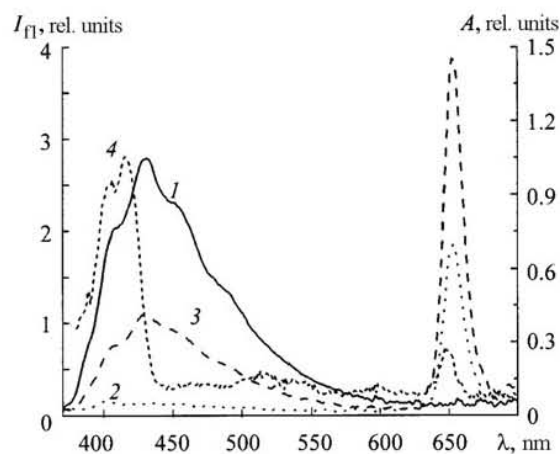


Fig. 1. Fluorescence spectra of donor unilaminar lipid vesicles dyed with DPHT (1), mTHPC (2), and simultaneously with mTHPC and DPHT (3); DMPC:DPHT=300:1; DMPC:mTHPC=400:1; λ_{exc} =354 nm; (4) absorption spectrum of mTHPC in the standard.

mixed suspension at temperatures of 40 and 55°C leads to a gradual increase over several hours in the intensity of the DPHT fluorescence intensity (I_{fl}) which is obviously related to the separation of the mTHPC and the lipid-bound marker in the donor vesicles. This effect is not a consequence of the redistribution of the covalent marker to acceptor ULV. The rate of exchange between lipid vesicles of the conjugates of the phospholipids with pyrene, which have analogous properties to the conjugates of DPHT has been estimated [8]. Based on the excimer fluorescence of pyrene it was shown that the rate of escape of the marked lipid from the ULV is extremely low. No more than 15% of the lipid molecules marked by the fluorescent marker were redistributed from ULV made from DMPC after 10 h of incubation at 37°C. Thus, the change in the fluorescence intensity of DPHT in the system studied here is caused by redistribution of mTHPC from donor to acceptor ULV.

The rate of emergence of mTHPC from the lipid vesicles is very sensitive to the temperature of the incubating medium. Incubation at low temperatures (11°C) does not produce any change in the fluorescence intensity of DPHT, which indicates that the localization of mTHPC in the donor liposomes is unchanged (Fig. 2, curve 1). At higher temperatures the fluorescence of DPHT flares up in the mixed ULV suspension. At 40°C the equilibrium distribution is reached after 10–15 h (curve 2) and at 55°C this process is completed over 2–3 h (curve 3). These large differences in the rate of redistribution of the photosensitizer are probably caused by thermally induced changes in the structure of the lipid bilayer of the donor ULV [9]. At low temperatures the state of the lipid bilayer corresponds to a gel phase, which is characterized by low mobility and dense packing of the lipid chains. When the temperature is increased beyond 21–23°C, a phase transition to a liquid crystal state, in which the lipid chains are disordered and are highly mobile, occurs in the lipid bilayer of DMPC ULV. These structural changes increase the rate at which the ligands escape from the ULV [9]. The temperature range within which the rate of escape of mTHPC increases coincides with the range of temperatures in which the phase state of the lipid bilayer changes (measured as 20–23°C).

These results show that the method based on determining the efficiency with which the electronic excitation energy is transferred between a membrane-bound fluorescent marker and mTHPC can be used for continuous monitoring of the redistribution of a photosensitizer from a ULV. This method provides the most information when donor ULV with mTHPC:DMPC < 1:200 are used. With high vesicle loading the accuracy of the quantitative estimate of the rate of release of mTHPC falls off sharply owing to the nonlinear dependence of the degree of quenching of DPHT on the mTHPC concentration in the vesicles.

Anisotropic fluorescence of mTHPC. The dependence of the anisotropy in the fluorescence of mTHPC on its concentration in the ULV was studied. For low loading of the ULV with the sensitizer (DMPC:mTHPC > 1000:1), the

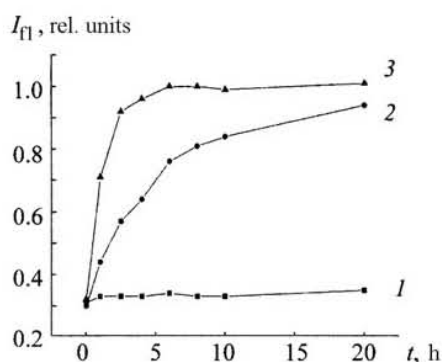


Fig. 2. Redistribution kinetics of mTHPC between donor and acceptor ULV made up of DMPC at incubation temperatures of 11 (1), 40 (2), and 55°C (3); the ratio of the concentrations of the donor and acceptor vesicles is 1:10, the donor ULV consist of DMPC:DPHT = 300:1, DMPC:mTHPC = 400:1; t is the incubation time for the mixed suspension of unilaminar lipid vesicles.

fluorescence of mTHPC is characterized by a high anisotropy ($r = 0.25$) (Fig. 3), which indicates rigid fixing of the mTHPC in the lipid bilayer. With increasing mTHPC content in the ULV, the anisotropy decreases, with complete depolarization of the fluorescence when the lipid:pigment ratio $< 50:1$. It has been shown [10, 11] that the basis of this concentration dependent fluorescence depolarization is direct Foerster energy transfer between monomer mTHPC molecules in the lipid bilayer. The existence of a unique relationship between r and the level of loading of the vesicles with mTHPC means that this fluorescence characteristic can be used to detect the redistribution of the photosensitizer from a ULV structure into analogous acceptor structures. Figure 4 shows the measured fluorescence anisotropy of mTHPC during incubation of dyed donor ULV in the presence of an excess of the same type of acceptor vesicles. Redistribution of the photosensitizer leads to a drop in the average concentration of mTHPC in the lipid phase and, as a consequence, to a rise in the anisotropy of its fluorescence. Using the dependence of r on the DMPC:mTHPC ratio (Fig. 3) as a calibration curve, it is possible to estimate the amount of mTHPC remaining in the donor ULV at any given time.

Measuring the fluorescence anisotropy to trace the kinetics of interliposomal redistribution of mTHPC yields results that are analogous to those obtained using a DPHT -tagged lipid. During low-temperature incubation, r remains constant for a sample in a mixed suspension. This indicates that mTHPC is essentially not escaping from the donor ULV over the entire incubation time (Fig. 4, curve 1). Raising the temperature of the incubation medium above the phase transition point of a DMPC liposome (23°C) speeds up the redistribution process significantly and, therefore, causes a significant increase in the fluorescence anisotropy (curves 2 and 3). Note that the characteristic redistribution times for mTHPC are essentially the same at a given temperature according to the two methods described here.

Photoinduced quenching of fluorescence of mTHPC. Another method used in this paper to detect the time variation in the emergence of mTHPC from ULV is based on the dependence of the relative fluorescence yield of this photosensitizer as part of a liposome on the photoexposure dose. It has been shown [4] that low dose exposure (0.5 J/cm²) of a suspension of loaded ULV to laser light at $\lambda = 650$ nm causes a reduction in the fluorescence intensity by more than 90%. The observed effect is not a result of a higher rate of photo-burnup of mTHPC in the lipid carriers, since destruction of the irradiated ULV by the detergent leads to complete restoration of the fluorescence intensity. A study of the light dependent fluorescence quenching suggests that its mechanism is related to the formation, in the ULV, of a small amount of quenchant which are primary photooxidation products of mTHPC [4]. Under conditions of efficient homogeneous transfer of excitation energy, even small amounts of quenchant molecules can lead to quenching of the fluorescence of the entire pool of mTHPC molecules within a lipid vesicle.

As a quantitative characteristic of the efficiency of photoinduced quenching, it is convenient in practice to use the normalized fluorescence intensity I_{norm} (or I/I_{X-100}), defined as the ratio of the fluorescence intensities of the irra-

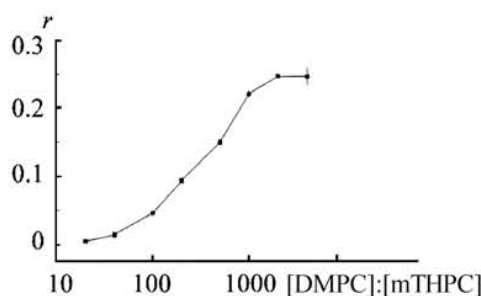


Fig. 3. The anisotropy of fluorescence in mTHPC in unilaminar lipid vesicles made of DMPC as a function of loading: $\lambda_{exc} = 435$ nm, $\lambda_{det} = 652$ nm.

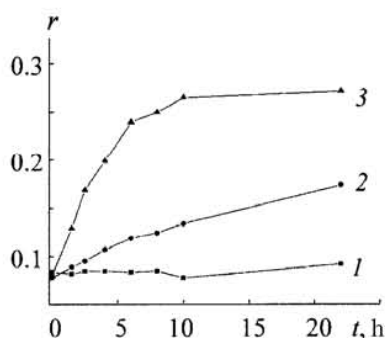


Fig. 4. Time variation of the anisotropy r in the fluorescence of mTHPC in a mixture of donor and acceptor unilaminar lipid vesicles made of DMPC at incubation temperatures of 11 (1), 40 (2), and 55°C (3); the donor ULV composition is mTHPC:DMPC = 1:100; the ratio of the concentrations of the donor and acceptor ULV is 1:10.

diated ULV before and after they are destroyed by the detergent. The magnitude of the irradiation dependent response depends strongly on the local concentration of mTHPC in the lipid bilayer, so that I_{norm} varies between 0.08 for ULV with DPPC:mTHPC = 10 to 0.82–0.84 for liposomal forms with minimal loading (DPPC:mTHPC > 1000). Similar dependences of I_{norm} on the degree of loading were obtained using ULV prepared from different lipids, including DMPC and distearoylphosphatidylcholine.

Measuring the normalized fluorescence intensity makes it possible to monitor the release of mTHPC from ULV. Figure 5 illustrates the variation in I_{norm} associated with the redistribution of the photosensitizer in a mixture of donor and acceptor liposomes made of DPPC. These data show that more than 20 h of incubation at 37°C is required to reach an equilibrium distribution of mTHPC in this system; this is indicative of a much lower rate of release of the photosensitizer from ULV made of DPPC compared to ULV made of DMPC.

It should be noted that a reduction in the local photosensitizer concentration in donor liposomes is not the main factor in the change of I_{norm} during redistribution of the photosensitizer in experiments with acceptor ULV. Here the main cause of the reduction in the efficiency of photoinduced quenching of the fluorescence is an increase in the pool of molecules that are localized in acceptor liposomes and, therefore, free of the influence of collective processes leading to quenching of the fluorescence. Compared to the methods described above, the technique of photoinduced fluorescence quenching affords a wider dynamic range for measurements of the sensitizer yield from liposomal carriers. Our data show that measuring the characteristics of photoinduced quenching provides a maximum accuracy in determining the release rate of mTHPC from ULV with loads (mol/mol) in the range of 0.5–10%. (The limit of

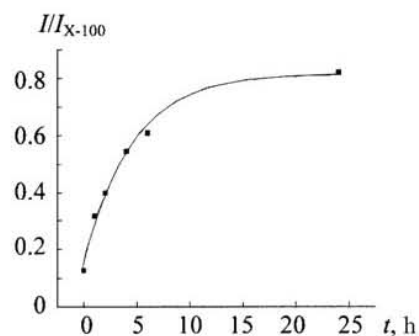


Fig. 5. Time variation of the normalized fluorescence of mTHPC in a mixture of donor and acceptor ULV made of DPPC; the composition of the donor ULV is mTHPC:DPPC = 1:20; the temperature of the medium is 37 C; λ_{exc} = 420 nm, λ_{det} = 652 nm.

sensitivity is 0.2%.) Measurements of fluorescence anisotropy are informative when ULV with loads $\leq 1\%$ are used; this is substantially below the amount of porphyrin photosensitizers in commercial liposomal molds (5–10%). Measurements of the normalized fluorescence are essentially independent of the type of acceptor structure to which mTHPC is bound after it emerges from the liposomal carriers. Thus, photoinduced quenching of fluorescence can be used to analyze pharmacokinetics in blood and in solid tissues [4, 12], as well as for detecting the kinetics of sensitizer redistribution in model studies.

Conclusion. The results reported here demonstrate that aspects of the fluorescence of *meta*-tetrahydroxyphenylchlorin incorporated in unilaminar lipid vesicles associated with its local concentration in the lipid bilayer can be used in the development of methods for continuous noninvasive monitoring of the release of mTHPC from lipid carriers in biological systems (e.g., of redistribution in blood serum). Using different fluorescence characteristics yields similar results on the rate of redistribution. According to our data the rate of release of sensitizer from unilaminar lipid vesicles is fairly low. It is comparable to the rate of destruction of liposomal forms in serum, so it becomes necessary to include the rate of release when analyzing the pharmacological behavior of mTHPC contained in biological systems.

Fluorescence anisotropy, fluorescence sensitization, and photoinduced fluorescence quenching have different sensitivities to the local photosensitizer concentration, and the efficiency with which they can be used depends on the degree of loading of the unilaminar lipid vesicles by the photosensitizer. For commercial liposomal mTHPC forms (with a sensitizer content of 10%), the most informative method is photoinduced fluorescence quenching. It can provide an exact quantitative estimate of the rate of redistribution of mTHPC immediately following the introduction of a liposomal preparation into a biological system.

REFERENCES

1. K. Lang, J. Mosinger, and D. M. Wagnerova, *Coord. Chem. Rev.*, **248**, 321–350 (2004).
2. T. M. Allen, C. B. Hansen, and D. E. L. de Menezes, *Adv. Drug Deliv. Rev.*, **16**, 267–284 (1995).
3. R. Bonnett, B. D. Djelal, A. Nguyen, and J. Porphir, *Phthaloc.*, **5**, No. 8, 652–661 (2001).
4. D. Kachatkou, S. Sasnouski, V. Zorin, T. Zorina, M. A. D’Hallewin, F. Guillemin, and L. Bezdetnaya, *Photochem. Photobiol.*, **85**, No. 3, 719–724 (2009).
5. S. Batzri and E. D. Korn, *Biochim. Biophys. Acta*, **298**, No. 4, 1015–1019 (1973).
6. H. Hauser, D. Oldani, and M. C. Phillips, *Biochemistry*, **12**, No. 22, 4507–4517 (1973).
7. V. Zorin, T. Zorina, and I. Mikhalovsky, *Proc. SPIE*, **2625**, 145–155 (1996).
8. V. P. Zorin, S. L. Sosnovskii, T. E. Zorina, I. I. Khludeev, L. N. Bolotina, and F. Gimya, *Dokl. NAN Belarusi*, **47**, No. 4, 96–99 (2003).

9. A. Fahr, P. V. Hoogevest, S. May, N. Bergstrand, and M. S. Leigh, *Eur. J. Pharm. Sci.*, **26**, Nos. 3–4, 251–265 (2005).
10. R. F. Chen and J. R. Knutson, *Anal. Biochem.*, **172**, 61–67 (1988).
11. A. A. Frolov, E. I. Zenkevich, G. P. Gurinovich, and G. A. Kochubeyev, *J. Photochem. Photobiol. B: Biol.*, **7**, 43–56 (1990).
12. M. A. D'Hallewin, D. Kochetkov, Y. Viry-Babel, A. Leroux, E. Werkmeister, D. Dumas, S. Gräfe, V. Zorin, F. Guillemain, and L. Bezdetnaya, *Lasers Surg. Med.*, **40**, No. 8, 543–549 (2008).

3. BINDING OF LIPOSOMAL MTHPC TO SERUM PROTEINS AND THE DESTRUCTION OF LIPOSOMES

The third part of the results is the article published in 2012 on the interaction of mTHPC encapsulated in conventional and PEGylated liposomes with serum proteins, with an emphasis on drug binding and liposomes destruction.

Interaction of Liposomal Formulations of Meta-tetra(hydroxyphenyl)chlorin (Temoporfin) with Serum Proteins: Protein Binding and Liposome Destruction

Vadzim Reshetov, Vladimir Zorin, Agnieszka Siupa, Marie-Ange D'Hallewin, François Guillemin and Lina Bezdetnaya

Photochem. Photobiol.; 2012. Accepted article, doi: 10.1111/j.1751-1097.2012.01176.x

The binding of liposomal mTHPC to human serum proteins was estimated using size-exclusion chromatography. It was found that the inclusion of mTHPC into Foslip® and Fospeg® did not affect equilibrium serum protein binding compared to solvent-based mTHPC. About 65% of the drug binds to high-density lipoproteins, and 35% - to low-density lipoproteins. No significant binding to albumin was found, indicating that liposomal mTHPC binds to lipoproteins in the monomer form, as opposed to Foscan®. Additionally, the rate of drug release from liposomes was estimated, and the results were consistent with those obtained by photoinduced fluorescence quenching. The measurements of the photoinduced quenching in the intact liposomes in serum indicated that the efflux of the drug was not the only process of mTHPC redistribution, but the destruction of liposomes was also involved.

We investigated the liposome destruction using the technique of nanoparticle tracking analysis. PEGylated liposomes were stable in serum for prolonged incubation times, while conventional liposomes showed much faster kinetics of disintegration. It was shown that the inclusion of mTHPC into liposomes increases the structural stability of the carriers. The input of both drug efflux and liposome destruction in overall release was discussed, combining the chromatography data with the destruction rate. At short incubation times the redistribution of mTHPC from Foslip® and Fospeg® proceeds by both drug release and liposomes destruction. At longer incubation times, the drug redistributes only by release.

Interaction of Liposomal Formulations of Meta-tetra(hydroxyphenyl)chlorin (Temoporfin) with Serum Proteins: Protein Binding and Liposome Destruction

Vadim Reshetov^{1,2}, Vladimir Zorin², Agnieszka Siupa³, Marie-Ange D'Hallewin¹, François Guillemin¹ and Lina Bezdetsnaya¹

¹Centre de Recherche en Automatique de Nancy, Université de Lorraine, CNRS UMR 7039, Centre Alexis Vautrin, Vandœuvre-Les-Nancy, France

²Laboratory of Biophysics and Biotechnology, Physics Faculty, Belarusian State University, Minsk, Belarus

³Nanosight Ltd., Arnesbury, UK

Received 23 November 2011, accepted 6 May 2012, DOI: 10.1111/j.1751-1097.2012.01176.x

ABSTRACT

mTHPC is a non polar photosensitizer used in photodynamic therapy. To improve its solubility and pharmacokinetic properties, liposomes were proposed as drug carriers. Binding of liposomal mTHPC to serum proteins and stability of drug carriers in serum are of major importance for PDT efficacy; however, neither was reported before. We studied drug binding to human serum proteins using size-exclusion chromatography. Liposomes destruction in human serum was measured by nanoparticle tracking analysis (NTA). Inclusion of mTHPC into conventional (Foslip[®]) and PEGylated (Fospeg[®]) liposomes does not affect equilibrium serum protein binding compared with solvent-based mTHPC. At short incubation times the redistribution of mTHPC from Foslip[®] and Fospeg[®] proceeds by both drug release and liposomes destruction. At longer incubation times, the drug redistributes only by release. The release of mTHPC from PEGylated vesicles is delayed compared with conventional liposomes, alongside with greatly decreased liposomes destruction. Thus, for long-circulation times the pharmacokinetic behavior of Fospeg[®] could be influenced by a combination of protein- and liposome-bound drug. The study highlights the modes of interaction of photosensitizer-loaded nanovesicles in serum to predict optimal drug delivery and behavior *in vivo* in preclinical models, as well as the novel application of NTA to assess the destruction of liposomes.

INTRODUCTION

Photodynamic therapy is an effective method of tumor treatment based on light-activated photosensitizer drugs that produce cytotoxic molecular species to eradicate the tumor (1). Meta-tetra(hydroxyphenyl)chlorin (mTHPC; Foscan[®], temoporfin; Biolitec GmbH, Jena, Germany) is a second-generation clinically approved photosensitizer. Its development, study and applications were very recently summarized in a comprehensive review (2). One of the problem associated with effective mTHPC delivery is its low-water solubility, which leads to

drug aggregation in biological media and decrease in photodynamic efficacy. Liposomes are considered to be one of the most common nanocarriers for water-insoluble drugs (3). Liposomes offer the advantage of drug monomerization and increase in photosensitizer photoactivity, as well as an enhanced permeability and retention (EPR) effect (4). Liposomal formulations of mTHPC (Foslip[®] and Fospeg[®] [Biolitec GmbH]), designed to improve the overall efficacy of the drug, have received considerable attention both in *in vitro* and *in vivo* studies (2).

The stability of liposomal formulation in terms of solute release and destruction of vesicle structure presents a challenge for successful application of lipid carriers. The problem of stability was extensively studied in different *in vitro* (5,6) and in preclinical models (5–7). Several pathways of prolonging stability and circulation times of liposomes in blood along with reduced uptake by reticuloendothelial system (RES) have been proposed, with sterical shielding of liposomal surface by polyethyleneglycol (PEG) groups being one of the most studied (4).

As intravenous injection is the accepted route of drug administration, this implies that plasma proteins are the structures of initial drug or drug carrier contact in the body. Binding of photosensitizers to plasma proteins influences a number of parameters affecting photodynamic treatment outcome (8). Thus, it is of the utmost importance to characterize the interaction of liposomes with serum proteins in terms of drug binding and stability in serum, which may contribute to the understanding of pharmacokinetics of liposomal formulations of the drug.

mTHPC release from lipid carriers to serum proteins (9) and liposomes (10) was recently estimated. Inclusion of mTHPC into liposomes considerably influenced physicochemical properties of nanocarriers (11), implying that the stability of mTHPC carriers may differ from that of unloaded liposomes. However, neither the relative distribution pattern of liposomal mTHPC between serum proteins nor the stability of mTHPC liposomal carrier in serum has been yet addressed.

The aim of the present study was to (1) evaluate the interaction and binding specificity of conventional and PEGylated liposomal mTHPC formulations (Foslip[®] and Fospeg[®])

*Corresponding author email: l.bolotina@nancy.unicancer.fr (Lina Bezdetsnaya)
© 2012 Wiley Periodicals, Inc.
Photochemistry and Photobiology © 2012 The American Society of Photobiology 0031-8655/12

[Biolitec GmbH]) to human serum proteins; and (2) assess the stability of liposomal formulations and determine the role of liposome destruction in the process of drug release.

MATERIALS AND METHODS

Photosensitizers. Photosensitizers mTHPC, Foslip[®] and Fospeg[®] were kindly provided by Biolitec GmbH. Foslip[®] is based on L- α -dipalmitoylphosphatidylcholine (DPPC), dipalmitoylphosphatidylglycerol (DPPG) and mTHPC, with a dye:lipid molar ratio of 1:12 and DPPC:DPPG ratio of 9:1 (wt/wt). Foslip[®] was reconstituted from lyophilized powder in distilled water. Fospeg[®] has the same composition as Foslip[®], with addition of distearoylphosphatidyl-ethanolamine-mPEG 2000 (DSPE-PEG) and has a DPPC:DSPE-PEG ratio of 9:1 (wt/wt) and dye:lipid molar ratio of 1:13. Fospeg[®] formulation was supplied in aqueous solution. Z-average diameter of liposomes, as measured by dynamic light scattering (DLS) on a Malvern ZetaSizer Nano (Malvern Instruments, UK), was 111 ± 8 nm (polydispersity index 0.113 ± 0.01) for Foslip[®] and 114 ± 7 nm (polydispersity index 0.108 ± 0.01) for Fospeg[®]. All experiments were performed in phosphate-buffered saline (PBS), pH 7.4 (Invitrogen, USA).

Preparation of liposomes. Unilamellar mTHPC-free liposomes were made by filter extrusion technique. Briefly, 18 mg mL^{-1} of DPPC (Avanti, Alabaster, USA) and 2 mg mL^{-1} of DPPG (Avanti) were dissolved in 1 mL of 99.6% ethanol. A thin film was obtained by removal of the solvent by rotary evaporation at 60°C . The film was hydrated in 1 mL of PBS and underwent three freeze-thaw cycles. The suspension was extruded 21 times through 100 nm polycarbonate Nuclepore[®] membranes using Avanti Mini-Extruder (Avanti) at 50°C . After extrusion liposomes were stored at 4°C .

Spectroscopic measurements. Absorption spectra were measured on PerkinElmer Lambda 35 (PerkinElmer, Waltham, USA) and Solar PV 1251 (Solar, Minsk, Belarus) spectrophotometers using 1 cm optical path quartz cuvettes. mTHPC concentration in liposomal samples was calculated from absorption spectrum in 99.6% ethanol using mTHPC molar extinction coefficient of $30\,000 \text{ m}^{-1} \text{ cm}^{-1}$ at 650 nm. Fluorescence spectra were recorded on PerkinElmer LS55B (PerkinElmer) and Solar SFL 1211A (Solar) spectrofluorimeters equipped with thermostated cuvette compartments (PTP-1 Peltier temperature controller in the case of LS55B) and magnetic stirring.

Photoinduced fluorescence quenching. In our recent article (12), we have described photoinduced fluorescence quenching of mTHPC in liposomal formulations. This phenomenon consists in significant mTHPC fluorescence decrease after irradiation of the sample with low-light doses, which is restored after the destruction of liposomes by neutral detergent. We considered the value of normalized fluorescence to be an indicator of photoinduced quenching. Normalized fluorescence was defined as the (I/I_{X-100}) ratio, where (I) is the mTHPC fluorescence intensity measured immediately after irradiation and (I_{X-100}) is the mTHPC fluorescence intensity measured after addition of 0.2% Triton[®] X-100 (Sigma-Aldrich, Lyon, France) to the sample. Samples containing liposomal mTHPC were irradiated by 17 mW 650 nm semiconductor laser for 30 s under continuous stirring at room temperature. All photoinduced fluorescence quenching measurements were carried out in triplicate. Measurements of normalized fluorescence allowed us to estimate the mTHPC local concentration in liposomes using a numerical method as previously described (9).

Serum preparation. Human blood was collected from healthy donors and coagulation was carried out according to established protocols. Venous blood was precipitated in a BD Vacutainer SST II Advance (BD Diagnostics, Le Pont de Claix, France) tube at room temperature for 30 min until clot formation. The sample was centrifuged for 10 min at 1500 g. The serum obtained was stored in test tubes at -18°C until use. Immediately prior to the experiment, serum was centrifuged at 400 g for 5 min and the supernatant was collected.

Size-exclusion chromatography. Chromatographic experiments were performed on a Sigma 2.5×40 cm column filled with Sepharose CL-6B gel (GE Healthcare, USA) pre-equilibrated with PBS, total bed volume 250 mL. Experimental conditions were as follows: sample volume 1.8 mL, flow speed 1.2 mL min^{-1} and fraction sample volume 1.6–2.0 mL. Fractions were collected by automated fraction collector. The flow speed was periodically checked during the separation, and fraction collection time was adjusted if necessary. The column was

washed with two volumes of buffer after each separation, and cleaned with 0.1% Triton[®] X-100 (Sigma-Aldrich) after three consequent uses according to gel supplier instructions. The column was stored at room temperature and the separation was carried out in partially light-protected environment to avoid mTHPC photobleaching effects.

Unless otherwise indicated, Foslip[®] and Fospeg[®] (final mTHPC concentration was $5.2 \cdot 10^{-6} \text{ M}$) were incubated with 50% human serum at 37°C for different times under light-protection. After incubation the sample was injected into the column using a three-way connector. A 100 μL aliquot of non separated sample was used as a reference.

Fractions with elution volume from 65 to 190 mL were collected and analyzed for protein and mTHPC content. mTHPC content in the chromatographic fractions was estimated by fluorescence intensity measured after the addition of 0.2% Triton[®] X-100 (Sigma-Aldrich) to the samples. Intensities were corrected for fraction volume. No background fluorescence of serum was registered in the spectral region of 630–670 nm. For photoinduced fluorescence quenching experiments, collected fractions were measured for mTHPC fluorescence before and after laser irradiation and after addition of Triton[®] detergent.

The total protein content in the separated fractions was determined by the modified Lowry method (13). Triglyceride and cholesterol concentrations were determined by enzymatic assay (Analysis Plus, Minsk, Belarus) according to Tietz (14) based on formation of 4-(*p*-benzoquinone-monoimino)-phenazon, which effectively absorbs light at 500 nm. Absorption of samples was measured and compared with external linear calibration curves for proteins, triglycerides and cholesterol.

Samples of Foslip[®] and Fospeg[®] were also incubated with 20% human serum at the same conditions as for 50% serum. Only liposomal fractions were collected, in which the drug release and photoinduced quenching were measured.

Experiments showed that the recovery of proteins from the serum samples was more than 95%. No significant retention of conventional or PEGylated liposomes was noted throughout the experiments (>90% liposomal mTHPC was recovered). Human serum albumin (HSA) and high-density lipoproteins (HDL) run separately through the column as reference samples were supplied by Sigma-Aldrich.

Nanoparticle tracking analysis. Liposome destruction upon incubation in serum was estimated using a novel technique of nanoparticle tracking analysis (NTA; 15), which tracks the movement of particle in solution independently and simultaneously with other particles. Diluted samples of liposomes incubated with serum proteins were injected into a viewing chamber of Nanosight NS500 system (Nanosight Ltd., Amesbury, UK) with on-board sample pump. Particles were visualized by a focused laser beam (405 nm 60 mW laser) passing through the chamber using onboard CCD camera. Video of particle motion was recorded at 30 frames per second, and at least 1500 tracks were completed during video analysis using Nanosight software NTA v.2.1 (Nanosight Ltd., Amesbury, UK). The samples were measured for 90 s with manual shutter and gain adjustments. Particle diameters were calculated from particle tracks using Stokes-Einstein equation.

To remove chylomicrons and consequently improve the resolution of the signal from serum proteins and liposomes, each sample of human serum was filtered with Millipore 0.2 μm Durapore PVDF (Millipore, Molsheim, France) syringe filter unit and Millipore Ultra-free-MC 0.1 μm (Millipore) centrifugal device prior to incubation with liposomes. Comparison of Foslip[®] and Fospeg[®] incubation in filtered and non filtered serum showed the same release rate of mTHPC, thus indicating the absence of filtration influence on drug release process.

Foslip[®], Fospeg[®] (final mTHPC concentration in sample $6.6 \cdot 10^{-6} \text{ M}$) and 20% filtered human serum were incubated in PBS (viscosity 1.05 cP at 19°C) at 37°C up to 24 h. A 200 μL aliquots were collected at different timepoints, diluted to 2 mL with PBS, cooled to 4°C , and kept light protected at 4°C until measurement (additional dilution was applied prior to measurement). Separate reference samples of Foslip[®] and Fospeg[®] (final mTHPC concentration in sample $6.6 \cdot 10^{-6} \text{ M}$) in PBS and 20% filtered human serum in PBS were measured after appropriate dilution. In the case of mTHPC-free liposomes, suspension with 0.058 mg mL^{-1} lipid was incubated with serum. Incubating serum sample for 24 h in PBS at 37°C did not result in protein aggregation as measured by NTA. Incubating liposomes in PBS for 24 h at 37°C increased diameter less than by 20 nm (PDI increase < 10%) as measured by DLS.

RESULTS

mTHPC redistribution to serum proteins

Binding of non liposomal mTHPC to serum proteins. The binding of liposomal mTHPC to serum proteins was analyzed with size-exclusion chromatography with Sepharose CL-6B gel. As a reference point, we studied the distribution of solvent-based mTHPC between serum proteins.

Figure 1A shows a typical chromatogram of serum sample fractionated in the column. The major amount of protein is eluting in 140–180 mL volume, with a maximum at 163 mL (Fig. 1A, curve 2). This peak corresponds to serum albumin and macroglobulins. This was confirmed by passing isolated HSA through the column (Fig. 1B, curve 1). Biochemical analysis of total cholesterol and triglycerol content allowed distinguishing between the different lipoprotein fractions of serum. The analysis of cholesterol content shows two bands with maxima at 118 and 154 mL (Fig. 1A, curve 3). HDL, when passed separately, were eluted in the volume of 140–165 mL, peaking at 154 mL (Fig. 1B, curve 2). The first band at 118 mL contained a higher amount of cholesterol and a twice higher triglyceride quantity than HDL fraction (data not shown), supplying evidence that this fraction corresponds to low-density lipoproteins (LDL; 16).

Separation of serum sample containing mTHPC allowed estimating the drug distribution pattern between serum proteins. According to fluorescence measurements of the collected fractions, mTHPC was eluted in two distinct bands with maxima at 118 and 154 mL (Fig. 1A, curve 1), corresponding to LDL and HDL bands. The intensity of the second peak was about two times higher, indicating that more than 60% of mTHPC was bound to HDL.

Binding of liposome-based mTHPC to serum proteins. Addition of Foslip[®] or Fospeg[®] to serum had no influence on the position of proteins elution bands. Figure 2 shows the fluorescence-registered elution profiles of serum samples (50% serum) after incubation with Foslip[®] or Fospeg[®] for 30 min, 2, 6 or 24 h. In contrast to solvent-based mTHPC, three bands containing mTHPC were registered. Apart from previously described LDL and HDL bands (118 and 154 mL, respectively), an additional narrow band with low-elution

volume (79 mL) appeared. This band corresponded to mTHPC in lipid vesicles. Indeed, Foslip[®] and Fospeg[®] in PBS elute from the column in a single peak at 79–80 mL (Fig. 2A, B insets).

The position (exclusion volume) of three mTHPC elution bands was independent of incubation time, however, their relative intensity changed. Increasing incubation time resulted in a progressive reduction in mTHPC fluorescence signal in the first band, indicating decrease in concentration of mTHPC bound to liposomes. At the same time protein-bound mTHPC concentration increased. After 24 h only a small liposomal mTHPC peak remained.

Comparing mTHPC content in liposome- and protein-based bands, we were able to estimate the percentage of released dye, as well as the quantitative distribution among serum proteins at different timepoints (Table 1). According to the data, release of mTHPC from Foslip[®] and Fospeg[®] to serum proteins follows different patterns. For Foslip[®] we observed a progressive increase in the release of mTHPC during 24 h of incubation, whereas for Fospeg[®], a high amount of drug was released over short incubation time, followed by a slower redistribution as compared with Foslip[®].

Notably, the ratio of HDL- and LDL-bound mTHPC is constant for all timepoints (1.9 for both liposomal formulations). The same ratio was found for solvent-based mTHPC incubated with serum (Table 1). Hence, the ratio does not depend on the incubation time or the pharmacological formulation.

The serum concentration of 50% was chosen to better approach physiological conditions. Our previous study (9) has shown that the drug release is only slightly dependent on serum concentration in the range of 2–50%. Indeed, the release of mTHPC from conventional or PEGylated liposomes in 20% serum (Table 1) was slightly lower compared to that in 50% serum. The values of drug release in 20% serum were used for comparison with liposomes destruction rate assessed in 20% of serum.

Photophysical properties of mTHPC in liposomal and protein fractions assessed by photoinduced fluorescence quenching. We further studied fluorescence characteristics of mTHPC in non

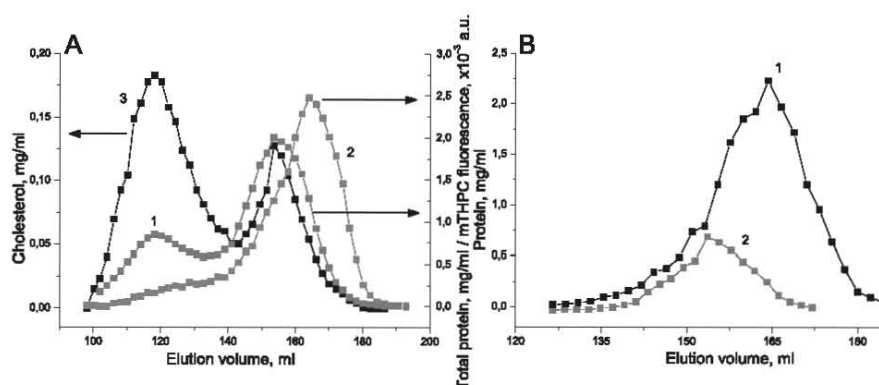


Figure 1. Elution of serum proteins and mTHPC from the chromatographic column. (A) Chromatogram of mTHPC incubated with 50% serum for 6 h, (1) mTHPC profile as measured by mTHPC fluorescence, (2) total protein profile, (3) cholesterol content profile. mTHPC concentration 5.2×10^{-6} M, serum concentration 50%. (B) Protein profiles of HSA (1) and HDL (2) passed separately through the chromatographic column.

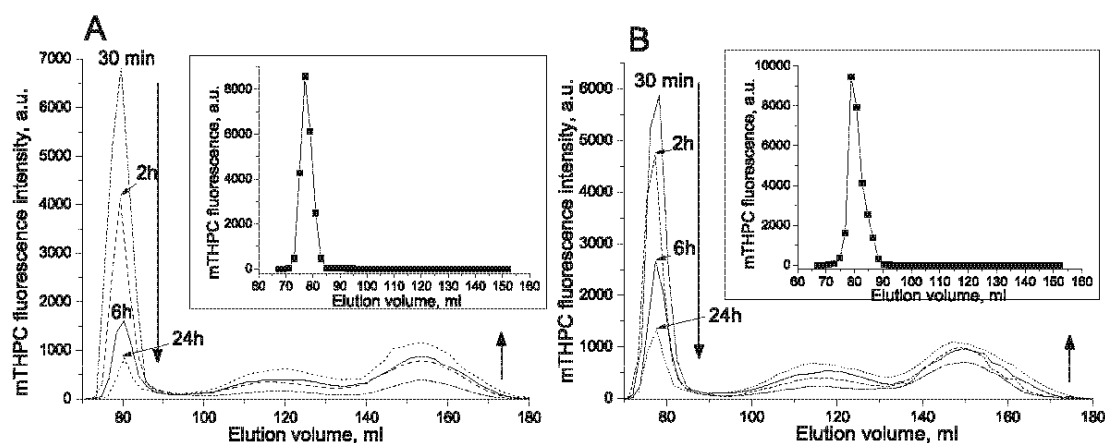


Figure 2. Distribution of mTHPC from Foslip[®] and Fospeg[®] to serum proteins after incubation for 30 min, 2, 6, 24 h. (A) Foslip[®], (B) Fospeg[®]. On insets the elution profiles of liposomes in PBS are shown.

Table 1. Interaction of liposomal mTHPC with lipoprotein fractions.

Formulation	Foslip [®]				Fospeg [®]				mTHPC
	0.5 h	2 h	6 h	24 h	0.5 h	2 h	6 h	24 h	
Incubation time	0.5 h	2 h	6 h	24 h	0.5 h	2 h	6 h	24 h	6 h
mTHPC released, %	22	54	76	91	42	54	60	74	n/a
Bound to LDL, %	8.2	18.3	25.9	31.1	15.0	18.5	20.7	25.0	31.5
Bound to HDL, %	14.8	35.7	50.1	59.9	27.0	35.5	39.3	49.0	68.5
mTHPC released, % (in 20% serum)	21.2	51.8	72.6	87.4	39.9	50.8	56.7	71.1	n/a
mTHPC:lipid ratio in intact liposomes*	1:12.5	1:17.5	1:24	1:46	1:15.9	1:18.4	1:24.1	1:34.8	n/a

SD of mTHPC amount released to serum proteins did not exceed 3%.

*Calculated from photoinduced fluorescence quenching data

detergent-treated fractions. For short incubation time the effect of photoinduced fluorescence quenching is expressed in the liposomal chromatographic fraction (70–90 mL) and is absent for protein-bound mTHPC (100–170 mL; Fig. 3A, C), indicating high and low local mTHPC concentrations, respectively. Increasing incubation time resulted in lower amplitude of photoinduced quenching both for Foslip[®] and Fospeg[®] (Fig. 3B, D), indicating a decrease in local mTHPC concentration in liposomes upon incubation in serum. Photoinduced quenching was also observed in HDL-bound mTHPC fraction after 6 h incubation (140–170 mL fraction); however, the amplitude was insignificant compared with liposomal fraction. This effect could be related to the high-enough local concentration of mTHPC in HDL provoking the energy transfer between mTHPC molecules.

The values of normalized fluorescence were used to calculate the drug:lipid ratios in conventional and PEGylated liposomes (Table 1). The mTHPC:lipid ratio changed only slightly in conventional liposomes after 30 min incubation in serum (1:12.5, corresponding to 4% release from intact liposomes) compared with Foslip[®] in buffer (1:12), whereas a significant percentage of drug (22%) was redistributed and bound to lipoproteins. After 2 and 6 h incubation, respectively, 31% and 50% of mTHPC was released from intact vesicles. This indicates that release may not be the only process implicated in mTHPC redistribution, but the structure of liposomes may also be disrupted. In contrast, at already 30 min incubation, 25% of mTHPC was released from intact Fospeg[®], based on the drug:lipid ratio of 1:15.9. Identical

values of normalized fluorescence were obtained for mTHPC-loaded liposomes incubated in 20% serum (data not shown).

Foslip[®] and Fospeg[®] vesicles destruction in serum assessed by NTA

The process of mTHPC redistribution in serum may proceed not only by drug release but also by disintegration of lipid vesicles. Structural stability of mTHPC liposomal carriers in serum was assessed by NTA, and particle size and concentration were calculated. Fig. 4A shows a screenshot of the light scattering video of the mixture of serum and liposomes. The large brighter particles of >100 nm size are visible on a background of smaller protein particles. Our studies have shown that 20% is the maximal serum concentration at which the liposomal particles can be well resolved in a mixture samples with mTHPC concentration of $6.6 \cdot 10^{-6}$ M.

Figure 4B shows typical results of NTA measurements, presented for Foslip[®] in PBS and Foslip[®] incubated with 20% serum for 5 min, 1, 3, 4.5, 6 or 24 h. As a reference a sample of 20% serum was measured, showing a concentration peak at 50–60 nm, with a negligible amount of particles larger than 120 nm (black line). Foslip[®] in PBS shows a broad population of particles from 50 to 180 nm with a maximum at 100 nm (Fig. 4B, red line). The position of the Fospeg[®] peak in PBS was identical to Foslip[®], whereas dye-free DPPC/DPPG liposomes peaked at 110 nm (data not shown).

Samples of serum incubated with Foslip[®] showed a distribution from 20 to 180 nm (Fig. 4B, dotted lines).

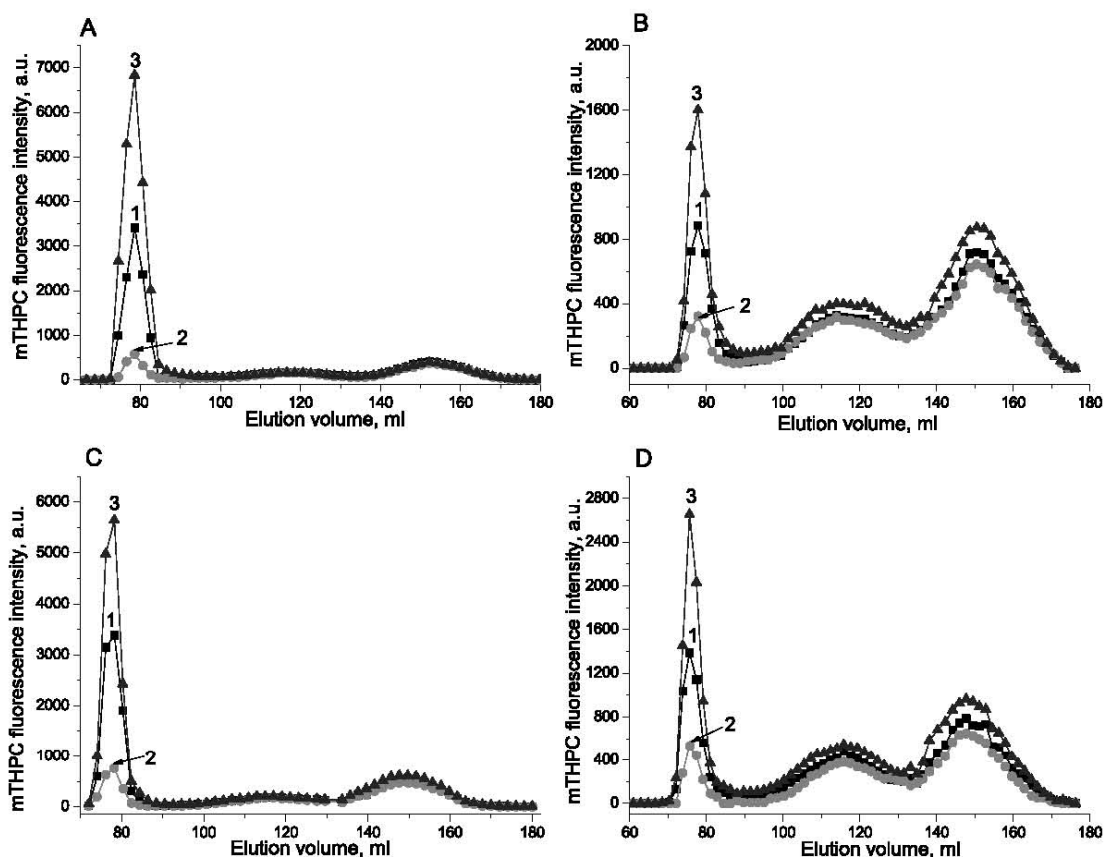


Figure 3. Photoinduced fluorescence quenching of chromatographic fractions. (A) Foslip[®] after 30 min, (B) Foslip[®] after 6 h, (C) Fospeg[®] after 30 min, (D) Fospeg[®] after 6 h incubation. (1) Fluorescence before irradiation, (2) fluorescence after irradiation, (3) fluorescence after addition of the neutral detergent.

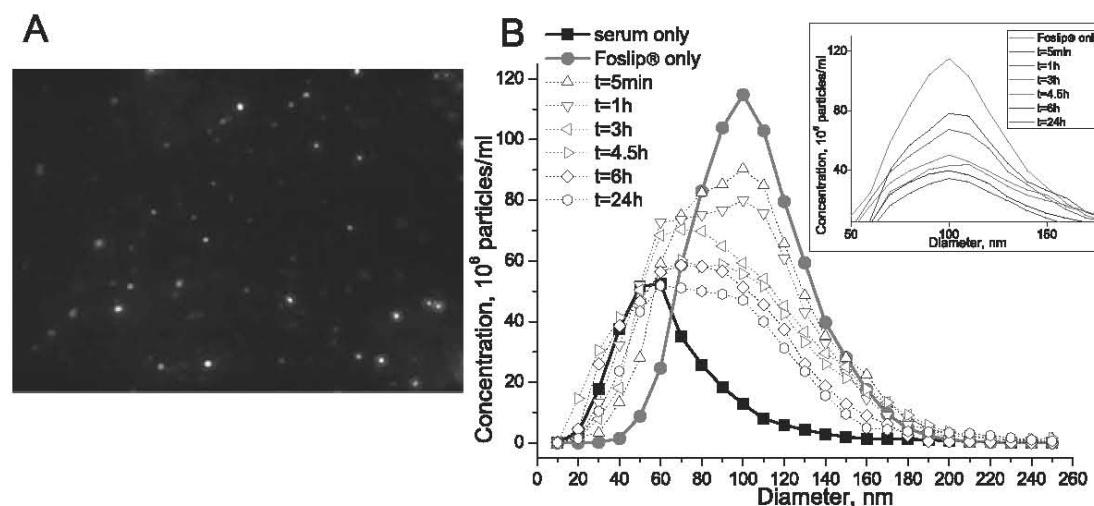


Figure 4. (A) Screenshot of original video file with light scattering particles. (B) Histograms of particle distribution of human serum, Foslip[®] in buffer and Foslip[®] incubated with serum. mTHPC concentration $6.6 \cdot 10^{-6}$ M, serum concentration 20%. On the inset the histograms of liposomes in serum after subtraction of serum part are shown.

Increasing incubation time led to a gradual shift of peak to smaller sizes and a decrease in large particle concentration. The shift apparently indicates the decrease in relative weight of

liposomal pool due to the destruction of liposomes. Indeed, after subtraction of the histogram of serum alone from the histogram of serum with liposomes, the position of the

liposomes distribution peak remained unchanged (Fig. 4B inset), but the concentration decreases with increasing incubation time. Qualitatively, the same histograms were obtained for Fospeg[®] and dye-free conventional liposomes as shown in Fig. 4B.

We used the value of 130-nm particles concentration to estimate the destruction of liposomes in serum (relative to liposome concentration in PBS). The peak value (100 nm) was not used to avoid input from serum particles at this size. Figure 5 shows the kinetics of liposomes destruction upon incubation in serum.

Foslip[®] particles are characterized by a fast destruction of a significant portion (27%) of liposomes during the first hour of incubation, followed by gradual decrease to *ca* 40% of intact liposomes after 24 h (Fig. 5, curve 2). Fospeg[®] proved to be much more stable than Foslip[®]. A small percentage of Fospeg[®] vesicles disappeared after introduction into serum (10%), and only an additional 18% are destroyed after 24 h incubation at 37°C (Fig. 5, curve 3). Dye-free liposomes had a lower stability than Foslip[®], with 40% of vesicles disintegrated after 1 h incubation, and only 25% liposomes intact after 24 h (Fig. 5, curve 1).

DISCUSSION

Binding of liposomal mTHPC to serum proteins

Plasma protein binding pattern is an important determinant influencing porphyrin pharmacokinetics and efficiency during PDT. Depending on the drug physico-chemical properties, porphyrin sensitizers generally bind to albumin (17), HDL and LDL (18).

Despite significant interest in liposomal formulations of mTHPC, relative binding to serum proteins has not yet been assessed. It was previously reported that the use of liposomal vehicles substantially changes the equilibrium percentage of lipoprotein-bound photosensitizers, such as benzoporphyrin derivative, hematoporphyrin and Zn(II)-phthalocyanine, compared with their aqueous preparations (19–21). Our data show that the equilibrium binding pattern of both Foslip[®] and

Fospeg[®] to serum proteins is identical to solvent-based drug (Table 1, Fig. 2). Indeed, mTHPC preferentially binds to lipoproteins, without significant portion of albumin-bound drug. These results correlate well with previous studies of solvent-based mTHPC in human serum (22,23). Thus, mTHPC incorporation into lipid vesicles does not affect its equilibrium serum protein distribution.

The relative distribution pattern remains unchanged over incubation, both for Foslip[®] and Fospeg[®] (Fig. 2, Table 1). This contrasts to solvent-based mTHPC, where the protein binding depends on the incubation time, with initial distribution of mTHPC to albumin, followed by progressive transfer to lipoproteins (23,24) to attain the equilibrium. The observed difference is due to mTHPC disaggregation with successive redistribution to serum proteins, whereas liposomal-based drug is mostly in monomer form. This may have an impact on the pharmacokinetics of mTHPC and its accumulation in tissues.

In the present article, binding of mTHPC to HDL is two times higher than to LDL. Nevertheless, as the ratio of HDL:LDL particles in human serum is more than 100:1 (25,26), this indicates a significant mTHPC affinity toward LDL. Binding of mTHPC to LDL may increase accumulation in tumor cells by LDL receptor-mediated endocytosis (27), both for solvent- and liposome-based mTHPC.

The rate of drug release from liposomes is an important parameter influencing the biodistribution of an active substance. In a recent modelisation study of non polar drug release kinetics from liposomes (28), it was discussed that high drug loading of liposomes tends to increase transfer rate. However, if attractive interactions between drug molecules in liposomes are present, the release is slowed down. The presence of interactions between mTHPC molecules in high drug-load liposomes was previously noted by our group (9,12). Thus, the two counter-acting effects obviously complicate the release of the mTHPC from liposomes.

As compared with other non polar drugs such as benzoporphyrin derivative (29), mTHPC release from liposomes is slow and proceeds on a timescale of hours. In contrast to conventional Foslip[®], a significant part of mTHPC releases fast during the first 30 min of Fospeg[®] incubation (Table 1). This was suggested to be the consequence of mTHPC localization in the PEG shell surrounding the liposomal surface and the lipid bilayer (9) and further supported by the group of E. Reddi with biphasic cellular uptake of Fospeg[®] (30). After this initial fast phase, mTHPC release from Fospeg[®] is slower compared with Foslip[®] (Table 1).

Disintegration of mTHPC lipid carriers in serum

The liposomal disintegration is of interest for the analysis of liposomal drug distribution. This holds particularly true for mTHPC as (1) the drug release is prolonged; and (2) the drug considerably affects the physical state of liposomes (11).

The transfer of lipid from liposomes has a highly destructive influence on the liposomal structure (31). Molecular mechanism of phospholipids transfer is envisioned as the phospholipids-apolipoprotein substitution in HDL particles, together with incorporation of additional phospholipids molecules in HDL without apolipoprotein loss (32). Serum apolipoproteins (A1 and E) are the most potent liposome-disrupting agents,

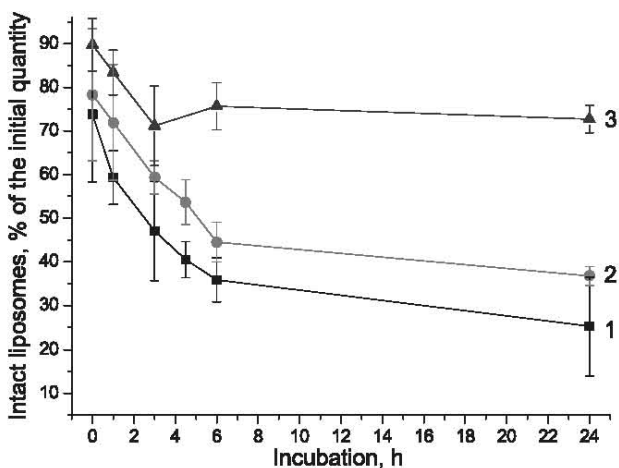


Figure 5. Kinetics of liposomes destruction in serum. (1) mTHPC-free DPPC/DPPG liposomes, (2) Foslip[®], (3) Fospeg[®]. 100% corresponds to liposomes concentration in buffer. Error bars represent SD values.

however, various serum proteins including complement components (5) and LDL (33) may also interact with lipid vesicles.

Most studies used indirect methods to register liposomal disintegration or aggregation, such as radioactive-labeled lipids (34) investigated by chromatography, fluorescent solutes like carboxyfluorescein (35) and energy transfer between labeled lipid molecules (36), electron microscopy (37). A few studies applied direct technique of DLS (37,38), which does not offer sufficient resolution for heterogeneous media, such as liposomes in serum. A recent study by Braeckmans *et al.* (39) used a fluorescence single particle tracking method to size the liposomes in serum and blood, but particle concentration could not be derived. NTA technique applied in this study supplies both size and particle concentration data and offers a superior resolution of heterogeneous mixtures compared with other methods (40).

The size of liposomes is a vital parameter for the efficacy of liposomal formulation (41). The increase of liposomal size leads to increased clearance by mononuclear phagocyte system, along with inhibiting the tumor targeting by EPR effect. Two important characteristics may be derived from the size NTA histograms of liposomes incubated with serum (Fig. 4B). First, incubation with serum does not cause significant Foslip[®] and Fospeg[®] aggregation, since the size distribution of mixture was not broadened as compared to liposomes in buffer at > 100 nm. Liposomal aggregation was reported earlier and was related to liposomes composition and charge (38,41). In agreement with our study, DPPC/DPPG/cholesterol liposomes (42) do not aggregate in serum, whereas liposome aggregation was reported for conventional and PEGylated liposomes with another composition (40). Second, the size of liposomes does not neither decrease upon incubation in serum as follows from the fixed position of the distribution peak at 100–110 nm (Fig. 4B inset). Therefore, consistent with the study (43), our results indicate that only liposomes disintegration takes place in serum without formation of smaller liposomes.

Our data further show that the destruction of conventional liposomes proceeds at a fast pace over the first 4 h of incubation, and is then considerably slowed down (Fig. 5). Indeed, more than 40% of Foslip[®] and dye-free liposomes are broken up during the first 3 h, whereas their concentration decreased only by 10–15% from 4 to 24 h incubation time (Fig. 5, curves 1, 2). The significant decrease in liposomes disintegration rate may be explained by several effects: (1) finite lipoproteins capability to accumulate additional phospholipids, thus decreasing their potency to attack liposomes upon saturation with phospholipids (34,42); (2) depletion of complement components (35); and (3) the low-rate adsorption of proteins on the liposome surface that hinder the access of apolipoproteins to the liposome surface (44). This suggests that serum concentration can influence the stability of liposomes. NTA resolution of liposomes in serum was limited to 20% serum and as such it is difficult to approximate liposomes disintegration profile in undiluted serum. However, the increase in serum concentration from 5% to 10% resulted in the increase in liposomes destruction from 29% to 35% after 2 h incubation (data not shown), compared with 40% destructed liposomes in 20% serum (Fig. 5). Therefore, we may suppose that further increase in serum concentration will not considerably augment liposomes destruction.

The inclusion of mTHPC into liposomes induces a slight increase in stability of formulation. About 10% more intact vesicles was noted for Foslip[®] in serum compared with dye-free liposomes (Fig. 5, curves 1, 2). It is worth noting that at 37°C Foslip[®] is in liquid crystalline state due to inclusion of mTHPC (phase transition at 35°C; 11), whereas dye-free liposomes are in gel state (phase transition at 42°C), suggesting that the state of lipid bilayer has a minor impact on vesicle destruction. However, the shift of lipid bilayer state from gel to liquid crystalline at 37°C increases the release rate of mTHPC from liposomes (9,10).

For Fospeg[®] the amount of destructed liposomes is much less (20% within 2 h and additional 8% at 24 h) than for conventional vesicles (Fig. 5, curve 3). PEG, occupying surface-adjacent space, excludes other macromolecules, limiting access of plasma proteins to liposome surface (37). PEG inclusion into formulation was shown to decrease protein binding values (5) compared with conventional liposomes.

Combining NTA results with the release kinetics of mTHPC (in 20% serum) and drug:lipid ratios in intact liposomes (Table 1), we conclude that at short incubation times mTHPC redistribution from Foslip[®] and Fospeg[®] to lipoproteins proceeds by both drug release and liposomes destruction.

However, the drug:lipid ratios (Table 1) obviously indicate that the input of mTHPC release from intact PEGylated liposomes is prevailing compared with their destruction. In contrast, the mTHPC release from Foslip[®] is of minor contribution compared with vesicles destruction. Indeed, the actual release of the drug from intact conventional liposomes, estimated by photoinduced quenching, accounts only partially for redistributed mTHPC. At long incubation times (> 6 h) the drug redistribution from Foslip[®] continues mostly by the release from liposomes, with a small percentage of destructed liposomes. PEGylated liposomes remain intact even after long incubation in serum, and mTHPC redistribution proceeds slowly only by drug release from the carrier. The association of mTHPC with lipoproteins is independent of the binding of phospholipids of destroyed liposomes, as the HDL/LDL-bound mTHPC ratio is constant in time (Table 1), whereas most of the lipids bind to HDL. It is worth noting that the amount of mTHPC residing in intact conventional liposomes is about 15% higher than in PEGylated ones after 30 min incubation in serum (relative value weighed to the product of destroyed liposomes (%) and released mTHPC (%), calculated from data in Fig. 5 and Table 1). However, at > 30 min incubation this value is always higher for Fospeg[®]. This implies that at prolonged incubation times Fospeg[®] may provide higher liposomal concentrations of mTHPC in plasma and a higher probability of cellular uptake as liposomal entity (30). Thus, an excellent serum stability of Fospeg[®], together with RES-avoiding properties (4) and utilization of the EPR effect for intact vesicles indicate promising application of these liposomes *in vivo*. The majority of drug injected in the form of conventional liposomes will be quickly redistributed from the carriers by means of liposome destruction and release, apart from liposome elimination from the blood flow.

CONCLUSIONS

The presented study of redistribution of mTHPC from Foslip[®] and Fospeg[®] in human serum *in vitro* as well as the stability of

liposomal formulations may provide insights into the *in vivo* behavior of these formulations. The equilibrium binding pattern of liposomal mTHPC to serum proteins is identical as the one observed for solvent-based drug. Incorporation of mTHPC into liposomes changes, however, the drug distribution immediately after injection. The release of mTHPC from PEGylated vesicles is delayed compared with conventional liposomes alongside with greatly decreased liposomes destruction. Thus, for long-circulation times the pharmacokinetic behavior of Fospeg[®] could be influenced by a combination of proteins-bound mTHPC as well as liposome-incorporated drug, attenuating the efficacy of shielded mTHPC liposomal formulations.

Acknowledgements—This work was supported by the research funds of Centre Alexis Vautrin, French Ligue Nationale contre le Cancer and by Belarusian Foundation for Fundamental Research (grant B11F-004). V.R. acknowledges the fellowship of the Ministry of Foreign and European affairs of France. We thank Biolitec (Jena, Germany) for providing mTHPC and its liposomal formulations.

REFERENCES

- Agostinis, P., K. Berg, K. A. Cengel, T. H. Foster, A. W. Girotti, S. O. Gollnick, S. M. Hahn, M. R. Hamblin, A. Juzeniene, D. Kessel, M. Korbelik, J. Moan, P. Mroz, D. Nowis, J. Piette, B. C. Wilson and J. Golab (2011) Photodynamic therapy of cancer: An update. *CA Cancer J. Clin.* **61**, 250–281.
- Senge, M. O. and J. C. Brandt (2011) Temoporfin (Foscan(R), 5,10,15,20-tetra(m-hydroxyphenyl)chlorin), a second generation photosensitizer. *Photochem. Photobiol.* **87**, 1240–1296.
- Fahr, A. and X. Liu (2007) Drug delivery strategies for poorly water-soluble drugs. *Expert Opin. Drug. Deliv.* **4**, 403–416.
- Derycke, A. S. and P. A. de Witte (2004) Liposomes for photodynamic therapy. *Adv. Drug Deliv. Rev.* **56**, 17–30.
- Semple, S. C., A. Chonn and P. R. Cullis (1998) Interactions of liposomes and lipid-based carrier systems with blood proteins: Relation to clearance behaviour *in vivo*. *Adv. Drug Deliv. Rev.* **32**, 3–17.
- Ishida, T., H. Harashima and H. Kiwada (2002) Liposome clearance. *Biosci. Rep.* **22**, 197–224.
- Hwang, K. J. and P. L. Beaumier (1988) Disposition of liposomes *in vivo*. In *Liposomes as Drug Carriers: Recent Trends and Progress*. (Edited by G. Gregoriadis), pp. 19–27. Wiley, Chichester, New York.
- Obochi, M. O. K., R. W. Boyle and J. E. v. Lier (1993) Biological activities of phthalocyanines. XIII. The effects of human serum components on the *in vitro* uptake and photodynamic activity of zinc phthalocyanine. *Photochem. Photobiol.* **57**, 634–640.
- Reshetov, V., D. Kachatkou, T. Shmigol, V. Zorin, M.-A. D'Hallewin, F. Guillemain and L. Bezdetsnaya (2011) Redistribution of meta-tetra(hydroxyphenyl)chlorin (m-THPC) from conventional and PEGylated liposomes to biological substrates. *Photochem. Photobiol. Sci.* **10**, 911–919.
- Hefesha, H., S. Loew, X. Liu, S. May and A. Fahr (2011) Transfer mechanism of temoporfin between liposomal membranes. *J. Control Release* **150**, 279–286.
- Kuntsche, J., I. Freisleben, F. Steimiger and A. Fahr (2010) Temoporfin-loaded liposomes: Physicochemical characterization. *Eur. J. Pharm. Sci.* **40**, 305–315.
- Kachatkou, D., S. Sasnouski, V. Zorin, T. Zorina, M. A. D'Hallewin, F. Guillemain and L. Bezdetsnaya (2009) Unusual photoinduced response of mTHPC liposomal formulation (Foslip). *Photochem. Photobiol.* **85**, 719–724.
- Lowry, O. H., N. J. Rosebrough, A. L. Farr and R. J. Randall (1951) Protein measurement with the Folin phenol reagent. *J. Biol. Chem.* **193**, 265–275.
- Tietz, N. W. (1995) *Clinical Guide to Laboratory Tests*. WB Saunders Co., Philadelphia.
- Malloy, A. and B. Carr (2006) Nanoparticle tracking analysis—The Halo™ system. *Part. Part. Syst. Charact.* **23**, 197–204.
- Silvander, M., M. Johnsson and K. Edwards (1998) Effects of PEG-lipids on permeability of phosphatidylcholine/cholesterol liposomes in buffer and in human serum. *Chem. Phys. Lipids* **97**, 15–26.
- Kessel, D., P. Thompson, K. Saatio and K. D. Nantwi (1987) Tumor localization and photosensitization by sulfonated derivatives of tetraphenylporphine. *Photochem. Photobiol.* **45**, 787–790.
- Maziere, J. C., P. Morliere and R. Santus (1991) The role of the low density lipoprotein receptor pathway in the delivery of lipophilic photosensitizers in the photodynamic therapy of tumours. *J. Photochem. Photobiol. B* **8**, 351–360.
- Richter, A. M., E. Waterfield, A. K. Jain, A. J. Canaan, B. A. Allison and J. G. Levy (1993) Liposomal delivery of a photosensitizer, benzoporphyrin derivative monoacid ring A (BPD), to tumor tissue in a mouse tumor model. *Photochem. Photobiol.* **57**, 1000–1006.
- Jori, G. (1990) Factors controlling the selectivity and efficiency of tumour damage in photodynamic therapy. *Lasers Med. Sci.* **5**, 115–120.
- Ginevra, F., S. Biffanti, A. Pagnan, R. Biolo, E. Reddi and G. Jori (1990) Delivery of the tumour photosensitizer zinc(II)-phthalocyanine to serum proteins by different liposomes: Studies *in vitro* and *in vivo*. *Cancer Lett.* **49**, 59–65.
- Michael-Titus, A. T., R. Whelpton and Z. Yaqub (1995) Binding of temoporfin to the lipoprotein fractions of human serum. *Br. J. Clin. Pharmacol.* **40**, 594–597.
- Hopkinson, H. J., D. I. Vernon and S. B. Brown (1999) Identification and partial characterization of an unusual distribution of the photosensitizer meta-tetrahydroxyphenyl chlorin (temoporfin) in human plasma. *Photochem. Photobiol.* **69**, 482–488.
- Sasnouski, S., V. Zorin, I. Khludayev, M. A. D'Hallewin, F. Guillemain and L. Bezdetsnaya (2005) Investigation of Foscan interactions with plasma proteins. *Biochim. Biophys. Acta* **1725**, 394–402.
- Blake, G. J., J. D. Otvos, N. Rifai and P. M. Ridker (2002) Low-density lipoprotein particle concentration and size as determined by nuclear magnetic resonance spectroscopy as predictors of cardiovascular disease in women. *Circulation* **106**, 1930–1937.
- El Harchaoui, K., B. J. Arsenault, R. Franssen, J. P. Despres, G. K. Hovingh, E. S. Stroes, J. D. Otvos, N. J. Wareham, J. J. Kastelein, K. T. Khaw and S. M. Boekholdt (2009) High-density lipoprotein particle size and concentration and coronary risk. *Ann. Intern. Med.* **150**, 84–93.
- Bonneau, S., P. Morliere and D. Brault (2004) Dynamics of interactions of photosensitizers with lipoproteins and membrane models: Correlation with cellular incorporation and subcellular distribution. *Biochem. Pharmacol.* **68**, 1443–1452.
- Loew, S., A. Fahr and S. May (2011) Modeling the release kinetics of poorly water-soluble drug molecules from liposomal nanocarriers. *J. Drug Deliv.* **2011**, Article ID 376548.
- Chowdhary, R. K., I. Shariff and D. Dolphin (2003) Drug release characteristics of lipid based benzoporphyrin derivative. *J. Pharm. Pharm. Sci.* **6**, 13–19.
- Compagnin, C., F. Moret, L. Celotti, G. Miotto, J. H. Woodhams, A. J. MacRobert, D. Scheglmann, S. Iratni and E. Reddi (2011) Meta-tetra(hydroxyphenyl)chlorin-loaded liposomes sterically stabilised with poly(ethylene glycol) of different length and density: Characterisation, *in vitro* cellular uptake and phototoxicity. *Photochem. Photobiol. Sci.* **10**, 1751–1759.
- Scherphof, G., F. Roerdink, M. Waite and J. Parks (1978) Disintegration of phosphatidylcholine liposomes in plasma as a result of interaction with high-density lipoproteins. *Biochim. Biophys. Acta* **542**, 296–307.
- Tall, A. R., I. Tabas and K. J. Williams (1986) Lipoprotein-liposome interactions. *Methods Enzymol.* **128**, 647–657.
- Comiskey, S. J. and T. D. Heath (1990) Serum-induced leakage of negatively-charged liposomes at nanomolar lipid concentrations. *Biochemistry* **29**, 3626–3631.
- Scherphof, G. L., J. Damen and J. Wilschut (1984) Interactions of liposomes with plasma proteins. In *Liposome Technology*, Vol. 3 (Edited by G. Gregoriadis), pp. 205–224. CRC Press, Boca Raton, Fla.

35. Harashima, H., Y. Ochi and H. Kiwada (1994) Kinetic modelling of liposome degradation in serum: Effect of size and concentration of liposomes *in vitro*. *Biopharm. Drug Dispos.* **15**, 217–225.
36. Madörin, M., P. van Hoogevest, R. Hilfiker and H. Leuenberger (2000) The use of fluorescence resonance energy transfer to study the disintegration kinetics of liposomes containing lysolecithin and oleic acid in rat plasma. *Pharm. Res.* **17**, 1118–1123.
37. Dos Santos, N., C. Allen, A. M. Doppen, M. Anantha, K. A. Cox, R. C. Gallagher, G. Karlsson, K. Edwards, G. Kenner, L. Samuels, M. S. Webb and M. B. Bally (2007) Influence of poly(ethylene glycol) grafting density and polymer length on liposomes: Relating plasma circulation lifetimes to protein binding. *Biochim. Biophys. Acta* **1768**, 1367–1377.
38. Foradada, M., A. Manzano, T. Roig, J. Estelrich and J. Bermúdez (1997) Serum-liposome interaction is an oxygen-dependent process. *Biochim. Biophys. Acta* **1345**, 43–55.
39. Braeckmans, K., K. Buyens, W. Bouquet, C. Vervaet, P. Joye, F. De Vos, L. Plawinski, L. Dœuvre, E. Angles-Cano, N. N. Sanders, J. Demeester and S. C. De Smedt (2010) Sizing nanomatter in biological fluids by fluorescence single particle tracking. *Nano Lett.* **10**, 4435–4442.
40. Filipe, V., A. Hawe and W. Jiskoot (2010) Critical evaluation of nanoparticle tracking analysis (NTA) by NanoSight for the measurement of nanoparticles and protein aggregates. *Pharm Res.* **27**, 796–810.
41. Nagayasu, A., K. Uchiyama and H. Kiwada (1999) The size of liposomes: A factor which affects their targeting efficiency to tumors and therapeutic activity of liposomal antitumor drugs. *Adv. Drug Deliv. Rev.* **40**, 75–87.
42. Oku, N., Y. Tokudome, Y. Namba, N. Saito, M. Endo, Y. Hasegawa, M. Kawai, H. Tsukada and S. Okada (1996) Effect of serum protein binding on real-time trafficking of liposomes with different charges analyzed by positron emission tomography. *Biochim. Biophys. Acta* **1280**, 149–154.
43. Scherphof, G. and H. Morselt (1984) On the size-dependent disintegration of small unilamellar phosphatidylcholine vesicles in rat plasma. Evidence of complete loss of vesicle structure. *Biochem. J.* **221**, 423–429.
44. Jung, S. H., S. K. Kim, E. H. Kim, S. H. Cho, K. S. Jeong, H. Seong and B. C. Shin (2010) Increased stability in plasma and enhanced cellular uptake of thermally denatured albumin-coated liposomes. *Colloids Surf. B Biointerfaces* **76**, 434–440.

General discussion

GENERAL DISCUSSION

Liposomes have been studied for many years as carrier systems for drugs [170, 243, 174] with advantages such as the enhancement of therapeutic efficacy with low drug dosage, reduction in toxicity of the encapsulated agent, improvement of pharmacokinetic profiles and targeting. Because of their characteristic small size, good solubilization efficiency and stability, liposomes may represent a good delivery system for non-polar PDT drugs. Incorporation into lipid vesicles allows for the monomerization of tetrapyrrolic photosensitizers, providing a high photosensitizing activity. An additional advantage of such systems is the possibility of passive targeting by the EPR effect. From this perspective, the development of mTHPC-PDT has been also shifted to the liposomal formulations of this effective photosensitizer. Despite a growing number of studies reporting on PDT with Foslip® or Fospeg®, there are only a few papers on the characterization of the drug in a lipid environment, including the photophysical properties, localization and drug release [283, 284, 119].

Spectroscopic characteristics of mTHPC in liposomes with varying drug:lipid ratios, described in the first part of the results, demonstrated an impact of dye-dye interactions at high liposomal drug loads. A decrease in the distance between drug molecules increased the probability of energy transfer, which led to significant depolarization and appearance of photoinduced fluorescence quenching (upon laser irradiation), which was first described in the study published by our group [119]. In high-drug load liposomes a marked decrease in fluorescence yield and spectral changes were noted, pointing to mTHPC aggregation. The strong resonance light scattering signal in Foslip®/Fospeg® indicated the presence of J-aggregates, with an even higher quantity of the aggregated drug in Fospeg®. This was later supported by another research team [284, 290] using fluorescence lifetime measurements.

An important part of liposomal drug characterization is the study of its localization within the carrier structure. The localization in the lipid bilayer was shown to influence the photooxidizing properties of porphyrins [254, 255]. Our results indicate that mTHPC possesses a heterogeneous distribution inside the lipid bilayer, with a 1:2 ratio of iodine-accessible to inaccessible drug. These results are in good agreement with the proposed pattern of porphyrin localization in liposomes [256].

An interesting peculiarity of mTHPC in Fospeg® is the localization of a part of mTHPC in the PEG shell, which affects the photophysical properties as shown in the first part of the results. This was supported by another study, where fluorescence lifetimes of mTHPC in PEGylated liposomes indicated the PS aggregation [284]. Besides, partial PEG localization of

mTHPC in polymeric nanoparticles resulted in a burst release of this fraction upon incubation in serum [285]. Evidently, the mTHPC localization may influence the release from conventional and PEGylated liposomes, which needs to be estimated. Therefore, a method of drug release is required, that would be applicable not only to model situations like buffer, model membranes or serum solution, but also to *in vivo* conditions.

We have proposed the use of photoinduced fluorescence quenching as a method to estimate the mTHPC concentration in liposomes [119]. Indeed, the changes in mTHPC distribution pattern in a biological system with a liposomal mTHPC formulation will be consistent with the changes in the photoinduced quenching amplitude. Compared to the methods of fluorescence anisotropy measurements and resonance energy transfer, we have shown in the second part of our results that the technique of photoinduced fluorescence quenching affords a wider dynamic range for measurements of the drug release from liposomal carriers, which is especially important in the case of high-drug load liposomes. Measuring the characteristics of photoinduced quenching provides a maximum degree of accuracy in determining the release rate of mTHPC from liposomes with loads (mol/mol) in the range of 0.2-10%. Measurements of fluorescence anisotropy are reliable for liposomes with mTHPC loads $\leq 1\%$, while energy transfer method using donor label tends to be informative with mTHPC loads of less than 0.5%. Such low drug loads do not correspond to commercially used drug formulations.

We have extensively studied the photoinduced quenching characteristics in a set of liposomes with different drug:lipid ratios. These measurements allowed us to construct a calibration curve, and, with the help of a numerical method, we recalculated the values of the photoinduced quenching amplitude into the relative percentage of the drug released from the liposomes at any given moment in a given system. This method of drug release is applicable both to *in vitro* systems and *in vivo* models and blood sampling, as it makes use of intrinsic mTHPC properties in a lipidic environment regardless of the surrounding milieu. The only requirement is to provide an excess of acceptor structures in the incubation medium over the concentration of mTHPC-loaded liposomes. This is easily fulfilled in *in vivo*, in contrast, e.g., to the method used to estimate the mTHPC interliposomal release by ion exchange columns [279].

We have also described the release of mTHPC from Foslip® and Fospeg® to liposomes and serum proteins. The information on the time scale necessary to establish an equilibrium drug distribution between the donor-acceptor structures is extremely important since it provides valuable indications as to the optimal pharmacokinetic parameters. The release of mTHPC from Foslip® was a slow one-phase process, the equilibrium being achieved after more than 8 h of incubation at physiological temperature. The pattern of mTHPC release from Foslip® is similar to the interliposomal transfer kinetics of conventional liposomal mTHPC with a very low drug

load, studied by Fahr and co-authors [275]. The differences between the two studies are obviously related to the extremely high drug load of Foslip®, and indeed underline the need to characterize the release of the drug from the carriers in the exact pharmacological formulation as intended for clinical use. Modeling the release from highly loaded liposomes was reported [276], and emphasized the complexity of such formulations. It was discussed that a high drug loading of liposomes tends to increase the transfer rate. However, if there are attractive interactions between drug molecules in liposomes, the release is slowed down. The presence of both effects in Foslip® and Fospeg®, described in our studies, may imply that they effectively counterbalance the release rate.

The release from Fospeg® presented a very different two-phase pattern. A significant amount of mTHPC was released after several minutes of incubation. During the slow phase (from 30 min onward) the rate of release was much lower compared to the fast phase. This behavior is explained by the presence of two mTHPC pools: in the PEG shell (burst release) and in the lipid bilayer (slow release). The rapid partial release of mTHPC from Fospeg® is likely to contribute to the *in vitro* behavior of Fospeg®. Indeed, biphasic uptake of mTHPC from Fospeg® by cancer cells was reported [284], which suggested a difference in the modality of mTHPC internalization from the free drug form. mTHPC could be released from liposomes into the incubation medium and be internalized when bound to lipoproteins, a process with a different time scale compared to liposome-bound mTHPC. An important point considering the release of mTHPC from both liposomal formulations is that it occurs with the lipid bilayer in the liquid-crystalline state, due to the influence of mTHPC on the liposomes [283].

Besides studying the release rate of mTHPC from liposomal carriers to serum proteins, it is equally important to determine the exact protein fractions that bind mTHPC, since this has a significant effect on the drug tumor binding. This issue was addressed in the third part of the results.

Our data indicated that the *equilibrium* binding pattern of Foslip®- and Fospeg®-formulated mTHPC is identical to solvent-based Foscan®, with about 65% of the drug binding to high-density lipoproteins, and 35% to low-density lipoproteins. The relative binding pattern of liposome-based mTHPC to proteins was independent of incubation time in serum. This is in direct contrast to Foscan®, where the protein binding depends on the incubation time, with initial distribution of mTHPC to albumin, followed by progressive transfer to lipoproteins to attain the equilibrium [89, 90, 88]. In the case of Foscan®, mTHPC undergoes disaggregation in serum with redistribution to serum proteins. In contrast, liposome-based mTHPC is mostly in the monomer form, thus liposomes may serve as drug monomerizers in the case of a burst release or sustained efflux of the drug in plasma. As only the monomer form of mTHPC is photoactive, and

as LDL-bound drug may be rapidly uptaken by cancer cells, this underlines the positive effect of liposomal formulations on the drug efficacy in case of PS release prior to liposome accumulation in the tumor.

Indeed, the absence of large mTHPC aggregation in Fospeg® may explain the higher efficacy of liposomal drug *vs.* Foscan®, reported in [284]. Although the cell uptake of Fospeg® was slower and reduced by 30-40% compared to Foscan®, this, however, led to only a slight reduction in the phototoxicity. While Foscan® will be partially uptaken as aggregates, mTHPC from Fospeg® would be uptaken in monomer form when bound to lipoproteins after release, or will be internalized within the liposomes.

The analysis of photoinduced quenching of mTHPC in liposomes after chromatographic separation of liposomes and serum proteins showed that the mTHPC efflux from liposomes alone could not be the only means of drug redistribution to serum proteins. This prompted us to conduct research into the liposomal stability in serum, and estimate the kinetics of liposome destruction. The technique of nanoparticle tracking analysis used in this study allowed for direct and quantitative analysis of liposome destruction. While Fospeg® is stable for 24 h incubation, Foslip® vesicles are gradually destroyed by serum proteins. Foslip® destruction showed two-phase kinetics - fast destruction over the first 4 h of incubation followed by a considerably slower process. An interesting possibility is the link between the rate of liposome destruction, mTHPC release and the influence of the drug on the physical state of the lipid bilayer. After 4 h a significant amount of mTHPC is already released from liposomes, which will have changed the phase transition temperature from below- to above-physiological values. As the liposomes in the gel state are less prone to destruction by the serum proteins, this could be another explanation of the slowing down of the destruction after 4 h incubation. This underlines the complex interrelation between the drug and the liposomal delivery system. It is to be noted that the inclusion of mTHPC into liposomes induces a slight increase in the stability of formulation compared to drug-free vesicles.

Combining the chromatography data with the destruction rate, we estimated the input of the drug efflux and liposome destruction to the overall release. At short incubation times the redistribution of mTHPC from Foslip® and Fospeg® proceeds by both drug release and liposomes destruction. At longer incubation times, the drug redistributes only by release. The input of mTHPC release from intact PEGylated liposomes is prevailing compared to their destruction. In contrast, the mTHPC release from Foslip® is of minor significance compared to vesicle destruction.

Thus, an excellent serum stability of Fospeg®, together with RES-avoiding properties and utilization of the EPR effect for intact vesicles point to good prospects for the application of

these liposomes *in vivo*. Indeed, a large percentage of mTHPC will be released to lipoproteins during the circulation, but the remainder of the drug would be delivered into the tumor in the liposomal form, which may occur significantly faster than by the lipoproteins pathway. In contrast, most of the drug injected in the form of conventional liposomes will be quickly redistributed from the carriers by means of liposome destruction and release, supplemented with the elimination of liposomes from the blood flow by RES. This will limit the role of conventional liposomes to simple drug monomerizers.

The present study presents a characterization of the behavior of liposomal mTHPC in biological media, which would need to be taken into account while designing efficient drug delivery systems. The method of photoinduced fluorescence quenching used for the drug release study can be supplemented with the technique of analyzing structural stability of liposomes. This would provide an integral approach to evaluating the absolute amount of liposomal and released drug in the blood circulation, which is important for pharmacokinetics analysis.

Conclusions and outlook

CONCLUSIONS AND OUTLOOK

The overarching aim of the present study was to provide the characterization of liposomal formulations of mTHPC *in vitro*.

The incorporation of mTHPC into liposomes influences their properties, just as the liposomes influence the properties of the drug. This interdependence leads to particular features in the liposomal mTHPC behavior. Localization of mTHPC in the PEG shell of Fospeg® greatly increases the transfer rate of this part of the drug to serum proteins, while the rest of mTHPC residing in the lipid bilayer is more protected from the rapid release. At the same time, inclusion of mTHPC into liposomes reduces the phase transition temperature of the lipid bilayer, which leads to increased drug release at physiological temperatures. Inclusion of mTHPC was found to enhance the structural integrity of liposomes.

Importantly, the existence of the photoinduced quenching effect allowed us to develop a technique to register drug release both *in vitro* and *in vivo*. The release is vital for the characterization of a liposomal system. A significant mTHPC efflux from both Foslip® and Fospeg® in the serum indicated that the drug will mostly end up bound to serum proteins and be delivered into the tumor in the monomer form by the same lipoproteins as for solvent-based Foscan®. At the same time, a lower release rate and the EPR effect of protein-indestructible and RES-protected Fospeg® may allow for a higher PDT efficacy than Foslip® prone to destruction by proteins and RES uptake. Presumably, steric stabilization and a lower release rate are sufficient to provide more vascular effect of PDT to Fospeg® compared to Foslip®.

Outlook

The continuation of this work lies in the search for the optimal drug release parameters related to PDT efficacy. Firstly, the *in vivo* study shall be conducted, comparing the pharmacokinetic parameters (including drug release from liposomes) and PDT efficacy of Foslip® and Fospeg®.

Secondly, the modulation of drug release rate from liposomes is an important study. For instance, preparation of PEGylated liposomes with slower or faster release rates than Fospeg® formulation described here will help determine the balance between the release rate and the PDT treatment outcome. Modulation of the drug release is possible by varying the lipid composition of the liposomal carriers, such as incorporating cholesterol or changing DPPC for higher phase transition lipids to rigidify the bilayer. Moreover, the high drug load present in Fospeg® may not necessarily be the most suitable option for efficient PDT. Decrease in the drug content will lead

to decrease in the release rate and the return of the lipid bilayer to the gel state at physiological temperatures, which may affect the PDT efficacy. Indeed, such formulation would have to be precisely characterized both *in vitro* and *in vivo*. The overall results of such work would be beneficial for understanding the behavior of any liposomal PDT drug.

Another direction of further research would be the development of a method to characterize the destruction of liposomal formulations *in vivo*. A combination of NTA technique and chromatography would seem to be the most straightforward approach, without the need to use specific markers like radioactive probes.

Fourthly, *in vivo* study of liposomal mTHPC-PDT should be complemented with the assessment of vascular damage using histological analysis and non-invasive methods like Doppler sonography or the measurements of partial oxygen pressure. To predict the clinical efficacy of liposomal mTHPC-PDT, the immune effect of PDT should be evaluated on immunocompetent animals. Finally, the efficacy of Foslip®/Fospeg®-PDT should be compared to Foscan® to directly prove the advantages of these 3rd generation photosensitizers.

References

REFERENCES

1. Agostinis, P., K. Berg, K. A. Cengel, T. H. Foster, A. W. Girotti, S. O. Gollnick, S. M. Hahn, M. R. Hamblin, A. Juzeniene, D. Kessel, M. Korbelik, J. Moan, P. Mroz, D. Nowis, J. Piette, B. C. Wilson and J. Golab. Photodynamic therapy of cancer: an update. *CA: a cancer journal for clinicians* 2011; 61: 250-81.
2. Allen, T. M., W. W. Cheng, J. I. Hare and K. M. Laginha. Pharmacokinetics and pharmacodynamics of lipidic nano-particles in cancer. *Anticancer Agents Med Chem* 2006; 6: 513-23.
3. Lipson, R. L. and E. J. Baldes. The photodynamic properties of a particular hematoporphyrin derivative. *Archives of dermatology* 1960; 82: 508-16.
4. Lipson, R. L., E. J. Baldes and A. M. Olsen. Further Evaluation of the Use of Hematoporphyrin Derivative As a New Aid for the Endoscopic Detection of Malignant Disease. *Diseases of the Chest* 1964; 46: 676-679.
5. Dougherty, T. J., J. E. Kaufman, A. Goldfarb, K. R. Weishaupt, D. Boyle and A. Mittleman. Photoradiation therapy for the treatment of malignant tumors. *Cancer research* 1978; 38: 2628-35.
6. Dougherty, T. J. An update on photodynamic therapy applications. *Journal of clinical laser medicine & surgery* 2002; 20: 3-7.
7. Dai, T., Y. Y. Huang and M. R. Hamblin. Photodynamic therapy for localized infections - state of the art. *Photodiagnosis and photodynamic therapy* 2009; 6: 170-88.
8. Wilson, B. C. and M. S. Patterson. The physics, biophysics and technology of photodynamic therapy. *Physics in medicine and biology* 2008; 53: 61-109.
9. Bergh, J. Quo vadis with targeted drugs in the 21st century? *Journal of clinical oncology : official journal of the American Society of Clinical Oncology* 2009; 27: 2-5.
10. Fojo, T. and C. Grady. How much is life worth? The \$440 Billion Question. *Journal of the National Cancer Institute* 2009; 101: 1033.
11. Nseyo, U. O., J. DeHaven, T. J. Dougherty, W. R. Potter, D. L. Merrill, S. L. Lundahl and D. L. Lamm. Photodynamic therapy (PDT) in the treatment of patients with resistant superficial bladder cancer: a long-term experience. *Journal of clinical laser medicine & surgery* 1998; 16: 61-8.
12. Usuda, J., H. Kato, T. Okunaka, K. Furukawa, H. Tsutsui, K. Yamada, Y. Suga, H. Honda, Y. Nagatsuka, T. Ohira, M. Tsuboi and T. Hirano. Photodynamic therapy (PDT) for lung cancers. *Journal of thoracic oncology : official publication of the International Association for the Study of Lung Cancer* 2006; 1: 489-93.
13. Fayter, D., M. Corbett, M. Heirs, D. Fox and A. Eastwood. A systematic review of photodynamic therapy in the treatment of pre-cancerous skin conditions, Barrett's oesophagus and cancers of the biliary tract, brain, head and neck, lung, oesophagus and skin. *Health Technol Assess* 2010; 14: 1-288.
14. Gao, F., Y. Bai, S. R. Ma, F. Liu and Z. S. Li. Systematic review: photodynamic therapy for unresectable cholangiocarcinoma. *Journal of hepato-biliary-pancreatic sciences* 2010; 17: 125-31.
15. Trachtenberg, J., A. Bogaards, R. A. Weersink, M. A. Haider, A. Evans, S. A. McCluskey, A. Scherz, M. R. Gertner, C. Yue, S. Appu, A. Aprikian, J. Savard, B. C. Wilson and M. Elhilali. Vascular targeted photodynamic therapy with palladium-bacteriopheophorbide photosensitizer for recurrent prostate cancer following definitive radiation therapy: assessment of safety and treatment response. *The Journal of urology* 2007; 178: 1974-9.
16. Eggener, S. E., P. T. Scardino, P. R. Carroll, M. J. Zelefsky, O. Sartor, H. Hricak, T. M. Wheeler, S. W. Fine, J. Trachtenberg, M. A. Rubin, M. Otori, K. Kuroiwa, M. Rossignol

- and L. Abenheim. Focal therapy for localized prostate cancer: a critical appraisal of rationale and modalities. *The Journal of urology* 2007; 178: 2260-7.
17. Biel, M. Advances in photodynamic therapy for the treatment of head and neck cancers. *Lasers in surgery and medicine* 2006; 38: 349-55.
 18. Hopper, C., A. Kubler, H. Lewis, I. B. Tan and G. Putnam. mTHPC-mediated photodynamic therapy for early oral squamous cell carcinoma. *International journal of cancer. Journal international du cancer* 2004; 111: 138-46.
 19. Nyst, H. J., R. L. van Veen, I. B. Tan, R. Peters, S. Spaniol, D. J. Robinson, F. A. Stewart, P. C. Levendag and H. J. Sterenborg. Performance of a dedicated light delivery and dosimetry device for photodynamic therapy of nasopharyngeal carcinoma: phantom and volunteer experiments. *Lasers in surgery and medicine* 2007; 39: 647-53.
 20. Brown, S. B., E. A. Brown and I. Walker. The present and future role of photodynamic therapy in cancer treatment. *The lancet oncology* 2004; 5: 497-508.
 21. Bell, S. Antibiotic Resistance: Is the End of an Era Near? *Neonatal Network: The Journal of Neonatal Nursing* 2003; 22: 47-54.
 22. Demidova, T. N. and M. R. Hamblin. Photodynamic therapy targeted to pathogens. *International journal of immunopathology and pharmacology* 2004; 17: 245-54.
 23. Tang, H. M., M. R. Hamblin and C. M. Yow. A comparative in vitro photoinactivation study of clinical isolates of multidrug-resistant pathogens. *Journal of infection and chemotherapy : official journal of the Japan Society of Chemotherapy* 2007; 13: 87-91.
 24. Schmidt-Erfurth, U. and T. Hasan. Mechanisms of action of photodynamic therapy with verteporfin for the treatment of age-related macular degeneration. *Survey of ophthalmology* 2000; 45: 195-214.
 25. Celli, J. P., B. Q. Spring, I. Rizvi, C. L. Evans, K. S. Samkoe, S. Verma, B. W. Pogue and T. Hasan. Imaging and photodynamic therapy: mechanisms, monitoring, and optimization. *Chemical reviews* 2010; 110: 2795-838.
 26. Nestor, M., M. Gold, A. Kauvar, A. Taub, R. Geronemus, E. Ritvo, M. Goldman, D. Gilbert, D. Richey, T. Alster, R. Anderson, D. Bank, A. Carruthers, J. Carruthers, D. Goldberg, C. Hanke, N. Lowe, D. Pariser, D. Rigel, P. Robins, J. Spencer and B. Zelickson. The use of photodynamic therapy in dermatology: results of a consensus conference. *J Drugs Dermatol.* 2006; 5: 140-154.
 27. Tschen, E. H., D. S. Wong, D. M. Pariser, F. E. Dunlap, A. Houlihan and M. B. Ferdon. Photodynamic therapy using aminolaevulinic acid for patients with nonhyperkeratotic actinic keratoses of the face and scalp: phase IV multicentre clinical trial with 12-month follow up. *British Journal of Dermatology* 2006; 155: 1262-1269.
 28. Shea, C. R., M. E. Sherwood, T. J. Flotte, N. Chen, M. Scholz and T. Hasan. Rhodamine 123 phototoxicity in laser-irradiated MGH-U1 human carcinoma cells studied in vitro by electron microscopy and confocal laser scanning microscopy. *Cancer research* 1990; 50: 4167-72.
 29. Smith, G., W. G. McGimpsey, M. C. Lynch, I. E. Kochevar and R. W. Redmond. An efficient oxygen independent two-photon photosensitization mechanism. *Photochem Photobiol* 1994; 59: 135-139.
 30. Sharman, W. M., C. M. Allen and J. E. van Lier. Role of activated oxygen species in photodynamic therapy. *Methods in enzymology* 2000; 319: 376-400.
 31. van Lier, J. E. and J. D. Spikes. The chemistry, photophysics and photosensitizing properties of phthalocyanines. *Ciba Foundation symposium* 1989; 146: 17-26.
 32. Baker, A. and J. R. Kanofsky. Quenching of singlet oxygen by biomolecules from L1210 leukemia cells. *Photochem Photobiol* 1992; 55: 523-8.
 33. Moan, J. and K. Berg. The photodegradation of porphyrins in cells can be used to estimate the lifetime of singlet oxygen. *Photochem Photobiol* 1991; 53: 549-553.

34. Dysart, J. S. and M. S. Patterson. Characterization of Photofrin photobleaching for singlet oxygen dose estimation during photodynamic therapy of MLL cells in vitro. *Physics in medicine and biology* 2005; 50: 2597-616.
35. Moan, J., K. Berg, E. Kvam, A. Western, Z. Malik, A. Ruck and H. Schneckenburger. Intracellular localization of photosensitizers. *Ciba Foundation symposium* 1989; 146: 95-107.
36. Dougherty, T. J., C. J. Gomer, G. Jori, D. Kessel, M. Korbelik, J. Moan and Q. Peng. Photodynamic Therapy. *Journal of the National Cancer Institute* 1998; 90: 889-905.
37. Dolmans, D. E., D. Fukumura and R. K. Jain. Photodynamic therapy for cancer. *Nature reviews. Cancer* 2003; 3: 380-7.
38. Henderson, B. W., S. M. Waldow, T. S. Mang, W. R. Potter, P. B. Malone and T. J. Dougherty. Tumor destruction and kinetics of tumor cell death in two experimental mouse tumors following photodynamic therapy. *Cancer research* 1985; 45: 572-6.
39. Kessel, D. and Y. Luo. Photodynamic therapy: a mitochondrial inducer of apoptosis. *Cell death and differentiation* 1999; 6: 28-35.
40. Trivedi, N. S., H. W. Wang, A. L. Nieminen, N. L. Oleinick and J. A. Izatt. Quantitative analysis of Pc 4 localization in mouse lymphoma (LY-R) cells via double-label confocal fluorescence microscopy. *Photochem Photobiol* 2000; 71: 634-9.
41. Oleinick, N. L., R. L. Morris and I. Belichenko. The role of apoptosis in response to photodynamic therapy: what, where, why, and how. *Photochemical & photobiological sciences : Official journal of the European Photochemistry Association and the European Society for Photobiology* 2002; 1: 1-21.
42. Bonneau, S., phanie and C. Vever-Bizet. Tetrapyrrole photosensitisers, determinants of subcellular localisation and mechanisms of photodynamic processes in therapeutic approaches. *Expert Opinion on Therapeutic Patents* 2008; 18: 1011-1025.
43. Kessel, D. Relocalization of cationic porphyrins during photodynamic therapy. *Photochemical & photobiological sciences : Official journal of the European Photochemistry Association and the European Society for Photobiology* 2002; 1: 837-40.
44. Dahle, J., O. Kaalhus, J. Moan and H. B. Steen. Cooperative effects of photodynamic treatment of cells in microcolonies. *Proceedings of the National Academy of Sciences of the United States of America* 1997; 94: 1773-8.
45. Reiners, J. J., Jr., P. Agostinis, K. Berg, N. L. Oleinick and D. Kessel. Assessing autophagy in the context of photodynamic therapy. *Autophagy* 2010; 6: 7-18.
46. Korbelik, M. and G. Kros. Cellular levels of photosensitisers in tumours: the role of proximity to the blood supply. *British journal of cancer* 1994; 70: 604-10.
47. Tromberg, B. J., A. Orenstein, S. Kimel, S. J. Barker, J. Hyatt, J. S. Nelson and M. W. Berns. In vivo tumor oxygen tension measurements for the evaluation of the efficiency of photodynamic therapy. *Photochem Photobiol* 1990; 52: 375-85.
48. Henderson, B. W. and V. H. Fingar. Oxygen limitation of direct tumor cell kill during photodynamic treatment of a murine tumor model. *Photochem Photobiol* 1989; 49: 299-304.
49. Gomer, C. J., N. Rucker and A. L. Murphree. Differential cell photosensitivity following porphyrin photodynamic therapy. *Cancer research* 1988; 48: 4539-42.
50. West, C. M., D. C. West, S. Kumar and J. V. Moore. A comparison of the sensitivity to photodynamic treatment of endothelial and tumour cells in different proliferative states. *International journal of radiation biology* 1990; 58: 145-56.
51. Snyder, J. W., W. R. Greco, D. A. Bellnier, L. Vaughan and B. W. Henderson. Photodynamic therapy: a means to enhanced drug delivery to tumors. *Cancer research* 2003; 63: 8126-31.
52. Henderson, B. W. and T. J. Dougherty. How does photodynamic therapy work? *Photochem Photobiol* 1992; 55: 145-157.

53. Henderson, B. W., S. O. Gollnick, J. W. Snyder, T. M. Busch, P. C. Kousis, R. T. Cheney and J. Morgan. Choice of oxygen-conserving treatment regimen determines the inflammatory response and outcome of photodynamic therapy of tumors. *Cancer research* 2004; 64: 2120-6.
54. Korbelik, M. PDT-associated host response and its role in the therapy outcome. *Lasers in surgery and medicine* 2006; 38: 500-8.
55. Kousis, P. C., B. W. Henderson, P. G. Maier and S. O. Gollnick. Photodynamic Therapy Enhancement of Antitumor Immunity Is Regulated by Neutrophils. *Cancer research* 2007; 67: 10501-10510.
56. Korbelik, M. and I. Cecic. Contribution of myeloid and lymphoid host cells to the curative outcome of mouse sarcoma treatment by photodynamic therapy. *Cancer letters* 1999; 137: 91-8.
57. Korbelik, M., G. Kroszl, J. Kroszl and G. J. Dougherty. The role of host lymphoid populations in the response of mouse EMT6 tumor to photodynamic therapy. *Cancer research* 1996; 56: 5647-52.
58. Jain, R. K. Delivery of molecular and cellular medicine to solid tumors. *Advanced drug delivery reviews* 2001; 46: 149-68.
59. Pogue, B. W., J. A. O'Hara, E. Demidenko, C. M. Wilmot, I. A. Goodwin, B. Chen, H. M. Swartz and T. Hasan. Photodynamic therapy with verteporfin in the radiation-induced fibrosarcoma-1 tumor causes enhanced radiation sensitivity. *Cancer research* 2003; 63: 1025-33.
60. Bachor, R., C. R. Shea, R. Gillies and T. Hasan. Photosensitized destruction of human bladder carcinoma cells treated with chlorin e6-conjugated microspheres. *Proceedings of the National Academy of Sciences of the United States of America* 1991; 88: 1580-4.
61. Allison, R. R., G. H. Downie, R. Cuenca, X.-H. Hu, C. J. H. Childs and C. H. Sibata. Photosensitizers in clinical PDT. *Photodiagnosis and photodynamic therapy* 2004; 1: 27-42.
62. Castano, A. P., T. N. Demidova and M. R. Hamblin. Mechanisms in photodynamic therapy: part one—photosensitizers, photochemistry and cellular localization. *Photodiagnosis and photodynamic therapy* 2004; 1: 279-293.
63. Plaetzer, K., B. Krammer, J. Berlanda, F. Berr and T. Kiesslich. Photophysics and photochemistry of photodynamic therapy: fundamental aspects. *Lasers in medical science* 2009; 24: 259-68.
64. Allison, R. R. and C. H. Sibata. Oncologic photodynamic therapy photosensitizers: a clinical review. *Photodiagnosis and photodynamic therapy* 2010; 7: 61-75.
65. Chan, W. S., J. F. Marshall, R. Svensen, J. Bedwell and I. R. Hart. Effect of sulfonation on the cell and tissue distribution of the photosensitizer aluminum phthalocyanine. *Cancer research* 1990; 50: 4533-8.
66. Woodburn, K., C. K. Chang, S. Lee, B. Henderson and D. Kessel. Biodistribution and PDT efficacy of a ketochlorin photosensitizer as a function of the delivery vehicle. *Photochem Photobiol* 1994; 60: 154-9.
67. Boyle, R. W. and D. Dolphin. Structure and Biodistribution Relationships of Photodynamic Sensitizers. *Photochem Photobiol* 1996; 64: 469-485.
68. Tannock, I. F. and D. Rotin. Acid pH in tumors and its potential for therapeutic exploitation. *Cancer research* 1989; 49: 4373-84.
69. Bonneau, S., P. Morliere and D. Brault. Dynamics of interactions of photosensitizers with lipoproteins and membrane-models: correlation with cellular incorporation and subcellular distribution. *Biochemical pharmacology* 2004; 68: 1443-52.
70. Cunderlikova, B., L. Gangeskar and J. Moan. Acid-base properties of chlorin e6: relation to cellular uptake. *Journal of photochemistry and photobiology. B, Biology* 1999; 53: 81-90.

71. Bonnett, R., R. White, U. Winfield and M. Berenbaum. Hydroporphyrins of the meso-tetra(hydroxyphenyl)porphyrin series as tumour photosensitizers. *Biochem J* 1989; 261: 277-280.
72. Ronn, A., M. Nouri, L. Lofgren, B. Steinberg, A. Westerborn, T. Windahl, M. Shikowitz and A. Abramson. Human tissue levels and plasma pharmacokinetics of temoporfin (Foscan, mTHPC). *Lasers in medical science* 1996; 11: 267-272.
73. Juzeniene, A., Q. Peng and J. Moan. Milestones in the development of photodynamic therapy and fluorescence diagnosis. *Photochemical & photobiological sciences : Official journal of the European Photochemistry Association and the European Society for Photobiology* 2007; 6: 1234-45.
74. Konan, Y. N., R. Gurny and E. Allemann. State of the art in the delivery of photosensitizers for photodynamic therapy. *Journal of photochemistry and photobiology. B, Biology* 2002; 66: 89-106.
75. Senge, M. O. and J. C. Brandt. Temoporfin (Foscan(R), 5,10,15,20-tetra(m-hydroxyphenyl)chlorin) - a second-generation photosensitizer. *Photochem Photobiol* 2011; 87: 1240-96.
76. Abulafi, A. M., M. L. DeJode, J. T. Allardice, J. K. Ansell and N. S. Williams. Adjuvant intraoperative photodynamic therapy in experimental colorectal cancer using a new photosensitizer. *The British journal of surgery* 1997; 84: 368-71.
77. Bonnett, R., P. Charlesworth, B. D. Djelal, S. Foley, D. J. McGarvey and T. George Truscott. Photophysical properties of 5,10,15,20-tetrakis(m-hydroxyphenyl)porphyrin (m-THPP), 5,10,15,20-tetrakis(m-hydroxyphenyl)chlorin (m-THPC) and 5,10,15,20-tetrakis(m-hydroxyphenyl)bacteriochlorin (m-THPBC): a comparative study. *Journal of the Chemical Society, Perkin Transactions 2* 1999: 325-328.
78. Savary, J. F., P. Grosjean, P. Monnier, C. Fontollet, G. Wagnieres, D. Braichotte and H. van den Bergh. Photodynamic therapy of early squamous cell carcinomas of the esophagus: a review of 31 cases. *Endoscopy* 1998; 30: 258-65.
79. Savary, J. F., P. Monnier, C. Fontollet, J. Mizeret, G. Wagnieres, D. Braichotte and H. van den Bergh. Photodynamic therapy for early squamous cell carcinomas of the esophagus, bronchi, and mouth with m-tetra (hydroxyphenyl) chlorin. *Archives of otolaryngology--head & neck surgery* 1997; 123: 162-8.
80. Copper, M., I. Tan, H. Oppelaar, M. Ruevekamp and F. Stewart. Meta-tetra(hydroxyphenyl)chlorin photodynamic therapy in early-stage squamous cell carcinoma of the head and neck. *Archives of otolaryngology--head & neck surgery* 2003; 129: 709-711.
81. Baas, P., A. E. Saarnak, H. Oppelaar, H. Neering and F. A. Stewart. Photodynamic therapy with meta-tetrahydroxyphenylchlorin for basal cell carcinoma: a phase I/II study. *The British journal of dermatology* 2001; 145: 75-8.
82. Moore, C. M., T. R. Nathan, W. R. Lees, C. A. Mosse, A. Freeman, M. Emberton and S. G. Bown. Photodynamic therapy using meso tetra hydroxy phenyl chlorin (mTHPC) in early prostate cancer. *Lasers in surgery and medicine* 2006; 38: 356-363.
83. Bown, S. G., A. Z. Rogowska, D. E. Whitelaw, W. R. Lees, L. B. Lovat, P. Ripley, L. Jones, P. Wyld, A. Gillams and A. W. Hatfield. Photodynamic therapy for cancer of the pancreas. *Gut* 2002; 50: 549-57.
84. Kruijt, B., A. van der Ploeg-van den Heuvel, H. S. de Bruijn, H. J. C. M. Sterenborg, A. Amelink and D. J. Robinson. Monitoring interstitial m-THPC-PDT in vivo using fluorescence and reflectance spectroscopy. *Lasers in surgery and medicine* 2009; 41: 653-664.
85. Tikhomirov, A. M., T. A. Shmigol, E. A. Kozhinova, A. A. Kiagova, L. N. Bezdetsnaia and A. Potapenko. [Investigation of aggregates of dyes by the method of resonance light scattering: correction of spectra]. *Biofizika* 2009; 54: 824-30.

86. Rezzoug, H., L. Bezdetnaya, O. A'Amar, J. L. Merlin and F. Guillemin. Parameters Affecting Photodynamic Activity of Foscan® or Meta-tetra(hydroxyphenyl)chlorin (mTHPC) In Vitro and In Vivo. *Lasers in medical science* 1998; 13: 119-125.
87. Sasnouski, S., D. Kachatkou, V. Zorin, F. Guillemin and L. Bezdetnaya. Redistribution of Foscan from plasma proteins to model membranes. *Photochemical & photobiological sciences : Official journal of the European Photochemistry Association and the European Society for Photobiology* 2006; 5: 770-7.
88. Sasnouski, S., V. Zorin, I. Khludeyev, M. A. D'Hallewin, F. Guillemin and L. Bezdetnaya. Investigation of Foscan interactions with plasma proteins. *Biochimica et biophysica acta* 2005; 1725: 394-402.
89. Michael-Titus, A. T., R. Whelpton and Z. Yaqub. Binding of temoporfin to the lipoprotein fractions of human serum. *British journal of clinical pharmacology* 1995; 40: 594-7.
90. Hopkinson, H. J., D. I. Vernon and S. B. Brown. Identification and partial characterization of an unusual distribution of the photosensitizer meta-tetrahydroxyphenyl chlorin (temoporfin) in human plasma. *Photochem Photobiol* 1999; 69: 482-8.
91. Ma, L. W., E. Bjørklund and J. Moan. Photochemotherapy of tumours with mesotetrahydroxyphenyl chlorin is pH dependent. *Cancer letters* 1999; 138: 197-201.
92. Ball, D. J., D. I. Vernon and S. B. Brown. The high photoactivity of m-THPC in photodynamic therapy. Unusually strong retention of m-THPC by RIF-1 cells in culture. *Photochem Photobiol* 1999; 69: 360-3.
93. Bombelli, C., G. Caracciolo, P. Di Profio, M. Diociaiuti, P. Luciani, G. Mancini, C. Mazzuca, M. Marra, A. Molinari, D. Monti, L. Toccaceli and M. Venanzi. Inclusion of a Photosensitizer in Liposomes Formed by DMPC/Gemini Surfactant: Correlation between Physicochemical and Biological Features of the Complexes. *J Med Chem* 2005; 48: 4882-4891.
94. Teiten, M. H., L. Bezdetnaya, P. Morliere, R. Santus and F. Guillemin. Endoplasmic reticulum and Golgi apparatus are the preferential sites of Foscan localisation in cultured tumour cells. *British journal of cancer* 2003; 88: 146-52.
95. Teiten, M. H., S. Marchal, M. A. D'Hallewin, F. Guillemin and L. Bezdetnaya. Primary photodamage sites and mitochondrial events after Foscan photosensitization of MCF-7 human breast cancer cells. *Photochem Photobiol* 2003; 78: 9-14.
96. Mitra, S., E. Maugain, L. Bolotine, F. Guillemin and T. H. Foster. Temporally and Spatially Heterogeneous Distribution of mTHPC in a Murine Tumor Observed by Two-color Confocal Fluorescence Imaging and Spectroscopy in a Whole-mount Model. *Photochem Photobiol* 2005; 81: 1123-1130.
97. Ma, L., J. Moan and K. Berg. Evaluation of a new photosensitizer, meso-tetrahydroxyphenyl-chlorin, for use in photodynamic therapy: a comparison of its photobiological properties with those of two other photosensitizers. *International journal of cancer. Journal international du cancer* 1994; 57: 883-8.
98. Kessel, D. Transport and localisation of m-THPC in vitro. *Int J Clin Pract* 1999; 53: 263-7.
99. Yow, C. M., J. Y. Chen, N. K. Mak, N. H. Cheung and A. W. Leung. Cellular uptake, subcellular localization and photodamaging effect of temoporfin (mTHPC) in nasopharyngeal carcinoma cells: comparison with hematoporphyrin derivative. *Cancer letters* 2000; 157: 123-31.
100. Marchal, S., L. Bezdetnaya and F. Guillemin. Modality of cell death induced by Foscan-based photodynamic treatment in human colon adenocarcinoma cell line HT29. *Biochemistry. Biokhimiia* 2004; 69: 45-9.
101. Ronn, A. M., J. Batti, C. J. Lee, D. Yoo, M. E. Siegel, M. Nouri, L. A. Lofgren and B. M. Steinberg. Comparative biodistribution of meta-Tetra(Hydroxyphenyl) chlorin in multiple species: clinical implications for photodynamic therapy. *Lasers in surgery and medicine* 1997; 20: 437-42.

102. Glanzmann, T., C. Hadjur, M. Zellweger, P. Grosjean, M. Forrer, J. P. Ballini, P. Monnier, H. van den Bergh, C. K. Lim and G. Wagnieres. Pharmacokinetics of tetra(m-hydroxyphenyl)chlorin in human plasma and individualized light dosimetry in photodynamic therapy. *Photochem Photobiol* 1998; 67: 596-602.
103. Jones, H. J., D. I. Vernon and S. B. Brown. Photodynamic therapy effect of m-THPC (Foscan) in vivo: correlation with pharmacokinetics. *British journal of cancer* 2003; 89: 398-404.
104. Triesscheijn, M., M. Ruevekamp, M. Aalders, P. Baas and F. A. Stewart. Outcome of mTHPC Mediated Photodynamic Therapy is Primarily Determined by the Vascular Response. *Photochem Photobiol* 2005; 81: 1161-1167.
105. Garrier, J., A. Bressenot, S. Grafe, S. Marchal, S. Mitra, T. H. Foster, F. Guillemin and L. Bezdetnaya. Compartmental targeting for mTHPC-based photodynamic treatment in vivo: Correlation of efficiency, pharmacokinetics, and regional distribution of apoptosis. *International journal of radiation oncology, biology, physics* 2010; 78: 563-71.
106. Veenhuizen, R., H. Oppelaar, M. Ruevekamp, J. Schellens, O. Dalesio and F. Stewart. Does tumour uptake of Foscan determine PDT efficacy? *International Journal of Cancer* 1997; 73: 236-239.
107. Ris, H. B., Q. Li, T. Krueger, C. K. Lim, B. Reynolds, U. Althaus and H. J. Altermatt. Photosensitizing effects of m-tetrahydroxyphenylchlorin on human tumor xenografts: correlation with sensitizer uptake, tumor doubling time and tumor histology. *International journal of cancer. Journal international du cancer* 1998; 76: 872-4.
108. Cecic, I., C. S. Parkins and M. Korbelik. Induction of systemic neutrophil response in mice by photodynamic therapy of solid tumors. *Photochem Photobiol* 2001; 74: 712-20.
109. Coutier, S., L. Bezdetnaya, S. Marchal, V. Melnikova, I. Belitchenko, J. L. Merlin and F. Guillemin. Foscan (mTHPC) photosensitized macrophage activation: enhancement of phagocytosis, nitric oxide release and tumour necrosis factor-alpha-mediated cytolytic activity. *British journal of cancer* 1999; 81: 37-42.
110. Wagnieres, G., C. Hadjur, P. Grosjean, D. Braichotte, J. F. Savary, P. Monnier and H. van den Bergh. Clinical evaluation of the cutaneous phototoxicity of 5,10,15,20-tetra(m-hydroxyphenyl)chlorin. *Photochem Photobiol* 1998; 68: 382-7.
111. Sibani, S. A., P. A. McCarron, A. D. Woolfson and R. F. Donnelly. Photosensitizer delivery for photodynamic therapy. Part 2: systemic carrier platforms. *Expert opinion on drug delivery* 2008; 5: 1241-54.
112. Ricchelli, F. Photophysical properties of porphyrins in biological membranes. *Journal of photochemistry and photobiology. B, Biology* 1995; 29: 109-18.
113. Brayden, D. J. Controlled release technologies for drug delivery. *Drug discovery today* 2003; 8: 976-8.
114. Allen, T., W. Cheng, J. Hare and K. Laginha. Pharmacokinetics and pharmacodynamics of lipidic nano-particles in cancer. *Anticancer Agents Med Chem* 2006; 6: 513-23.
115. Puri, A., K. Loomis, B. Smith, J. Lee, A. Yavlovich, E. Heldman and R. Blumenthal. Lipid-based nanoparticles as pharmaceutical drug carriers: from concepts to clinic. *Crit Rev Ther Drug Carrier Syst* 2009; 26: 523-80.
116. Allen, T. M. and P. R. Cullis. Drug delivery systems: entering the mainstream. *Science* 2004; 303: 1818-22.
117. Chatterjee, D. K., L. S. Fong and Y. Zhang. Nanoparticles in photodynamic therapy: an emerging paradigm. *Advanced drug delivery reviews* 2008; 60: 1627-37.
118. Peer, D., J. M. Karp, S. Hong, O. C. Farokhzad, R. Margalit and R. Langer. Nanocarriers as an emerging platform for cancer therapy. *Nat Nano* 2007; 2: 751-760.
119. Kachatkou, D., S. Sasnouski, V. Zorin, T. Zorina, M. A. D'Hallewin, F. Guillemin and L. Bezdetnaya. Unusual photoinduced response of mTHPC liposomal formulation (Foslip). *Photochem Photobiol* 2009; 85: 719-24.

120. Northfelt, D. W., B. J. Dezube, J. A. Thommes, R. Levine, J. H. Von Roenn, G. M. Dosik, A. Rios, S. E. Krown, C. DuMond and R. D. Mamelok. Efficacy of pegylated-liposomal doxorubicin in the treatment of AIDS-related Kaposi's sarcoma after failure of standard chemotherapy. *Journal of clinical oncology : official journal of the American Society of Clinical Oncology* 1997; 15: 653-9.
121. Vasey, P. A., S. B. Kaye, R. Morrison, C. Twelves, P. Wilson, R. Duncan, A. H. Thomson, L. S. Murray, T. E. Hilditch, T. Murray, S. Burtles, D. Fraier, E. Frigerio and J. Cassidy. Phase I clinical and pharmacokinetic study of PK1 [N-(2-hydroxypropyl)methacrylamide copolymer doxorubicin]: first member of a new class of chemotherapeutic agents-drug-polymer conjugates. Cancer Research Campaign Phase I/II Committee. *Clinical cancer research : an official journal of the American Association for Cancer Research* 1999; 5: 83-94.
122. Gabizon, A., H. Shmeeda and Y. Barenholz. Pharmacokinetics of pegylated liposomal Doxorubicin: review of animal and human studies. *Clinical pharmacokinetics* 2003; 42: 419-36.
123. Cabanes, A., K. E. Briggs, P. C. Gokhale, J. A. Treat and A. Rahman. Comparative in vivo studies with paclitaxel and liposome-encapsulated paclitaxel. *International journal of oncology* 1998; 12: 1035-40.
124. Maeda, H., J. Wu, T. Sawa, Y. Matsumura and K. Hori. Tumor vascular permeability and the EPR effect in macromolecular therapeutics: a review. *Journal of controlled release : official journal of the Controlled Release Society* 2000; 65: 271-84.
125. Davis, M. E., Z. G. Chen and D. M. Shin. Nanoparticle therapeutics: an emerging treatment modality for cancer. *Nature reviews. Drug discovery* 2008; 7: 771-82.
126. Petros, R. A. and J. M. DeSimone. Strategies in the design of nanoparticles for therapeutic applications. *Nature reviews. Drug discovery* 2010; 9: 615-27.
127. Malam, Y., M. Loizidou and A. M. Seifalian. Liposomes and nanoparticles: nanosized vehicles for drug delivery in cancer. *Trends in pharmacological sciences* 2009; 30: 592-9.
128. Wang, J., M. Sui and W. Fan. Nanoparticles for Tumor Targeted Therapies and Their Pharmacokinetics. *Current Drug Metabolism* 2010; 11: 129-141.
129. Jain, R. K. and T. Stylianopoulos. Delivering nanomedicine to solid tumors. *Nature reviews. Clinical oncology* 2010; 7: 653-64.
130. Farokhzad, O. C. and R. Langer. Impact of nanotechnology on drug delivery. *ACS nano* 2009; 3: 16-20.
131. Schroeder, A., D. A. Heller, M. M. Winslow, J. E. Dahlman, G. W. Pratt, R. Langer, T. Jacks and D. G. Anderson. Treating metastatic cancer with nanotechnology. *Nature reviews. Cancer* 2012; 12: 39-50.
132. Park, J. H., G. von Maltzahn, L. L. Ong, A. Centrone, T. A. Hatton, E. Ruoslahti, S. N. Bhatia and M. J. Sailor. Cooperative nanoparticles for tumor detection and photothermally triggered drug delivery. *Adv Mater* 2010; 22: 880-5.
133. von Maltzahn, G., A. Centrone, J.-H. Park, R. Ramanathan, M. J. Sailor, T. A. Hatton and S. N. Bhatia. SERS-Coded Gold Nanorods as a Multifunctional Platform for Densely Multiplexed Near-Infrared Imaging and Photothermal Heating. *Advanced Materials* 2009; 21: 3175-3180.
134. Choi, H. S., W. Liu, P. Misra, E. Tanaka, J. P. Zimmer, B. Itty Ipe, M. G. Bawendi and J. V. Frangioni. Renal clearance of quantum dots. *Nature biotechnology* 2007; 25: 1165-70.
135. Choi, H. S., W. Liu, F. Liu, K. Nasr, P. Misra, M. G. Bawendi and J. V. Frangioni. Design considerations for tumour-targeted nanoparticles. *Nature nanotechnology* 2010; 5: 42-7.
136. Mrsny, R. Active Targeting Strategies in Cancer with a Focus on Potential Nanotechnology Applications. In *Nanotechnology for Cancer Therapy* 2006 pp. 19-42. CRC Press.

137. Juillerat-Jeanneret, L. The targeted delivery of cancer drugs across the blood-brain barrier: chemical modifications of drugs or drug-nanoparticles? *Drug discovery today* 2008; 13: 1099-106.
138. Fang, J.-Y. and S. A. Al-Suwayeh. Nanoparticles as delivery carriers for anticancer prodrugs. *Expert opinion on drug delivery* 2012; 9: 657-669.
139. Koo, O. M., I. Rubinstein and H. Onyuksel. Role of nanotechnology in targeted drug delivery and imaging: a concise review. *Nanomedicine : nanotechnology, biology, and medicine* 2005; 1: 193-212.
140. Jaracz, S., J. Chen, L. V. Kuznetsova and I. Ojima. Recent advances in tumor-targeting anticancer drug conjugates. *Bioorganic & medicinal chemistry* 2005; 13: 5043-54.
141. Rzigalinski, B. A. and J. S. Strobl. Cadmium-containing nanoparticles: perspectives on pharmacology and toxicology of quantum dots. *Toxicology and applied pharmacology* 2009; 238: 280-8.
142. Duncan, R. Polymer conjugates as anticancer nanomedicines. *Nature reviews. Cancer* 2006; 6: 688-701.
143. Couvreur, P. and C. Vauthier. Nanotechnology: intelligent design to treat complex disease. *Pharmaceutical research* 2006; 23: 1417-50.
144. Danson, S., D. Ferry, V. Alakhov, J. Margison, D. Kerr, D. Jowle, M. Brampton, G. Halbert and M. Ranson. Phase I dose escalation and pharmacokinetic study of pluronic polymer-bound doxorubicin (SP1049C) in patients with advanced cancer. *British journal of cancer* 2004; 90: 2085-91.
145. Torchilin, V. P. Recent advances with liposomes as pharmaceutical carriers. *Nature reviews. Drug discovery* 2005; 4: 145-160.
146. Lopes de Menezes, D. E., L. M. Pilarski and T. M. Allen. In vitro and in vivo targeting of immunoliposomal doxorubicin to human B-cell lymphoma. *Cancer research* 1998; 58: 3320-30.
147. Kukowska-Latallo, J. F., K. A. Candido, Z. Cao, S. S. Nigavekar, I. J. Majoros, T. P. Thomas, L. P. Balogh, M. K. Khan and J. R. Baker, Jr. Nanoparticle targeting of anticancer drug improves therapeutic response in animal model of human epithelial cancer. *Cancer research* 2005; 65: 5317-24.
148. Gradishar, W. J., S. Tjulandin, N. Davidson, H. Shaw, N. Desai, P. Bhar, M. Hawkins and J. O'Shaughnessy. Phase III trial of nanoparticle albumin-bound paclitaxel compared with polyethylated castor oil-based paclitaxel in women with breast cancer. *Journal of clinical oncology : official journal of the American Society of Clinical Oncology* 2005; 23: 7794-803.
149. Hrkach, J. S., M. T. Peracchia, A. Domb, N. Lotan and R. Langer. Nanotechnology for biomaterials engineering: structural characterization of amphiphilic polymeric nanoparticles by ¹H NMR spectroscopy. *Biomaterials* 1997; 18: 27-30.
150. Matsumura, Y., T. Hamaguchi, T. Ura, K. Muro, Y. Yamada, Y. Shimada, K. Shirao, T. Okusaka, H. Ueno, M. Ikeda and N. Watanabe. Phase I clinical trial and pharmacokinetic evaluation of NK911, a micelle-encapsulated doxorubicin. *British journal of cancer* 2004; 91: 1775-81.
151. Bonacucina, G., M. Cespi, M. Misici-Falzi and G. F. Palmieri. Colloidal soft matter as drug delivery system. *Journal of Pharmaceutical Sciences* 2009; 98: 1-42.
152. Kojima, C., K. Kono, K. Maruyama and T. Takagishi. Synthesis of Polyamidoamine Dendrimers Having Poly(ethylene glycol) Grafts and Their Ability To Encapsulate Anticancer Drugs. *Bioconjugate chemistry* 2000; 11: 910-917.
153. Shah, D. S., T. Sakthivel, I. Toth, A. T. Florence and A. F. Wilderspin. DNA transfection and transfected cell viability using amphipathic asymmetric dendrimers. *International Journal of Pharmaceutics* 2000; 208: 41-48.

154. Buse, J. and A. El-Aneed. Properties, engineering and applications of lipid-based nanoparticle drug-delivery systems: current research and advances. *Nanomedicine (Lond)* 2010; 5: 1237-60.
155. Zhang, L., F. X. Gu, J. M. Chan, A. Z. Wang, R. S. Langer and O. C. Farokhzad. Nanoparticles in medicine: therapeutic applications and developments. *Clinical pharmacology and therapeutics* 2008; 83: 761-9.
156. Bangham, A. D., M. M. Standish and J. C. Watkins. Diffusion of univalent ions across the lamellae of swollen phospholipids. *Journal of molecular biology* 1965; 13: 238-52.
157. Gregoriadis, G., E. J. Wills, C. P. Swain and A. S. Tavill. Drug-carrier potential of liposomes in cancer chemotherapy. *Lancet* 1974; 1: 1313-6.
158. Bitounis, D., R. Fanciullino, A. Iliadis and J. Ciccolini. Optimizing Druggability through Liposomal Formulations: New Approaches to an Old Concept. *ISRN Pharmaceutics* 2012; 2012: 11.
159. Samad, A., Y. Sultana and M. Aqil. Liposomal drug delivery systems: an update review. *Current drug delivery* 2007; 4: 297-305.
160. Ulrich, A. Biophysical Aspects of Using Liposomes as Delivery Vehicles. *Bioscience Reports* 2002; 22: 129-150.
161. Papahadjopoulos, D. and H. K. Kimelberg *Phospholipid vesicles (liposomes) as models for biological membranes: their properties and interactions with cholesterol and proteins*. Elsevier, 1974 Amsterdam; New York.
162. Lasic, D. D. The mechanism of vesicle formation. *Biochem J* 1988; 256: 1-11.
163. Goldbach, P., H. Brochart, P. Wehrlé and A. Stamm. Sterile filtration of liposomes: Retention of encapsulated carboxyfluorescein. *International Journal of Pharmaceutics* 1995; 117: 225-230.
164. Lasic, D. D. *Liposomes from Physics to Applications*. Elsevier, 1993 Amsterdam; New York.
165. Slingerland, M., H. J. Guchelaar and H. Gelderblom. Liposomal drug formulations in cancer therapy: 15 years along the road. *Drug discovery today* 2012; 17: 160-6.
166. Gregoriadis, G. *Liposome technology: liposome preparation and related techniques*. Taylor & Francis, 2007 London.
167. Torchilin, V. P. Passive and active drug targeting: drug delivery to tumors as an example. *Handbook of experimental pharmacology* 2010: 3-53.
168. Lobatto, M. E., V. Fuster, Z. A. Fayad and W. J. Mulder. Perspectives and opportunities for nanomedicine in the management of atherosclerosis. *Nature reviews. Drug discovery* 2011; 10: 835-52.
169. Barenholz, Y. Liposome application: problems and prospects. *Current Opinion in Colloid & Interface Science* 2001; 6: 66-77.
170. Storm, G. and D. J. Crommelin. Colloidal systems for tumor targeting. *Hybridoma* 1997; 16: 119-25.
171. Abra, R. M. and C. A. Hunt. Liposome disposition in vivo. III. Dose and vesicle-size effects. *Biochimica et biophysica acta* 1981; 666: 493-503.
172. Moghimi, S. M. Mechanisms of splenic clearance of blood cells and particles: towards development of new splenotropic agents. *Advanced drug delivery reviews* 1995; 17: 103-115.
173. Klibanov, A. L., K. Maruyama, A. M. Beckerleg, V. P. Torchilin and L. Huang. Activity of amphiphatic poly(ethylene glycol) 5000 to prolong the circulation time of liposomes depends on the liposome size and is unfavorable for immunoliposome binding to target. *Biochimica et biophysica acta* 1991; 1062: 142-8.
174. Drummond, D. C., O. Meyer, K. Hong, D. B. Kirpotin and D. Papahadjopoulos. Optimizing liposomes for delivery of chemotherapeutic agents to solid tumors. *Pharmacological reviews* 1999; 51: 691-743.

175. Drummond, D. C., C. O. Noble, M. E. Hayes, J. W. Park and D. B. Kirpotin. Pharmacokinetics and in vivo drug release rates in liposomal nanocarrier development. *J Pharm Sci* 2008; 97: 4696-740.
176. Gregoriadis, G. and J. Senior. Control of fate and behaviour of liposomes in vivo. *Progress in clinical and biological research* 1982; 102 pt A: 263-79.
177. Papahadjopoulos, D., K. Jacobson, S. Nir and T. Isac. Phase transitions in phospholipid vesicles. Fluorescence polarization and permeability measurements concerning the effect of temperature and cholesterol. *Biochimica et biophysica acta* 1973; 311: 330-48.
178. Allen, T. M. and C. Hansen. Pharmacokinetics of stealth versus conventional liposomes: effect of dose. *Biochimica et biophysica acta* 1991; 1068: 133-41.
179. Kamps, J. A. and G. L. Scherphof. Biodistribution and uptake of liposomes in vivo. *Methods in enzymology* 2004; 387: 257-66.
180. Gaumet, M., A. Vargas, R. Gurny and F. Delie. Nanoparticles for drug delivery: the need for precision in reporting particle size parameters. *European journal of pharmaceuticals and biopharmaceutics : official journal of Arbeitsgemeinschaft fur Pharmazeutische Verfahrenstechnik e.V* 2008; 69: 1-9.
181. Patel, H. M. and S. M. Moghimi. Serum-mediated recognition of liposomes by phagocytic cells of the reticuloendothelial system - The concept of tissue specificity. *Advanced drug delivery reviews* 1998; 32: 45-60.
182. Dobrovolskaia, M. A. and S. E. McNeil. Immunological properties of engineered nanomaterials. *Nature nanotechnology* 2007; 2: 469-78.
183. Hoffman, A. S. The origins and evolution of "controlled" drug delivery systems. *Journal of controlled release : official journal of the Controlled Release Society* 2008; 132: 153-63.
184. Yan, X., G. L. Scherphof and J. A. Kamps. Liposome opsonization. *Journal of liposome research* 2005; 15: 109-39.
185. Senior, J., J. C. Crawley and G. Gregoriadis. Tissue distribution of liposomes exhibiting long half-lives in the circulation after intravenous injection. *Biochimica et biophysica acta* 1985; 839: 1-8.
186. Semple, S. C. and A. Chonn. Liposome-Blood Protein Interactions in Relation to Liposome Clearance. *Journal of liposome research* 1996; 6: 33-60.
187. Oja, C. D., S. C. Semple, A. Chonn and P. R. Cullis. Influence of dose on liposome clearance: critical role of blood proteins. *Biochimica et biophysica acta* 1996; 1281: 31-7.
188. Owens, D. E., 3rd and N. A. Peppas. Opsonization, biodistribution, and pharmacokinetics of polymeric nanoparticles. *Int J Pharm* 2006; 307: 93-102.
189. Guo, L. S., R. L. Hamilton, J. Goerke, J. N. Weinstein and R. J. Havel. Interaction of unilamellar liposomes with serum lipoproteins and apolipoproteins. *Journal of lipid research* 1980; 21: 993-1003.
190. Scherphof, G., F. Roerdink, M. Waite and J. Parks. Disintegration of phosphatidylcholine liposomes in plasma as a result of interaction with high-density lipoproteins. *Biochimica et biophysica acta* 1978; 542: 296-307.
191. Chobanian, J. V., A. R. Tall and P. I. Brecher. Interaction between unilamellar egg yolk lecithin vesicles and human high density lipoprotein. *Biochemistry* 1979; 18: 180-187.
192. Jonas, A. Interaction of bovine serum high density lipoprotein with mixed vesicles of phosphatidylcholine and cholesterol. *Journal of lipid research* 1979; 20: 817-24.
193. Tall, A. R., I. Tabas and K. J. Williams. Lipoprotein-liposome interactions. *Methods in enzymology* 1986; 128: 647-57.
194. Semple, S. C., A. Chonn and P. R. Cullis. Interactions of liposomes and lipid-based carrier systems with blood proteins: Relation to clearance behaviour in vivo. *Adv Drug Deliv Rev* 1998; 32: 3-17.
195. Shahrokh, Z. and A. V. Nichols. Particle size interconversion of human low density lipoproteins during incubation of plasma with phosphatidylcholine vesicles. *Biochem Biophys Res Commun* 1982; 108: 888-95.

196. Damen, J., J. Regts and G. Scherphof. Transfer of [14C]phosphatidylcholine between liposomes and human plasma high density lipoprotein Partial purification of a transfer-stimulating plasma factor using a rapid transfer assay. *Biochimica et Biophysica Acta (BBA) - Lipids and Lipid Metabolism* 1982; 712: 444-452.
197. Lalanne, F. and G. Ponsin. Mechanism of the phospholipid transfer protein-mediated transfer of phospholipids from model lipid vesicles to high density lipoproteins. *Biochimica et biophysica acta* 2000; 1487: 82-91.
198. Epstein-Barash, H., D. Gutman, E. Markovsky, G. Mishan-Eisenberg, N. Koroukhov, J. Szebeni and G. Golomb. Physicochemical parameters affecting liposomal bisphosphonates bioactivity for restenosis therapy: internalization, cell inhibition, activation of cytokines and complement, and mechanism of cell death. *Journal of controlled release : official journal of the Controlled Release Society* 2010; 146: 182-95.
199. Ogihara-Umeda, I. and S. Kojima. Increased delivery of gallium-67 to tumors using serum-stable liposomes. *Journal of nuclear medicine : official publication, Society of Nuclear Medicine* 1988; 29: 516-23.
200. Charrois, G. J. and T. M. Allen. Drug release rate influences the pharmacokinetics, biodistribution, therapeutic activity, and toxicity of pegylated liposomal doxorubicin formulations in murine breast cancer. *Biochimica et biophysica acta* 2004; 1663: 167-77.
201. Kaasgaard, T. and T. L. Andresen. Liposomal cancer therapy: exploiting tumor characteristics. *Expert opinion on drug delivery* 2010; 7: 225-43.
202. Song, G., H. Wu, K. Yoshino and W. C. Zamboni. Factors affecting the pharmacokinetics and pharmacodynamics of liposomal drugs. *Journal of liposome research* 2012.
203. Lindner, L. H. and M. Hossann. Factors affecting drug release from liposomes. *Current opinion in drug discovery & development* 2010; 13: 111-23.
204. Fahr, A. and J. Seelig. Liposomal formulations of Cyclosporin A: a biophysical approach to pharmacokinetics and pharmacodynamics. *Crit Rev Ther Drug Carrier Syst* 2001; 18: 141-72.
205. Hillaireau, H. and P. Couvreur. Nanocarriers' entry into the cell: relevance to drug delivery. *Cellular and Molecular Life Sciences* 2009; 66: 2873-2896.
206. Ringsdorf, H. Structure and properties of pharmacologically active polymers. *Journal of Polymer Science: Polymer Symposia* 1975; 51: 135-153.
207. Gabizon, A. A. Liposome circulation time and tumor targeting: implications for cancer chemotherapy. *Advanced drug delivery reviews* 1995; 16: 285-294.
208. Allen, T. M. and A. Chonn. Large unilamellar liposomes with low uptake into the reticuloendothelial system. *FEBS Letters* 1987; 223: 42-46.
209. Liu, D., F. Liu and Y. K. Song. Monosialoganglioside GM1 shortens the blood circulation time of liposomes in rats. *Pharmaceutical research* 1995; 12: 508-12.
210. Ishida, T., M. Harada, X. Y. Wang, M. Ichihara, K. Irimura and H. Kiwada. Accelerated blood clearance of PEGylated liposomes following preceding liposome injection: effects of lipid dose and PEG surface-density and chain length of the first-dose liposomes. *Journal of controlled release : official journal of the Controlled Release Society* 2005; 105: 305-17.
211. Allen, C., N. Dos Santos, R. Gallagher, G. N. Chiu, Y. Shu, W. M. Li, S. A. Johnstone, A. S. Janoff, L. D. Mayer, M. S. Webb and M. B. Bally. Controlling the physical behavior and biological performance of liposome formulations through use of surface grafted poly(ethylene glycol). *Bioscience reports* 2002; 22: 225-50.
212. Gabizon, A. and D. Papahadjopoulos. Liposome formulations with prolonged circulation time in blood and enhanced uptake by tumors. *Proceedings of the National Academy of Sciences of the United States of America* 1988; 85: 6949-53.
213. Scherphof, G. L., H. Morselt and T. M. Allen. Intrahepatic Distribution of Long-Circulating Liposomes Containing Poly(ethylene Glycol) Distearoyl Phosphatidylethanolamine. *Journal of liposome research* 1994; 4: 213-228.

214. Allen, T. M. Liposomes. Opportunities in drug delivery. *Drugs* 1997; 54 Suppl 4: 8-14.
215. van Vlerken, L. E., T. K. Vyas and M. M. Amiji. Poly(ethylene glycol)-modified nanocarriers for tumor-targeted and intracellular delivery. *Pharmaceutical research* 2007; 24: 1405-14.
216. Elbert, D. L. and J. A. Hubbell. Surface Treatments of Polymers for Biocompatibility. *Annual Review of Materials Science* 1996; 26: 365-294.
217. Kjellander, R. and E. Florin. Water structure and changes in thermal stability of the system poly(ethylene oxide)-water. *Journal of the Chemical Society, Faraday Transactions 1: Physical Chemistry in Condensed Phases* 1981; 77: 2053-2077.
218. de Gennes, P. G. Conformations of Polymers Attached to an Interface. *Macromolecules* 1980; 13: 1069-1075.
219. Immordino, M. L., F. Dosio and L. Cattel. Stealth liposomes: review of the basic science, rationale, and clinical applications, existing and potential. *International journal of nanomedicine* 2006; 1: 297-315.
220. Torchilin, V. P. and M. I. Papisov. Why do Polyethylene Glycol-Coated Liposomes Circulate So Long?: Molecular Mechanism of Liposome Steric Protection with Polyethylene Glycol: Role of Polymer Chain Flexibility. *Journal of liposome research* 1994; 4: 725-739.
221. Chonn, A., S. C. Semple and P. R. Cullis. Association of blood proteins with large unilamellar liposomes in vivo. Relation to circulation lifetimes. *The Journal of biological chemistry* 1992; 267: 18759-65.
222. Johnstone, S. A., D. Masin, L. Mayer and M. B. Bally. Surface-associated serum proteins inhibit the uptake of phosphatidylserine and poly(ethylene glycol) liposomes by mouse macrophages. *Biochimica et biophysica acta* 2001; 1513: 25-37.
223. Ahl, P. L., S. K. Bhatia, P. Meers, P. Roberts, R. Stevens, R. Dause, W. R. Perkins and A. S. Janoff. Enhancement of the in vivo circulation lifetime of L-alpha-distearoylphosphatidylcholine liposomes: importance of liposomal aggregation versus complement opsonization. *Biochimica et biophysica acta* 1997; 1329: 370-82.
224. Palmer, T. N., V. J. Caride, M. A. Caldecourt, J. Twickler and V. Abdullah. The mechanism of liposome accumulation in infarction. *Biochimica et biophysica acta* 1984; 797: 363-8.
225. Torchilin, V. P., A. N. Lukyanov, Z. Gao and B. Papahadjopoulos-Sternberg. Immunomicelles: Targeted pharmaceutical carriers for poorly soluble drugs. *Proceedings of the National Academy of Sciences* 2003; 100: 6039-6044.
226. Narang, A. S. and S. Varia. Role of tumor vascular architecture in drug delivery. *Advanced drug delivery reviews* 2011; 63: 640-58.
227. Fang, J., H. Nakamura and H. Maeda. The EPR effect: Unique features of tumor blood vessels for drug delivery, factors involved, and limitations and augmentation of the effect. *Advanced drug delivery reviews* 2011; 63: 136-51.
228. Matsumura, Y. and H. Maeda. A new concept for macromolecular therapeutics in cancer chemotherapy: mechanism of tumoritropic accumulation of proteins and the antitumor agent smancs. *Cancer research* 1986; 46: 6387-92.
229. Andresen, T. L., S. S. Jensen and K. Jorgensen. Advanced strategies in liposomal cancer therapy: problems and prospects of active and tumor specific drug release. *Progress in lipid research* 2005; 44: 68-97.
230. Yuan, F., M. Dellian, D. Fukumura, M. Leunig, D. A. Berk, V. P. Torchilin and R. K. Jain. Vascular permeability in a human tumor xenograft: molecular size dependence and cutoff size. *Cancer research* 1995; 55: 3752-6.
231. Padera, T. P., B. R. Stoll, J. B. Tooredman, D. Capen, E. di Tomaso and R. K. Jain. Pathology: cancer cells compress intratumour vessels. *Nature* 2004; 427: 695.
232. Adisheshaiah, P. P., J. B. Hall and S. E. McNeil. Nanomaterial standards for efficacy and toxicity assessment. *Wiley interdisciplinary reviews. Nanomedicine and nanobiotechnology* 2010; 2: 99-112.

233. Wang, X., J. Li, Y. Wang, K. J. Cho, G. Kim, A. Gjyzezi, L. Koenig, P. Giannakakou, H. J. Shin, M. Tighiouart, S. Nie, Z. G. Chen and D. M. Shin. HFT-T, a targeting nanoparticle, enhances specific delivery of paclitaxel to folate receptor-positive tumors. *ACS nano* 2009; 3: 3165-74.
234. Gupta, B. and V. P. Torchilin. Monoclonal antibody 2C5-modified doxorubicin-loaded liposomes with significantly enhanced therapeutic activity against intracranial human brain U-87 MG tumor xenografts in nude mice. *Cancer immunology, immunotherapy : CII* 2007; 56: 1215-23.
235. Abra, R. M., R. B. Bankert, F. Chen, N. K. Egilmez, K. Huang, R. Saville, J. L. Slater, M. Sugano and S. J. Yokota. The next generation of liposome delivery systems: recent experience with tumor-targeted, sterically-stabilized immunoliposomes and active-loading gradients. *Journal of liposome research* 2002; 12: 1-3.
236. Beija, M., R. Salvayre, N. Lauth-de Viguerie and J. D. Marty. Colloidal systems for drug delivery: from design to therapy. *Trends in biotechnology* 2012.
237. Keene, J. P., D. Kessel, E. J. Land, R. W. Redmond and T. G. Truscott. Direct detection of singlet oxygen sensitized by haematoporphyrin and related compounds. *Photochem Photobiol* 1986; 43: 117-20.
238. Chen, Y., A. Gryshuk, S. Achilefu, T. Ohulchansky, W. Potter, T. Zhong, J. Morgan, B. Chance, P. N. Prasad, B. W. Henderson, A. Oseroff and R. K. Pandey. A novel approach to a bifunctional photosensitizer for tumor imaging and phototherapy. *Bioconjugate chemistry* 2005; 16: 1264-74.
239. Chen, Y., R. Miclea, T. Srikrishnan, S. Balasubramanian, T. J. Dougherty and R. K. Pandey. Investigation of human serum albumin (HSA) binding specificity of certain photosensitizers related to pyropheophorbide-a and bacteriopheophorbide by circular dichroism spectroscopy and its correlation with in vivo photosensitizing efficacy. *Bioorganic & medicinal chemistry letters* 2005; 15: 3189-92.
240. Donnelly, R. F., P. A. McCarron, D. I. Morrow, S. A. Sibani and A. D. Woolfson. Photosensitizer delivery for photodynamic therapy. Part 1: Topical carrier platforms. *Expert opinion on drug delivery* 2008; 5: 757-66.
241. Damoiseau, X., H. J. Schuitmaker, J. W. Lagerberg and M. Hoebeke. Increase of the photosensitizing efficiency of the Bacteriochlorin a by liposome-incorporation. *Journal of photochemistry and photobiology. B, Biology* 2001; 60: 50-60.
242. Chen, B., B. W. Pogue and T. Hasan. Liposomal delivery of photosensitising agents. *Expert opinion on drug delivery* 2005; 2: 477-487.
243. Derycke, A. S. and P. A. de Witte. Liposomes for photodynamic therapy. *Advanced drug delivery reviews* 2004; 56: 17-30.
244. Jin, C. S. and G. Zheng. Liposomal nanostructures for photosensitizer delivery. *Lasers in surgery and medicine* 2011; 43: 734-48.
245. Ricchelli, F., S. Gobbo, G. Moreno, C. Salet, L. Brancalion and A. Mazzini. Photophysical properties of porphyrin planar aggregates in liposomes. *European Journal of Biochemistry* 1998; 253: 760-765.
246. Ribo, J. M., J. Crusats, J.-A. Farrera and M. L. Valero. Aggregation in water solutions of tetrasodium diprotonated meso-tetrakis(4-sulfonatophenyl)porphyrin. *Journal of the Chemical Society, Chemical Communications* 1994: 681-682.
247. Wang, Z. J., Y. Y. He, C. G. Huang, J. S. Huang, Y. C. Huang, J. Y. An, Y. Gu and L. J. Jiang. Pharmacokinetics, tissue distribution and photodynamic therapy efficacy of liposomal-delivered hypocrellin A, a potential photosensitizer for tumor therapy. *Photochem Photobiol* 1999; 70: 773-80.
248. Zimcik, P., M. Miletin, K. Kopecky, Z. Musil, P. Berka, V. Horakova, H. Kucerova, J. Zbytovska and D. Brault. Influence of aggregation on interaction of lipophilic, water-insoluble azaphthalocyanines with DOPC vesicles. *Photochem Photobiol* 2007; 83: 1497-504.

249. Delanaye, L., M. A. Bahri, F. Tfibel, M. P. Fontaine-Aupart, A. Mouithys-Mickalad, B. Heine, J. Piette and M. Hoebeke. Physical and chemical properties of pyropheophorbide-a methyl ester in ethanol, phosphate buffer and aqueous dispersion of small unilamellar dimyristoyl-L-alpha-phosphatidylcholine vesicles. *Photochemical & photobiological sciences : Official journal of the European Photochemistry Association and the European Society for Photobiology* 2006; 5: 317-25.
250. Brault, D., C. Vever-Bizet and T. Le Doan. Spectrofluorimetric study of porphyrin incorporation into membrane models--evidence for pH effects. *Biochimica et biophysica acta* 1986; 857: 238-50.
251. Ehrenberg, B., Z. Malik and Y. Nitzan. Fluorescence spectral changes of hematoporphyrin derivative upon binding to lipid vesicles, Staphylococcus aureus and Escherichia coli cells. *Photochem Photobiol* 1985; 41: 429-35.
252. Lang, K., J. Mosinger and D. M. Wagnerová. Photophysical properties of porphyrinoid sensitizers non-covalently bound to host molecules; models for photodynamic therapy. *Coordination Chemistry Reviews* 2004; 248: 321-350.
253. Chowdhary, R. K., I. Shariff and D. Dolphin. Drug release characteristics of lipid based benzoporphyrin derivative. *J Pharm Pharm Sci* 2003; 6: 13-19.
254. Lavi, A., H. Weitman, R. T. Holmes, K. M. Smith and B. Ehrenberg. The Depth of Porphyrin in a Membrane and the Membrane's Physical Properties Affect the Photosensitizing Efficiency. *Biophys J* 2002; 82: 2101-2110.
255. Bronshtein, I., M. Afri, H. Weitman, A. A. Frimer, K. M. Smith and B. Ehrenberg. Porphyrin Depth in Lipid Bilayers as Determined by Iodide and Parallax Fluorescence Quenching Methods and Its Effect on Photosensitizing Efficiency. *Biophys J* 2004; 87: 1155-1164.
256. Herenyi, L., D. Veres, S. Bekasi, I. Voszka, K. Modos, G. Csik, A. D. Kaposi and J. Fidy. Location of mesoporphyrin in liposomes determined by site-selective fluorescence spectroscopy. *The journal of physical chemistry. B* 2009; 113: 7716-24.
257. Mojzisova, H., S. Bonneau, P. Maillard, K. Berg and D. Brault. Photosensitizing properties of chlorins in solution and in membrane-mimicking systems. *Photochemical & Photobiological Sciences* 2009; 8: 778-787.
258. Borovkov, V. V., M. Anikin, K. Wasa and Y. Sakata. Structurally Controlled Porphyrin-Aggregation Process in Phospholipid Membranes. *Photochem Photobiol* 1996; 63: 477-482.
259. Derycke, A. S., A. Kamuhabwa, A. Gijssens, T. Roskams, D. De Vos, A. Kasran, J. Huwyler, L. Missiaen and P. A. de Witte. Transferrin-conjugated liposome targeting of photosensitizer AlPcS4 to rat bladder carcinoma cells. *J Natl Cancer Inst* 2004; 96: 1620-30.
260. Postigo, F., M. L. Sagrista, M. A. De Madariaga, S. Nonell and M. Mora. Photosensitization of skin fibroblasts and HeLa cells by three chlorin derivatives: Role of chemical structure and delivery vehicle. *Biochimica et biophysica acta* 2006; 1758: 583-96.
261. Qualls, M. M. and D. H. Thompson. Chloroaluminum phthalocyanine tetrasulfonate delivered via acid-labile diacylphosphatidylcholine-folate liposomes: intracellular localization and synergistic phototoxicity. *International journal of cancer. Journal international du cancer* 2001; 93: 384-92.
262. Milanese, C., F. Sorgato and G. Jori. Photokinetic and ultrastructural studies on porphyrin photosensitization of HeLa cells. *International journal of radiation biology* 1989; 55: 59-69.
263. Gijssens, A., A. Derycke, L. Missiaen, D. De Vos, J. Huwyler, A. Eberle and P. de Witte. Targeting of the photocytotoxic compound AlPcS4 to HeLa cells by transferrin conjugated PEG-liposomes. *International journal of cancer. Journal international du cancer* 2002; 101: 78-85.

264. Richter, A. M., E. Waterfield, A. K. Jain, A. J. Canaan, B. A. Allison and J. G. Levy. Liposomal delivery of a photosensitizer, benzoporphyrin derivative monoacid ring A (BPD), to tumor tissue in a mouse tumor model. *Photochem Photobiol* 1993; 57: 1000-1006.
265. Allison, B. A., M. T. Crespo, A. K. Jain, A. M. Richter, Y. N. Hsiang and J. G. Levy. Delivery of Benzoporphyrin Derivative, a Photosensitizer, into Atherosclerotic Plaque of Watanabe Heritable Hyperlipidemic Rabbits and Balloon-Injured New Zealand Rabbits. *Photochem Photobiol* 1997; 65: 877-883.
266. Jiang, F., L. Lilge, J. Grenier, Y. Li, M. D. Wilson and M. Chopp. Photodynamic therapy of U87 human glioma in nude rat using liposome-delivered photofrin. *Lasers in surgery and medicine* 1998; 22: 74-80.
267. Igarashi, A., H. Konno, T. Tanaka, S. Nakamura, Y. Sadzuka, T. Hirano and Y. Fujise. Liposomal photofrin enhances therapeutic efficacy of photodynamic therapy against the human gastric cancer. *Toxicology letters* 2003; 145: 133-41.
268. Davis, R. K., R. Straight and Z. Kereszti. Comparison of photosensitizers in saline and liposomes for tumor photodynamic therapy and skin phototoxicity. *The Laryngoscope* 1990; 100: 682-6.
269. Mayhew, E., L. Vaughan, A. Panus, M. Murray and B. W. Henderson. Lipid-associated methylpheophorbide-a (hexyl-ether) as a photodynamic agent in tumor-bearing mice. *Photochem Photobiol* 1993; 58: 845-51.
270. Ichikawa, K., T. Hikita, N. Maeda, Y. Takeuchi, Y. Namba and N. Oku. PEGylation of liposome decreases the susceptibility of liposomal drug in cancer photodynamic therapy. *Biological & pharmaceutical bulletin* 2004; 27: 443-4.
271. Shabbits, J. A., G. N. C. Chiu and L. D. Mayer. Development of an in vitro drug release assay that accurately predicts in vivo drug retention for liposome-based delivery systems. *Journal of Controlled Release* 2002; 84: 161-170.
272. Mayer, L. D., P. R. Cullis and M. B. Bally. The Use of Transmembrane pH Gradient-Driven Drug Encapsulation in the Pharmacodynamic Evaluation of Liposomal Doxorubicin. *Journal of liposome research* 1994; 4: 529-553.
273. Fahr, A., P. v. Hoogevest, S. May, N. Bergstrand and M. L. S. Leigh. Transfer of lipophilic drugs between liposomal membranes and biological interfaces: Consequences for drug delivery. *European Journal of Pharmaceutical Sciences* 2005; 26: 251-265.
274. Decker, D. E., S. M. Vroegop, T. G. Goodman, T. Peterson and S. E. Buxser. Kinetics and thermodynamics of emulsion delivery of lipophilic antioxidants to cells in culture. *Chemistry and Physics of Lipids* 1995; 76: 7-25.
275. Hefesha, H., S. Loew, X. Liu, S. May and A. Fahr. Transfer mechanism of temoporfin between liposomal membranes. *Journal of controlled release : official journal of the Controlled Release Society* 2011; 150: 279-86.
276. Loew, S., A. Fahr and S. May. Modeling the Release Kinetics of Poorly Water-Soluble Drug Molecules from Liposomal Nanocarriers. *Journal of Drug Delivery* 2011; 2011.
277. Washington, C. Drug release from microdisperse systems: a critical review. *International Journal of Pharmaceutics* 1990; 58: 1-12.
278. Henriksen, I., S. A. Sande, G. Smistad, T. Ågren and J. Karlsen. In vitro evaluation of drug release kinetics from liposomes by fractional dialysis. *International Journal of Pharmaceutics* 1995; 119: 231-238.
279. Fahr, A. and X. Liu. Utilization of liposomes for studying drug transfer and uptake. *Methods Mol Biol* 2010; 606: 1-10.
280. Petersen, S., A. Fahr and H. Bunjes. Flow Cytometry as a New Approach To Investigate Drug Transfer between Lipid Particles. *Molecular Pharmaceutics* 2010; 7: 350-363.
281. Hioki, A., A. Wakasugi, K. Kawano, Y. Hattori and Y. Maitani. Development of an in Vitro Drug Release Assay of PEGylated Liposome Using Bovine Serum Albumin and High Temperature. *Biological and Pharmaceutical Bulletin* 2010; 33: 1466-1470.

282. Dragicevic-Curic, N. and A. Fahr. Liposomes in topical photodynamic therapy. *Expert opinion on drug delivery* 2012.
283. Kuntsche, J., I. Freisleben, F. Steiniger and A. Fahr. Temoporfin-loaded liposomes: physicochemical characterization. *European journal of pharmaceutical sciences : official journal of the European Federation for Pharmaceutical Sciences* 2010; 40: 305-15.
284. Compagnin, C., F. Moret, L. Celotti, G. Miotto, J. H. Woodhams, A. J. MacRobert, D. Scheglmann, S. Iratni and E. Reddi. Meta-tetra(hydroxyphenyl)chlorin-loaded liposomes sterically stabilised with poly(ethylene glycol) of different length and density: characterisation, in vitro cellular uptake and phototoxicity. *Photochemical & photobiological sciences : Official journal of the European Photochemistry Association and the European Society for Photobiology* 2011; 10: 1751-9.
285. Rojnik, M., P. Kocbek, F. Moret, C. Compagnin, L. Celotti, M. J. Bovis, J. H. Woodhams, A. J. MacRobert, D. Scheglmann, W. Helfrich, M. J. Verkaik, E. Papini, E. Reddi and J. Kos. In vitro and in vivo characterization of temoporfin-loaded PEGylated PLGA nanoparticles for use in photodynamic therapy. *Nanomedicine (Lond)* 2012; 7: 663-77.
286. Kiesslich, T., J. Berlanda, K. Plaetzer, B. Krammer and F. Berr. Comparative characterization of the efficiency and cellular pharmacokinetics of Foscan- and Foslip-based photodynamic treatment in human biliary tract cancer cell lines. *Photochemical & photobiological sciences : Official journal of the European Photochemistry Association and the European Society for Photobiology* 2007; 6: 619-27.
287. Berlanda, J., T. Kiesslich, V. Engelhardt, B. Krammer and K. Plaetzer. Comparative in vitro study on the characteristics of different photosensitizers employed in PDT. *Journal of photochemistry and photobiology. B, Biology* 2010; 100: 173-80.
288. Compagnin, C., L. Bau, M. Mognato, L. Celotti, G. Miotto, M. Arduini, F. Moret, C. Fede, F. Selvestrel, I. M. Rio Echevarria, F. Mancin and E. Reddi. The cellular uptake of meta-tetra(hydroxyphenyl)chlorin entrapped in organically modified silica nanoparticles is mediated by serum proteins. *Nanotechnology* 2009; 20: 345101.
289. Lassalle, H. P., D. Dumas, S. Grafe, M. A. D'Hallewin, F. Guillemain and L. Bezdetsnaya. Correlation between in vivo pharmacokinetics, intratumoral distribution and photodynamic efficiency of liposomal mTHPC. *Journal of controlled release : official journal of the Controlled Release Society* 2009; 134: 118-24.
290. Bovis, M. J., J. H. Woodhams, M. Loizidou, D. Scheglmann, S. G. Bown and A. J. MacRobert. Improved in vivo delivery of m-THPC via pegylated liposomes for use in photodynamic therapy. *Journal of controlled release : official journal of the Controlled Release Society* 2012; 157: 196-205.
291. D'Hallewin, M. A., D. Kochetkov, Y. Viry-Babel, A. Leroux, E. Werkmeister, D. Dumas, S. Grafe, V. Zorin, F. Guillemain and L. Bezdetsnaya. Photodynamic therapy with intratumoral administration of Lipid-Based mTHPC in a model of breast cancer recurrence. *Lasers in surgery and medicine* 2008; 40: 543-9.
292. Petri, A., E. Alexandratou, M. Kyriazi, M. Rallis, V. Roussis and D. Yova. Combination of Fospeg-IPDT and a natural antioxidant compound prevents photosensitivity in a murine prostate cancer tumour model. *Photodiagnosis and photodynamic therapy* 2012; 9: 100-8.
293. Buchholz, J., B. Kaser-Hotz, T. Khan, C. Rohrer Bley, K. Melzer, R. A. Schwendener, M. Roos and H. Walt. Optimizing photodynamic therapy: in vivo pharmacokinetics of liposomal meta-(tetrahydroxyphenyl)chlorin in feline squamous cell carcinoma. *Clinical cancer research : an official journal of the American Association for Cancer Research* 2005; 11: 7538-44.
294. Svensson, J., A. Johansson, S. Gräfe, B. Gitter, T. Trebst, N. Bendsoe, S. Andersson-Engels and K. Svanberg. Tumor selectivity at short times following systemic administration of a liposomal temoporfin formulation in a murine tumor model. *Photochem Photobiol* 2007; 83: 1211-1219.

295. Buchholz, J., M. Wergin, H. Walt, S. Gräfe, C. R. Bley and B. Kaser-Hotz. Photodynamic Therapy of Feline Cutaneous Squamous Cell Carcinoma Using a Newly Developed Liposomal Photosensitizer: Preliminary Results Concerning Drug Safety and Efficacy. *Journal of Veterinary Internal Medicine* 2007; 21: 770-775.
296. Ohlerth, S., D. Lalahová, J. Buchholz, M. Roos, H. Walt and B. Kaser-Hotz. Changes in vascularity and blood volume as a result of photodynamic therapy can be assessed with power Doppler ultrasonography. *Lasers in surgery and medicine* 2006; 38: 229-234.
297. de Visscher, S. A., S. Kascakova, H. S. de Bruijn, A. P. van den Heuvel, A. Amelink, H. J. Sterenborg, D. J. Robinson, J. L. Roodenburg and M. J. Witjes. Fluorescence localization and kinetics of mTHPC and liposomal formulations of mTHPC in the window-chamber tumor model. *Lasers in surgery and medicine* 2011; 43: 528-36.
298. Pegaz, B., E. Debefve, J. P. Ballini, G. Wagnieres, S. Spaniol, V. Albrecht, D. V. Scheglmann, N. E. Nifantiev, H. van den Bergh and Y. N. Konan-Kouakou. Photothrombic activity of m-THPC-loaded liposomal formulations: pre-clinical assessment on chick chorioallantoic membrane model. *European journal of pharmaceutical sciences : official journal of the European Federation for Pharmaceutical Sciences* 2006; 28: 134-40.

Scientific output

SCIENTIFIC OUTPUT

1. ARTICLES IN PEER-REVIEWED JOURNALS

1. M. Pernot, T. Bastogne, N.P.E. Barry, B. Therrien, G. Koellensperger, S. Hann, **V. Reshetov** and M. Barberi-Heyob. System Biology Approach for in vivo Photodynamic Therapy Optimization of Ruthenium-Porphyrin Compounds // *J Photochem Photobiol B* 2012, **115**, 80-89.

2. B. Maherani, E. Arab-tehrany, A. Kheiriloom, **V. Reshetov**, M. J. Stebe, M. Linder. Optimization and Characterization of Liposome Formulation By Mixture Design // *Analyst* 2012, **137**, 773-786.

3. J. Garrier, **V. Reshetov**, V. Zorin, F. Guillemin, L. Bezdetnaya. Contrasting facets of nanoparticles-based phototherapy: photo-damage and photo-regeneration // Book chapter in *Photodynamic therapy: New research*. Nova Publishers 2012 (in print).

4. **V. Reshetov**, M. Artemyev, V. Zorin. Fluorescence quenching of CdSe/ZnS quantum dots in solution and in lipid vesicles (in Russian) // *Proceedings of National Academy of Sciences of Belarus* 2008, 52-54.

2. MAJOR ORAL COMMUNUCATIONS

1. **V. Reshetov**, D. Kachatkou, D. Scheglmann, T.E. Zorina, S. Grafe, F. Guillemin, L. Bolotine, V. Zorin. Photophysical properties of mTHPC in conventional and pegylated unilamellar lipid vesicles // *13th Congress of the European Society for Photobiology*, 5-10 September 2009, Wroclaw, Poland. – Book of abstracts. – 2009. – P.97-98.

2. **V. Reshetov**, A. Siupa, L. Bezdetnaya, V. Zorin. Interactions of mTHPC liposomal formulations with serum proteins // *14th Congress of the European Society for Photobiology*, September 1-6, 2011, Geneva, Switzerland. – Book of abstracts. – 2011. – P.90-91.

3. **V.A. Reshetov**, T.E. Zorina, M.-A. D'Hallewin, L. Bolotine, V.P. Zorin. Comparison of techniques of drug redistribution registration from nanosized carriers in biological systems // *Optical techniques and nano-tools for material and life sciences*, 15-19 June 2010, Minsk, Belarus. – Contributed papers. – 2010. – P.193-199.

4. **Reshetov V.A.**, Shmigol T.A., Potapenko A.Ya., Bolotine L.N., Zorin V.P. Resonance light scattering spectra of meta-tetra(hydroxyphenyl)chlorin in liposomes // *Molecular, membrane and cell fundamentals of biosystems functioning*, 23-25 June 2010, Minsk, Belarus. – Contributed papers. – 2010. – P.295-297.

5. **Reshetov V.A.**, Zorina T.E., D'Hallewin M.-A., Bolotine L.N., Zorin V.P. Redistribution of meta-tetra(hydroxyphenyl)chlorin from conventional and pegylated liposomes// *Molecular, membrane and cell fundamentals of biosystems functioning*, 23-25 June 2010, Minsk, Belarus. – Contributed papers. – 2010. – P.289-291.

3. POSTERS

1. **V. Reshetov**, V. Zorin, L. Bolotine. Interaction of mTHPC liposomal formulations with serum proteins // *3rd Joint Meeting of the French Society for Photobiology and the Italian Society for Photobiology*, 25-26 October 2010, Paris, France. – Abstracts. – 2010.

2. **Reshetov V.**, François A., Lassalle H., Dumas D., Filipe V., Zorin V., Bezdetnaya L. Formulations liposomales pour le traitement des cancers: relations entre propriétés physico-chimique, libération de la drogue, dégradation du vecteur, localisation intra-tumorale et efficacité de traitement // *7^{ème} Journée Claude Huriet de la Recherche Biomedicale*, 2 March 2012, Nancy, France. – Book of abstracts. – 2012. – P. E32.

4. COMMUNICATIONS PRESENTED BY COLLABORATORS

1. V.P. Zorin, D.S. Kachatkou, **V.A. Reshetov**, T.E. Zorina, M.-A. D'Hallewin, F. H. Guillemin, L.N. Bezdetnaya. Kinetics of mTHPC release from liposomes // *12th World Congress of the International Photodynamic Association*, Seattle, USA, 11-15 June 2009. – Meeting Report. – P.80.

2. J. Garrier, **V. Reshetov**, D. Dumas, V. Zorin, A. François, M.-A. D'Hallewin, F. Guillemin, L. Bezdetnaya. Spatio-temporal redistribution of mTHPC from lipid nanovesicles in chick chorioallantoic membrane model // *3rd Joint Meeting of the French Society for Photobiology and the Italian Society for Photobiology*, 25-26 October 2010, Paris, France. – Abstracts. – 2010.

3. J. Garrier, **V. Reshetov**, C. Ruch, F. Guillemin, V. Zorin, L. Bezdetnaya. Vascular damage photoinduced by liposomal formulations of mTHPC in xenografted CAM: influence of drug release // *14th Congress of the European Society for Photobiology*, September 1-6, 2011, Geneva, Switzerland. – Book of abstracts. – 2011. – P.90.

4. J. Garrier, **V. Reshetov**, A. François, S. Gräfe, V. Filipe, W. Jiskoot, F. Guillemin, V. Zorin, L. Bezdetnaya. Vascular and cellular damage photoinduced in Chorioallantoic Membrane model by Foslip[®] and Fospeg[®]: influence of mTHPC release from liposomes // *36th Meeting of the American Society for Photobiology*, 23-27 June 2012, Montreal, Canada. – Book of abstracts. – 2012. – P. 56-57.

5. Zorin V.P., **Reshetov V.A.**, Zorina T.E., D'Hallewin M-A., Guillemin F., Bezdetsnaya L.N. Photophysical and kinetic properties of meta-tetra-hydroxyphenylchlorin in lipid nanovesicles // *XI International Conference on physical and coordination chemistry of porphyrins and their analogues*, 10-14 June 2011, Odessa, Ukraine. – Book of abstracts. – 2011. – P.36.

Summary in French

RESUME DE LA THESE EN FRANÇAIS

Depuis de nombreuses années, les liposomes ont été évalués en tant que systèmes de transport des drogues et décrits comme présentant divers avantages tels que l'amélioration de l'efficacité thérapeutique accompagnée d'une diminution de la dose de drogue nécessaire et de sa toxicité, de l'amélioration de son profil pharmacocinétique et de son ciblage. De part leur petite taille caractéristique, leur pouvoir de solubilisation et leur stabilité, les liposomes constituent un système parfaitement adapté à la délivrance de drogues photosensibilisantes non-polaires. L'incorporation de photosensibilisateurs (PS) tétrapyrroliques dans les vésicules lipidiques permet leur monomérisation et leur confère une activité photosensibilisante élevée. De tels systèmes offrent également la possibilité de faire un ciblage passif de tissus grâce à l'effet de perméabilité et de rétention renforcées (enhanced permeability and retention effect, EPR).

Le but global de cette étude a été de caractériser *in vitro* les formulations liposomales de la méta-tétrahydroxyphénylchlorine (mTHPC, Foscan[®]), un PS de 2nde génération actuellement le plus efficace sur le marché. Malgré un nombre croissant d'études portant sur la thérapie photodynamique (PDT) avec des formulations liposomales de mTHPC (Foslip[®] et Fospeg[®]), seuls quelques articles ont abordé la caractérisation de la drogue dans un environnement lipidique incluant ses propriétés photophysiques, sa localisation et sa redistribution.

L'étude des caractéristiques spectroscopiques de la mTHPC liposomale avec des ratios drogue/lipide variables, décrite dans la première partie des résultats, a démontré un impact des interactions entre les molécules de mTHPC en présence d'une forte concentration locale dans les liposomes. Une diminution de la distance entre les molécules de mTHPC a augmenté la probabilité de transfert d'énergie conduisant ainsi à une dépolarisation significative et à l'apparition d'un phénomène appelé le « photoinduced quenching » (PFQ) initialement décrit par notre laboratoire en 2009. En effet, dans des liposomes possédant une forte concentration locale en mTHPC, une nette diminution du rendement quantique de fluorescence ainsi que des changements spectraux ont été observés, témoignant ainsi de l'agrégation de la mTHPC. Le fort signal de RLS (« resonance light scattering ») observé dans le Foslip[®] et le Fospeg[®] a indiqué la présence d'agrégats de type J avec une quantité plus élevée de molécules agrégées dans le Fospeg[®].

Une partie importante de la caractérisation de la drogue liposomale repose sur l'étude de sa localisation dans le liposome lui-même. Nos résultats ont indiqués que la mTHPC possède une

distribution hétérogène à l'intérieur de la bicouche lipidique, avec un ratio iodine accessible : iodine non accessible de 1:2. Une particularité intéressante dans la formulation de type Fospeg[®] est la localisation d'une partie de la mTHPC dans la couche externe de polyéthylène glycol (PEG), ce qui affecte les propriétés photophysiques comme montré dans la première partie des résultats. De façon évidente, la localisation de la mTHPC semblait influencer sa redistribution à partir des liposomes conventionnels et PEGylés et a donc fait l'objet d'une évaluation. Par conséquent, une méthode de redistribution de la drogue était nécessaire et devait être applicable non seulement aux différents modèles *in vitro* (solution tampon, membranes, solution de sérum) mais également aux modèles *in vivo*.

Nous avons donc proposé l'utilisation du PFQ en tant que méthode d'estimation de la concentration locale de mTHPC dans les liposomes. En effet, les changements de distribution de la mTHPC dans un système biologique en fonction de la formulation liposomale utilisée sont corrélés à un changement dans l'amplitude du PFQ. Nous avons montré dans la seconde partie de nos résultats que, comparée aux méthodes classiques de mesure de l'anisotropie de fluorescence et de FRET (« Förster resonance energy transfer »), la technique de PFQ offrait une gamme dynamique plus large pour les mesures de redistribution de la drogue à partir des transporteurs liposomaux, ce qui est particulièrement important dans le cas de liposomes ayant une forte concentration locale en drogue. Mesurer les caractéristiques du PFQ fournit un degré de précision maximum dans la détermination du taux de redistribution de la mTHPC à partir des liposomes avec des charges (mol/mol) de l'ordre de 0.2-10%. Les mesures d'anisotropie de fluorescence sont valables pour des liposomes avec des charges de mTHPC $\leq 1\%$, alors que la méthode de transfert d'énergie utilisant un marqueur donneur n'a tendance à être qu'informatrice avec des charges de mTHPC inférieures à 0.5%. Des charges si peu élevées ne correspondent pas aux formulations de drogue commercialement disponibles.

Nous avons étudié en détails les caractéristiques du PFQ dans une gamme de liposomes présentant différents ratios drogues-lipides. Ces mesures ont permis de construire une courbe de calibration, et, avec l'aide d'une méthode numérique, nous avons converti les valeurs de l'amplitude du PFQ en un pourcentage relatif de drogue redistribuée à partir des liposomes en fonction du temps et pour un système donné. Cette méthode de redistribution de la drogue est applicable à la fois dans les systèmes *in vitro* et dans les modèles *in vivo* et les échantillons de sang, puisqu'elle utilise les propriétés intrinsèques de la mTHPC dans un environnement lipidique sans tenir compte du milieu environnant. La seule condition requise est de fournir un excédent de molécules acceptrices dans le milieu d'incubation par rapport à la concentration des liposomes contenant de la mTHPC.

Nous avons également décrit la redistribution de la mTHPC à partir de Foslip® et de Fospeg® vers les liposomes et les protéines du sérum. Les informations concernant l'échelle de temps nécessaire à l'établissement d'une distribution de drogue équilibrée entre les structures donneuses-acceptrices sont extrêmement importantes car elles fournissent des indications intéressantes sur les paramètres pharmacocinétiques optimum. La redistribution de la mTHPC à partir du Foslip® est un processus monophasique lent, l'équilibre étant atteint après plus de 8 heures d'incubation à température physiologique.

La redistribution à partir du Fospeg® a présenté quant à elle un profil biphasique très différent de celui observé pour le Foslip®. Une quantité significative de mTHPC a été relarguée après plusieurs minutes d'incubation. Pendant la phase lente (de 30 minutes et plus), le taux de redistribution a été beaucoup plus faible comparé à celui observé durant la phase rapide. Ce comportement est expliqué par la présence de deux pools de mTHPC : le premier dans la couche externe de PEG (redistribution rapide) et le second dans la bicouche lipidique (redistribution lente). La redistribution partielle et rapide de la mTHPC à partir du Fospeg® contribue vraisemblablement au comportement du Fospeg® *in vitro*. Un point important concernant la redistribution de la mTHPC à partir des deux formulations liposomales est qu'elle s'effectue lorsque la bicouche lipidique des liposomes est dans un état liquide-cristallin, dû à l'influence de la mTHPC sur les liposomes.

En plus d'étudier le taux de redistribution de la mTHPC à partir des transporteurs liposomaux vers les protéines du sérum, il est également important de déterminer les fractions exactes de protéines qui se lient à la mTHPC. En effet, cela a un impact significatif sur l'accumulation tumorale de la drogue. Ce point a été présenté dans la troisième partie des résultats.

Nos données ont indiqué que les profils de liaison à l'équilibre du Foslip® et du Fospeg® étaient identiques à celui du Foscan® en solution, avec à peu près 65% de la drogue liée aux lipoprotéines de haute densité (HDL), et 35% aux lipoprotéines de faible densité (LDL). Le profil relatif de liaison de la mTHPC liposomale aux protéines a été démontré comme indépendant du temps d'incubation dans le sérum. C'est en contraste direct avec le Foscan®, où la liaison aux protéines dépend du temps d'incubation, avec une distribution initiale de la mTHPC sur l'albumine, suivie par un transfert progressif aux lipoprotéines pour atteindre l'équilibre. Dans le cas du Foscan®, la mTHPC subit une désagrégation dans le sérum avec une redistribution vers les protéines du sérum. A l'inverse, la mTHPC liposomale est majoritairement

sous forme monomérique, par conséquent les liposomes peuvent être utilisés pour monomériser les drogues dans le cas d'une redistribution rapide ou prolonger l'efflux de la drogue dans le plasma. Etant donné que seule la forme monomérique de la mTHPC est photoactive, et que la drogue liée aux LDL peut être rapidement captée par les cellules cancéreuses, cela souligne l'effet positif des formulations liposomales sur l'efficacité de la drogue dans le cas d'une redistribution du PS avant l'accumulation de liposomes dans la tumeur.

L'analyse du PFQ de la mTHPC dans les liposomes après une chromatographie d'exclusion des liposomes et des protéines du sérum a montré que l'efflux de la mTHPC à partir des liposomes seuls ne pouvait pas être le seul moyen de redistribution de la drogue vers les protéines du sérum. Cela nous a conduits à faire des recherches portant sur la stabilité des liposomes dans le sérum, et à estimer les cinétiques de destruction des liposomes. La technique d'analyse du suivi des nanoparticules (nanoparticle tracking analysis, NTA) utilisée dans cette étude a permis une analyse directe et quantitative de la destruction des liposomes. Alors que le Fospeg[®] était stable durant une incubation de 24 heures, les vésicules de Foslip[®] ont été progressivement détruites par les protéines du sérum. La destruction du Foslip[®] a montré une cinétique biphasique : une rapide destruction durant les 4 premières heures suivie par un processus extrêmement lent. Il est à noter que l'inclusion de mTHPC dans les liposomes induit une augmentation légère de la stabilité de la formulation liposomale comparée aux vésicules exemptes de drogue.

En associant les données chromatographiques avec le taux de destruction, nous avons estimé l'impact de l'efflux de la drogue et de la destruction des liposomes dans le relargage global. A des temps d'incubation courts, le relargage de la mTHPC à partir du Foslip[®] et du Fospeg[®] s'effectue à la fois par une redistribution de la drogue et par la destruction des liposomes. A des temps d'incubation plus longs, l'efflux de la drogue se fait uniquement par le processus de redistribution. L'impact de la redistribution de la mTHPC à partir de liposomes PEGylés intacts est prévalent comparé à leur destruction. A l'inverse, la redistribution de la mTHPC à partir du Foslip[®] ne présente que peu d'importance comparée à la destruction des vésicules.

Ainsi, l'excellente stabilité du Fospeg[®] dans le sérum, associé à ses propriétés de furtivité vis à vis du système réticulo-endothélial (RES) et l'utilisation de l'effet EPR suggèrent de bonnes perspectives pour l'application de ces liposomes *in vivo*. En effet, un large pourcentage de la mTHPC est redistribué vers les lipoprotéines dans la circulation, mais le reste de la drogue serait délivrée dans la tumeur sous forme liposomale, ce qui peut se produire

significativement plus rapidement que par la voie des lipoprotéines. On peut donc supposer que la stabilisation stérique et un taux de redistribution plus faible sont suffisants pour fournir un effet plus vasculaire de la PDT pour le Fospeg[®] que pour le Foslip[®]. A l'inverse, la majorité de la drogue injectée sous forme de liposomes conventionnels sera relarguée rapidement des transporteurs au moyen de la destruction des liposomes et de la redistribution additionnées d'une élimination des liposomes du flux sanguin par le RES. Cela limite donc le rôle des liposomes conventionnels à de simples monomérisateurs de drogue.

La présente étude présente une caractérisation du comportement de la mTHPC liposomale dans le milieu biologique, paramètre qui devrait être pris en compte lors de l'identification et de l'évaluation de systèmes de délivrances efficaces. La méthode du PFQ utilisée pour l'étude de la redistribution de la drogue peut être complétée par la technique d'analyse de la stabilité structurelle des liposomes. Cela fournirait une approche intégrale pour évaluer la quantité absolue de drogue liposomale et relarguée dans la circulation sanguine ayant un impact direct sur l'analyse pharmacocinétique.

La poursuite de ce travail réside dans la recherche de paramètres optimaux de redistribution de la drogue afin de potentialiser l'efficacité de la PDT. L'étude *in vivo* devra être conduite en comparant les paramètres pharmacocinétiques (incluant la redistribution de la drogue à partir des liposomes) et l'efficacité thérapeutique du Foslip[®] et du Fospeg[®]. De plus, la modulation du taux de redistribution de la drogue à partir des liposomes est une composante essentielle. Ainsi, la préparation de liposomes PEGylés avec des taux de redistribution plus lents ou plus rapides que ceux du Fospeg[®] décrits ici aideront à déterminer l'équilibre à respecter entre le taux de redistribution et l'efficacité thérapeutique de la PDT.

Photodynamic therapy (PDT) is a photochemical-based modality of cancer treatment that uses a combination of a photosensitizer, light and molecular oxygen. Application of liposomal nanocarriers to deliver photosensitizers to tumor targets has become a major direction of PDT research.

The present study investigates conventional and sterically stabilized liposomal formulations of the photosensitizer mTHPC, Foslip® and Fospeg®, with a view to determine the parameters for optimizing liposomal PDT. The characterization of *in vitro* behaviour of liposomal mTHPC was conducted, with an emphasis on drug localization, aggregation state and photophysical properties of the compounds in liposomes. We demonstrated the monomeric state of mTHPC in lipid vesicles and a partial localisation of mTHPC in Fospeg® in a PEG shell, while the main part was bound to the lipid bilayer. We further studied the drug release kinetics and binding pattern to serum proteins and the destruction of liposomes in serum. With this aim, a fluorescence-based methodology of estimating mTHPC release both *in vitro* and *in vivo* was developed, as well as an *in vitro* assay to characterize liposome destruction. The release of mTHPC from PEGylated liposomes was delayed compared with conventional liposomes along with greatly diminished liposome destruction. Knowledge of these parameters allows to better predict the drug release rate, pharmacological parameters and *in vivo* tumoricidal effect. The PDT treatment could be more advantageous with Fospeg® compared to mTHPC embedded in conventional liposomes.

Keywords: Photodynamic therapy, mTHPC, liposomes, drug release, liposome destruction, protein binding.

La thérapie photodynamique (PDT) est une modalité de traitement du cancer qui utilise la combinaison d'un photosensibilisant, de la lumière et d'oxygène moléculaire. L'application de nanosubstances liposomales pour délivrer les photosensibilisants dans la tumeur est devenu un sujet important de la recherche en PDT.

La présente étude porte sur les formulations liposomales conventionnelles et stériquement stabilisées de photosensibilisant mTHPC, Foslip® et Fospeg®, dans le but de déterminer les paramètres pour l'optimisation de la PDT liposomale. La caractérisation du comportement *in vitro* de la mTHPC liposomale a été étudiée, particulièrement sa localisation, l'état d'agrégation et les propriétés photophysiques des drogues dans les liposomes. Nous avons démontré l'état monomérique de la mTHPC dans les vésicules lipidiques et une localisation partielle du mTHPC dans Fospeg® dans la partie PEG des liposomes, alors que la majeure partie est liée à la bicouche lipidique. Nous avons ensuite étudié les cinétiques de relargage des drogues, le mode de liaison aux protéines et la destruction des liposomes dans le sérum. Dans ce but, une méthodologie basée sur la fluorescence pour estimer le relargage de la mTHPC à la fois *in vitro* et *in vivo* a été développée, ainsi que d'un essai *in vitro* pour caractériser la destruction des liposomes. Le relargage de la mTHPC des liposomes PEGylés a été retardé par rapport aux liposomes conventionnels et la destruction des liposomes a été considérablement diminuée. La connaissance de tous ces paramètres permet de mieux prédire le taux de relargage de la drogue, les paramètres pharmacologiques et l'effet tumoricide *in vivo*. Le traitement PDT pourrait être plus avantageux avec le Fospeg® comparé à la mTHPC incorporée dans les liposomes conventionnels.

Mots-clé : Thérapie photodynamique, mTHPC, liposomes, relargage de drogue, destruction de liposomes, liaison aux protéines